Experimental Dark Matter Searches - Part 2

Carsten B Krauss
carsten.krauss@ualberta.ca

Aug 2 2019
TRISEP summer school at TRIUMF

WIMP Searches

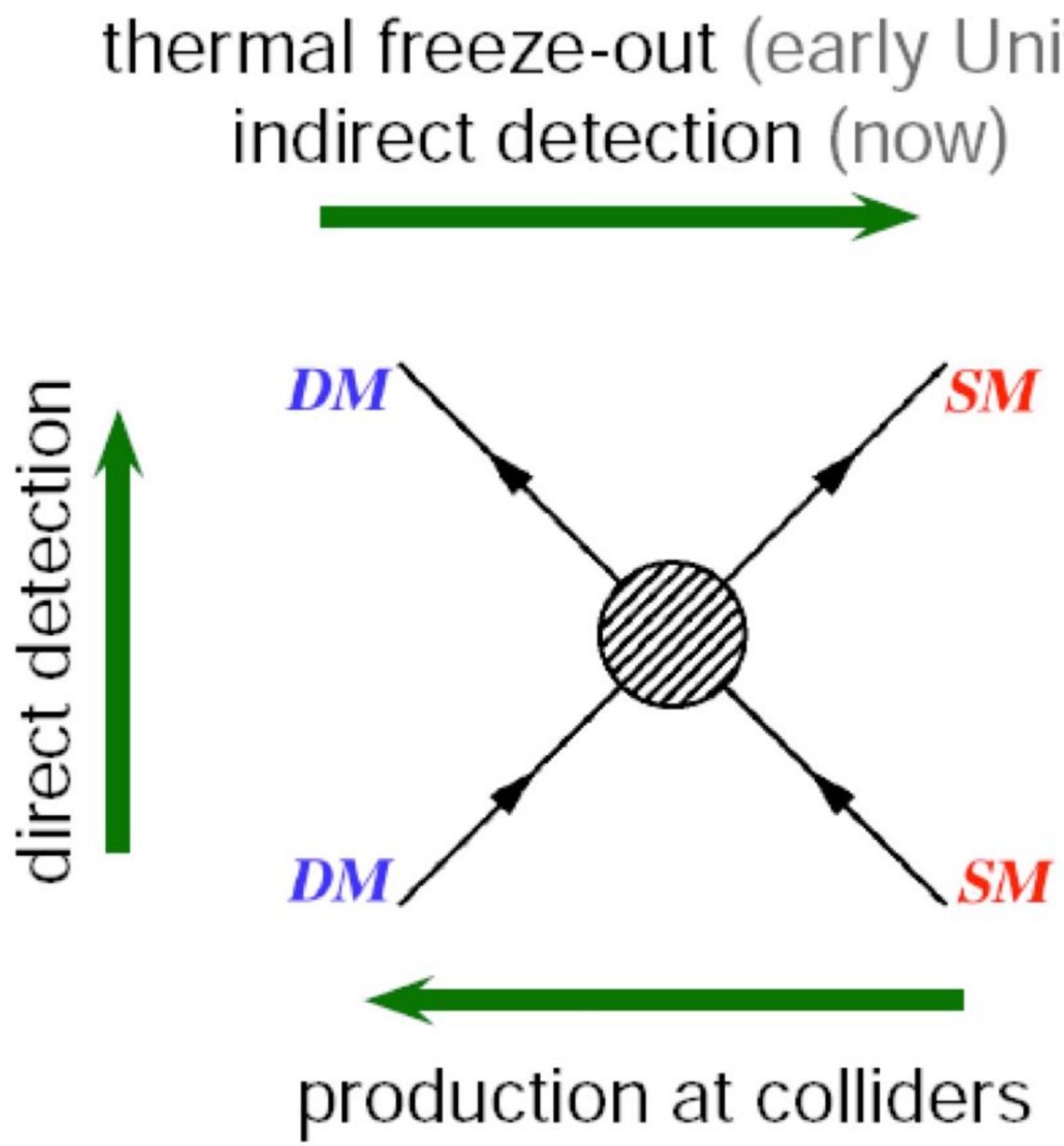

From Wednesday's lecture by G. Gelmini

WIMP Searches

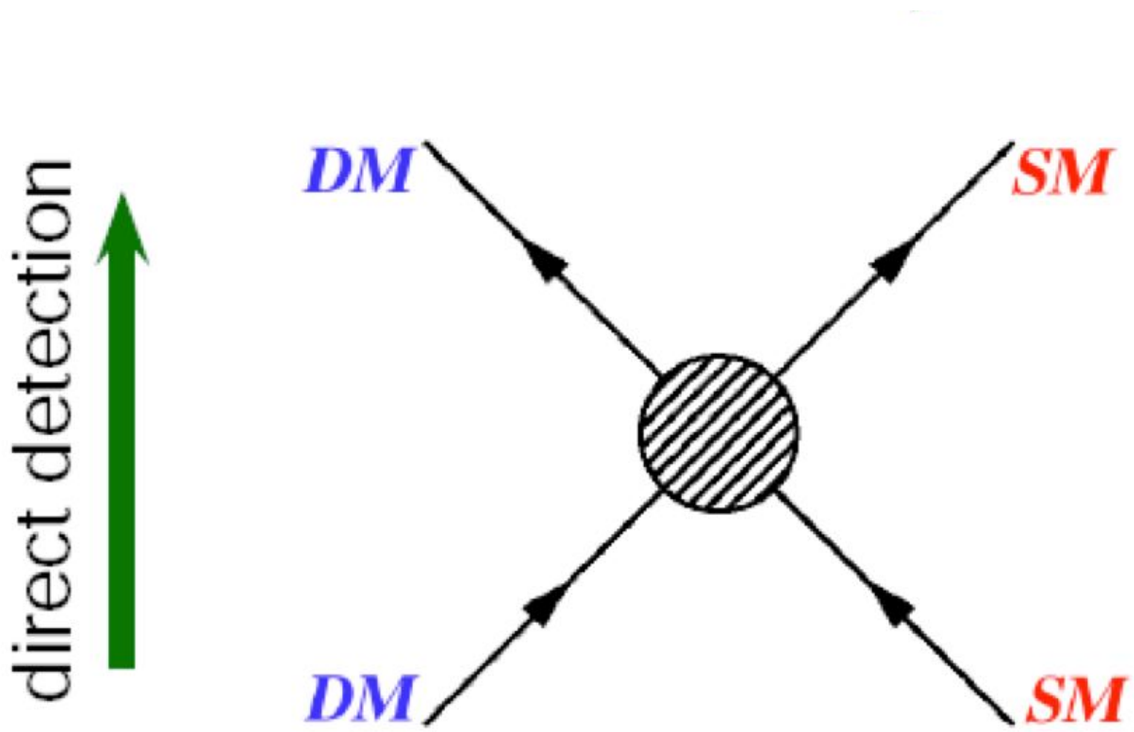

From Wednesday's lecture by G. Gelmini

Signal

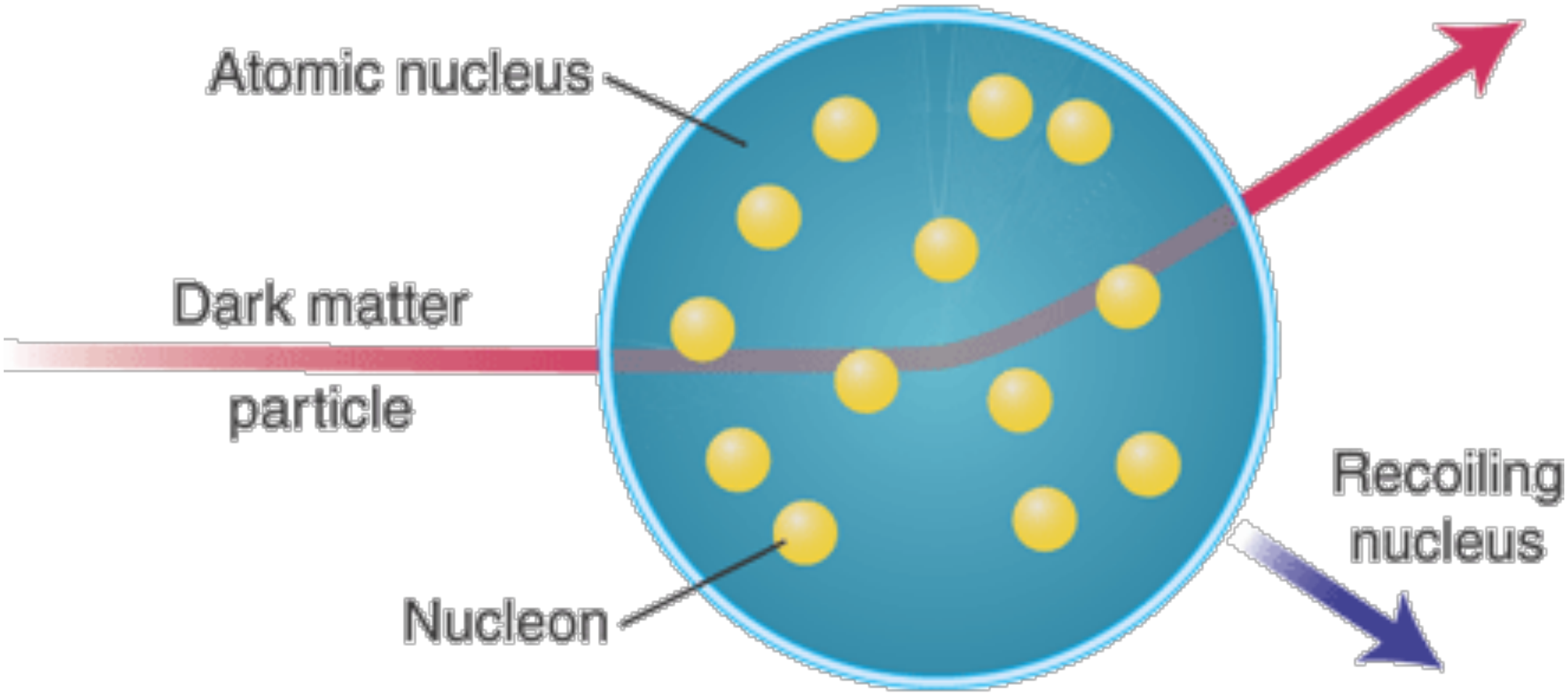

- Coherent scattering off the whole target nucleus

Science 26 Nov 2004:Vol. 306, Issue 5701, pp. 1485-1488

Recoil spectrum

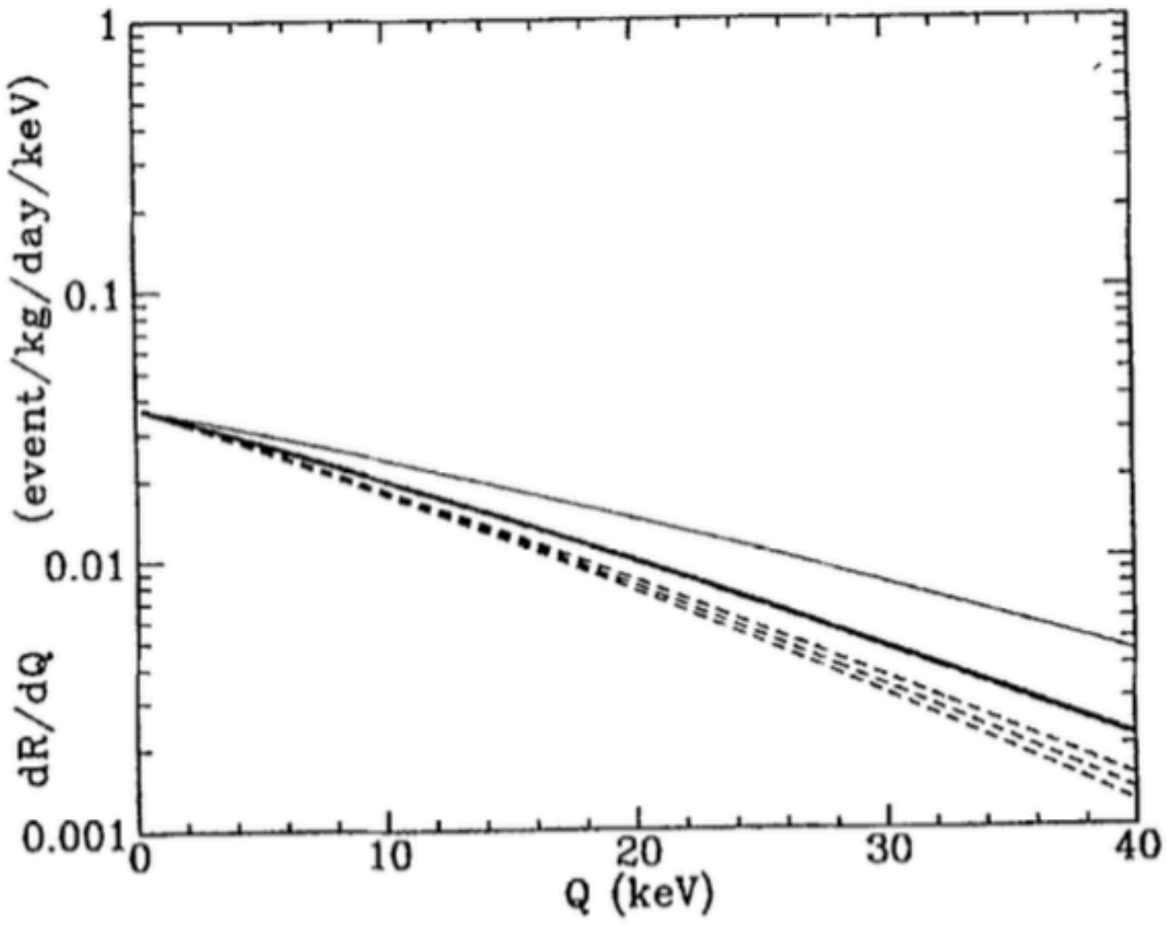

Fig. 22. Theoretical differential event rate [Eq. (8.17)] versus deposited energy for several different nuclear form factors. An arbitrary cross section of $\sigma_0 = 4 \times 10^{-36}\,\mathrm{cm}^2$ was chosen, with $m_\chi = 40$ GeV and $m_N = 68$ GeV, and standard values of the other parameters. The heavy solid line shows the best-estimate (i.e., the Woods–Saxon) form factor [Eq. (7.33)] for scalar interactions, while the long-dashed line (which falls on top of the heavy solid line) shows the exponential form factor [Eq. (7.31)]. The light solid line shows $F(Q) = 1$ (no form factor). The three spin form factors for germanium (Table 5) are shown as short-dashed lines.

[1] Jungmann, Kamionkowski, Griest, Supersymmetric Dark Matter, Physics Reports 267. 267 (2006) 179.

Galactic Dark Matter Density Profile

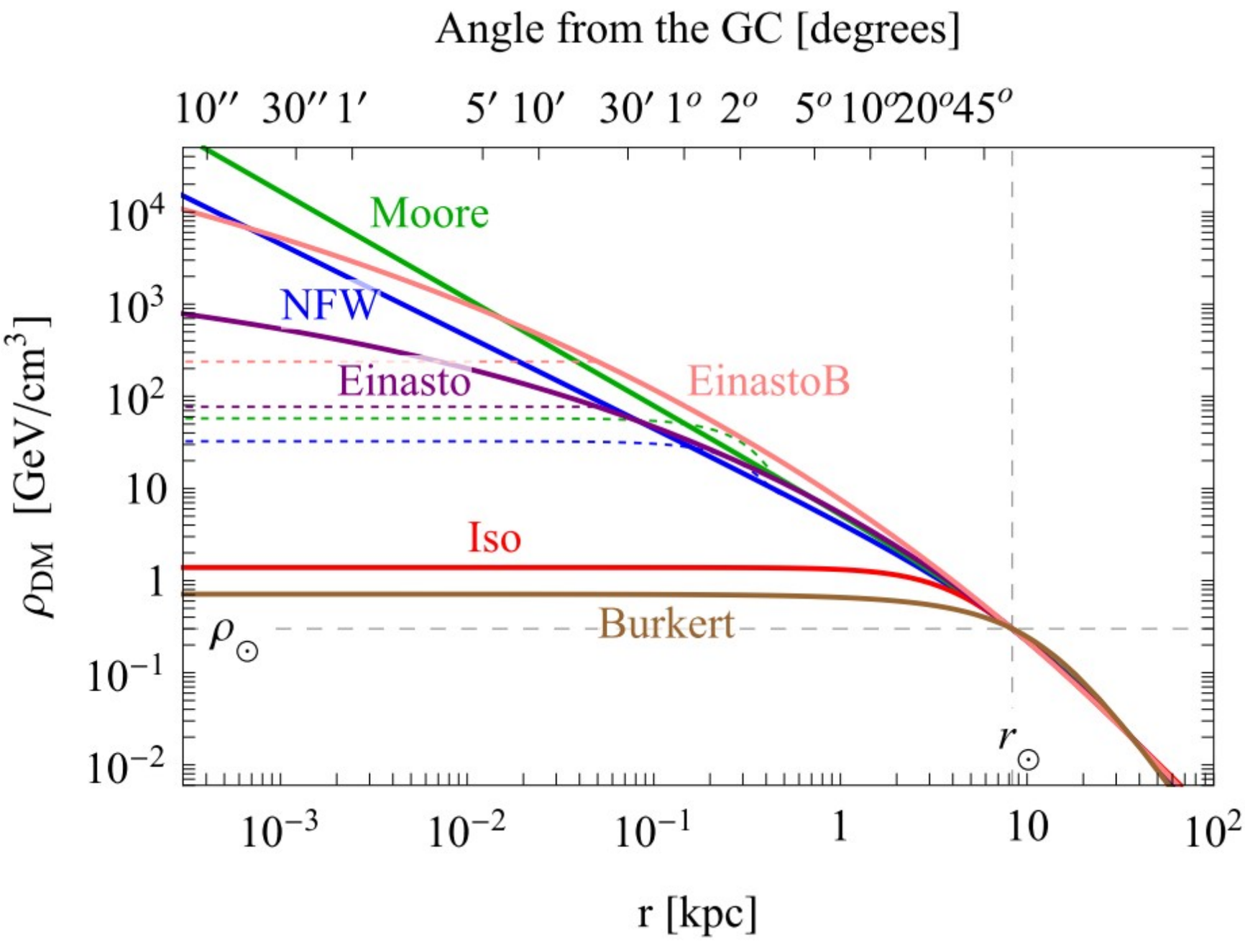

Standard Halo

- ρ_{DM}= 0.3 GeV cm^{-3}, v_{esc} = 544 km/s, v_0 = 220 km/s, and v_{Earth} = 30 km/s.

- To compare experiments, check that they use the same parameters!

- This is a super active field of research too, there is almost no way that these standard parameters are true: the halo is more complex for sure. It contains a history of past galactic mergers and other interesting astrophysics

Direct detection

- Canonical WIMP searches
    - Spin dependent and
    - Spin independent
- Low mass WIMP searches
- Directional dark matter search experiments

The Pioneers

- Classical germanium detectors
- Bolometric searches
  - Germanium, $CaWO_4$
- NaI Scintillators

First Dark Matter Searches

- Germanium detectors with their outstanding energy resolution and low background allowed for the first direct measurements of dark matter

- These detectors were originally build for the search for neutrinoless double beta decay and the event rate at low energies could be turned into an exclusion limit

Geometries of Ge Detectors

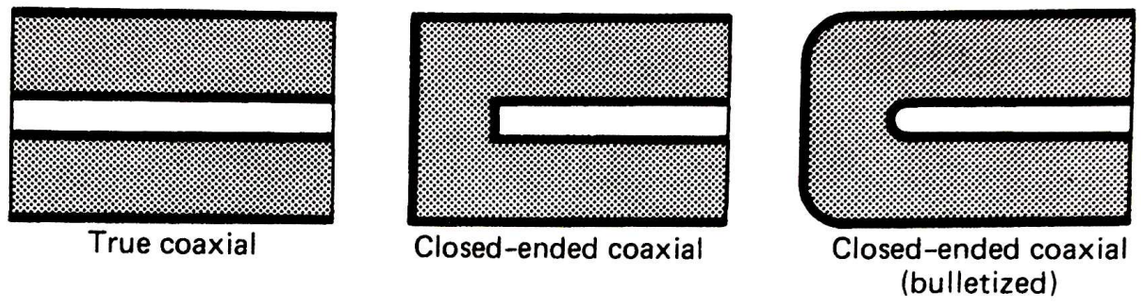

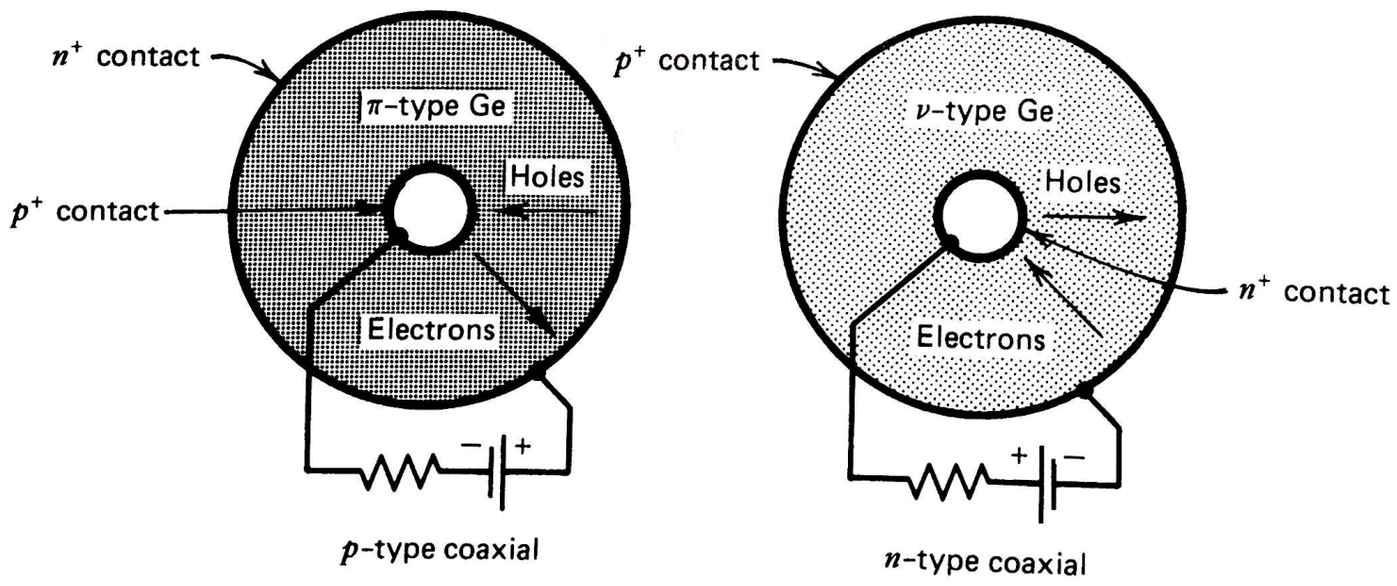

Knoll

Ge Detector X-Ray Image

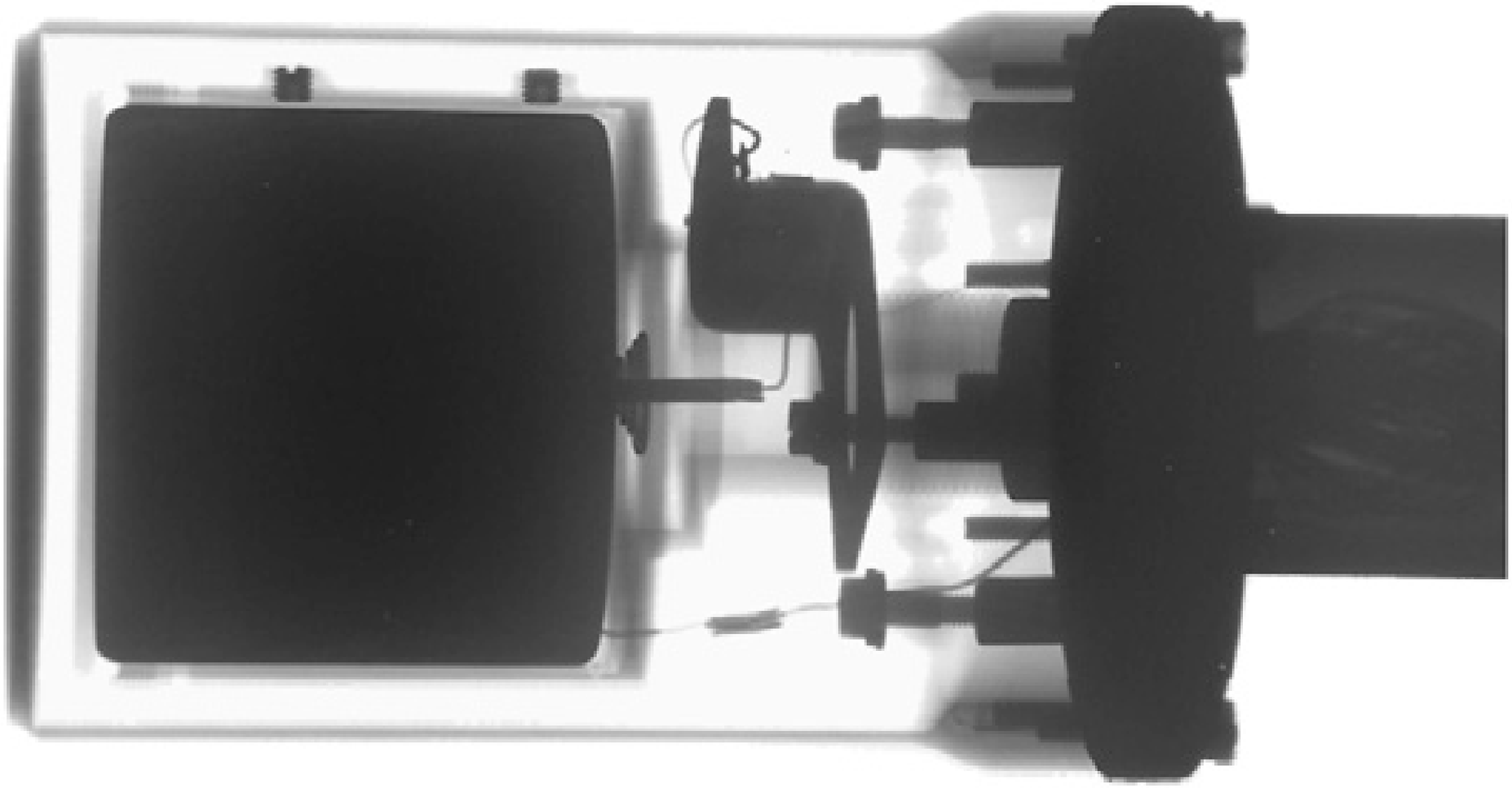

Fig. 2. An X-ray image of the detector showing the internal components of the housing.

Budjáš, D., Heisel, M., Maneschg, W., & Simgen, H. (2009). Optimisation of the MC-model of a p-type Ge-spectrometer for the purpose of efficiency determination. *Applied Radiation and Isotopes*, *67*(5), 706–710. doi:10.1016/j.apradiso.2009.01.015

Detector schematics

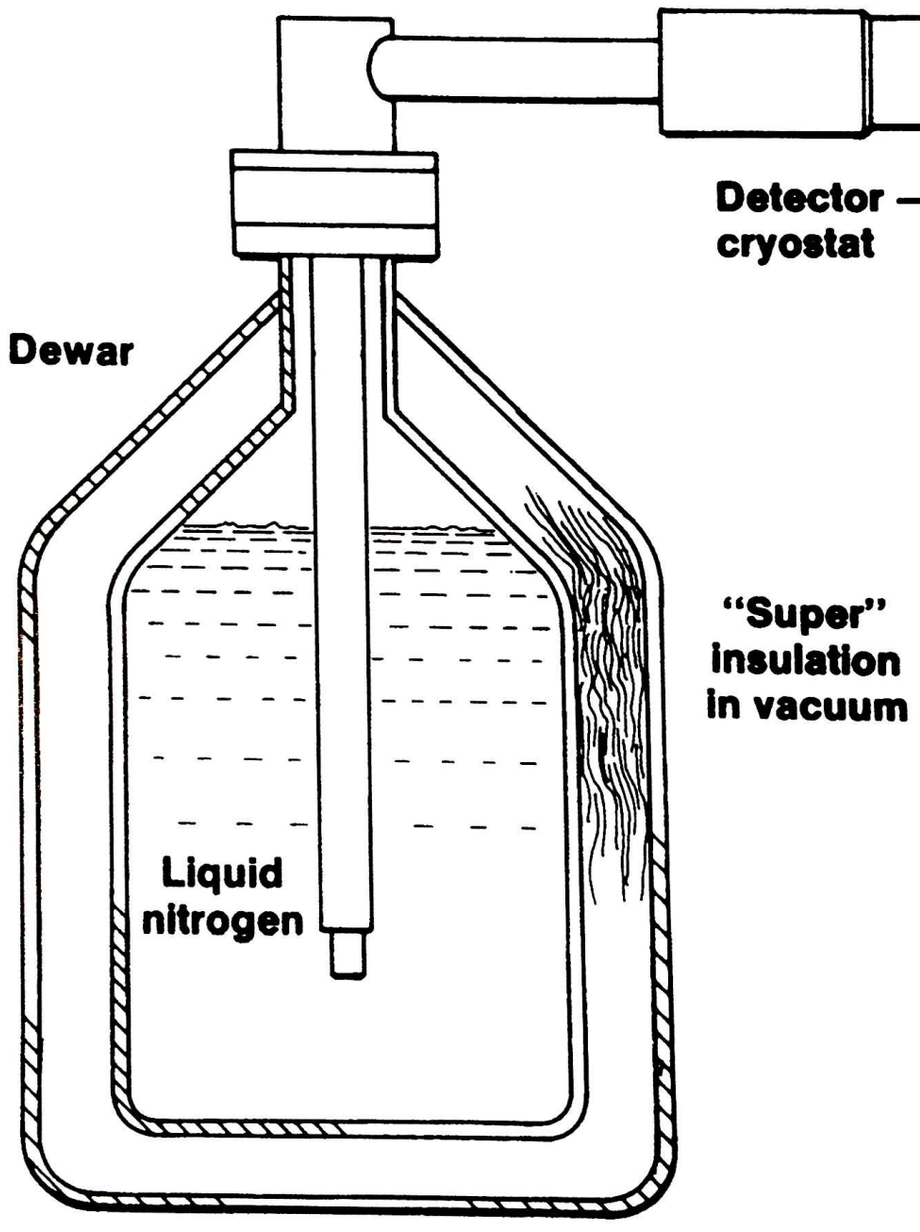

Knoll

Detector schematics

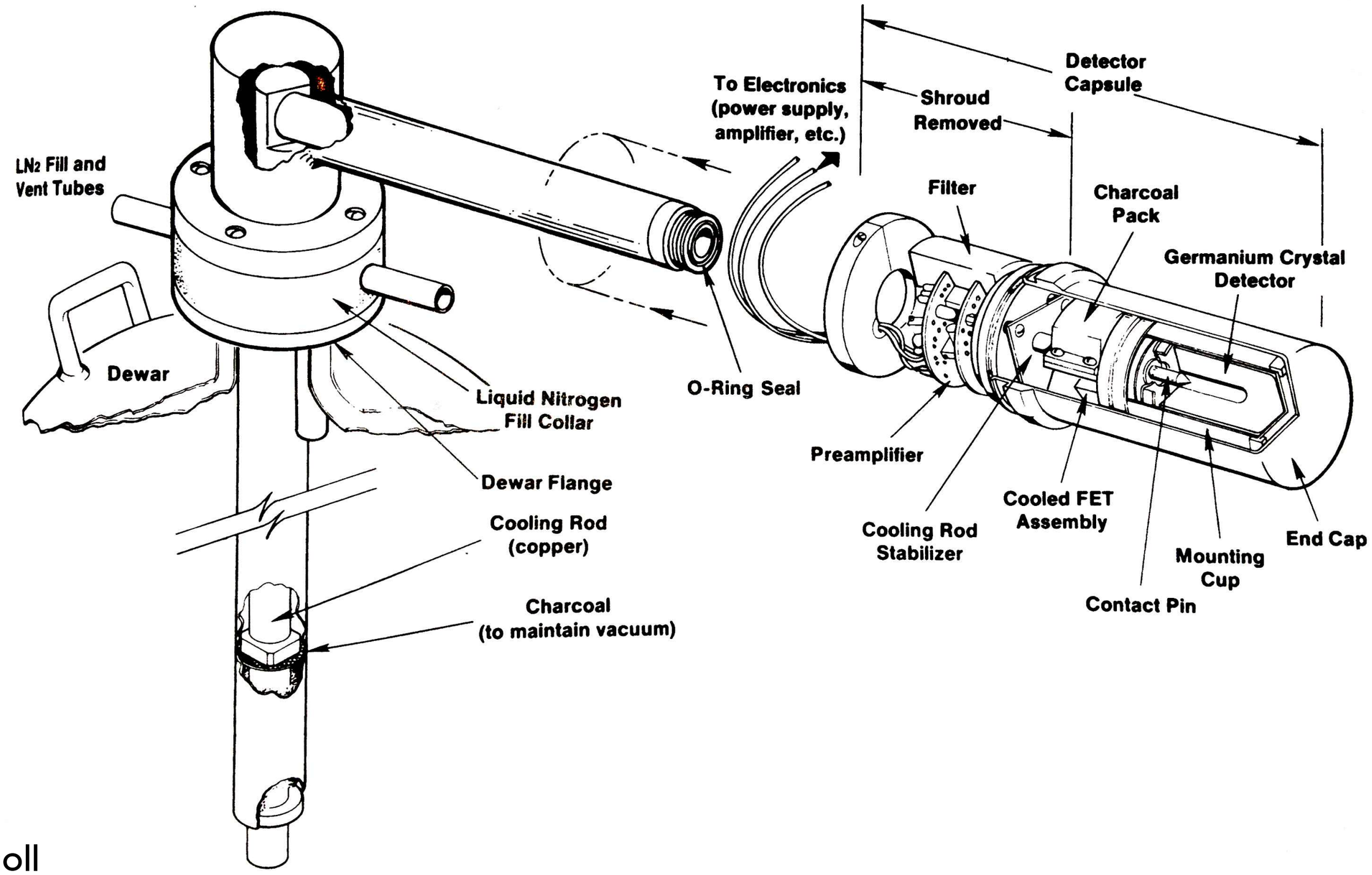

Knoll

The Heidelberg Moscow Experiment

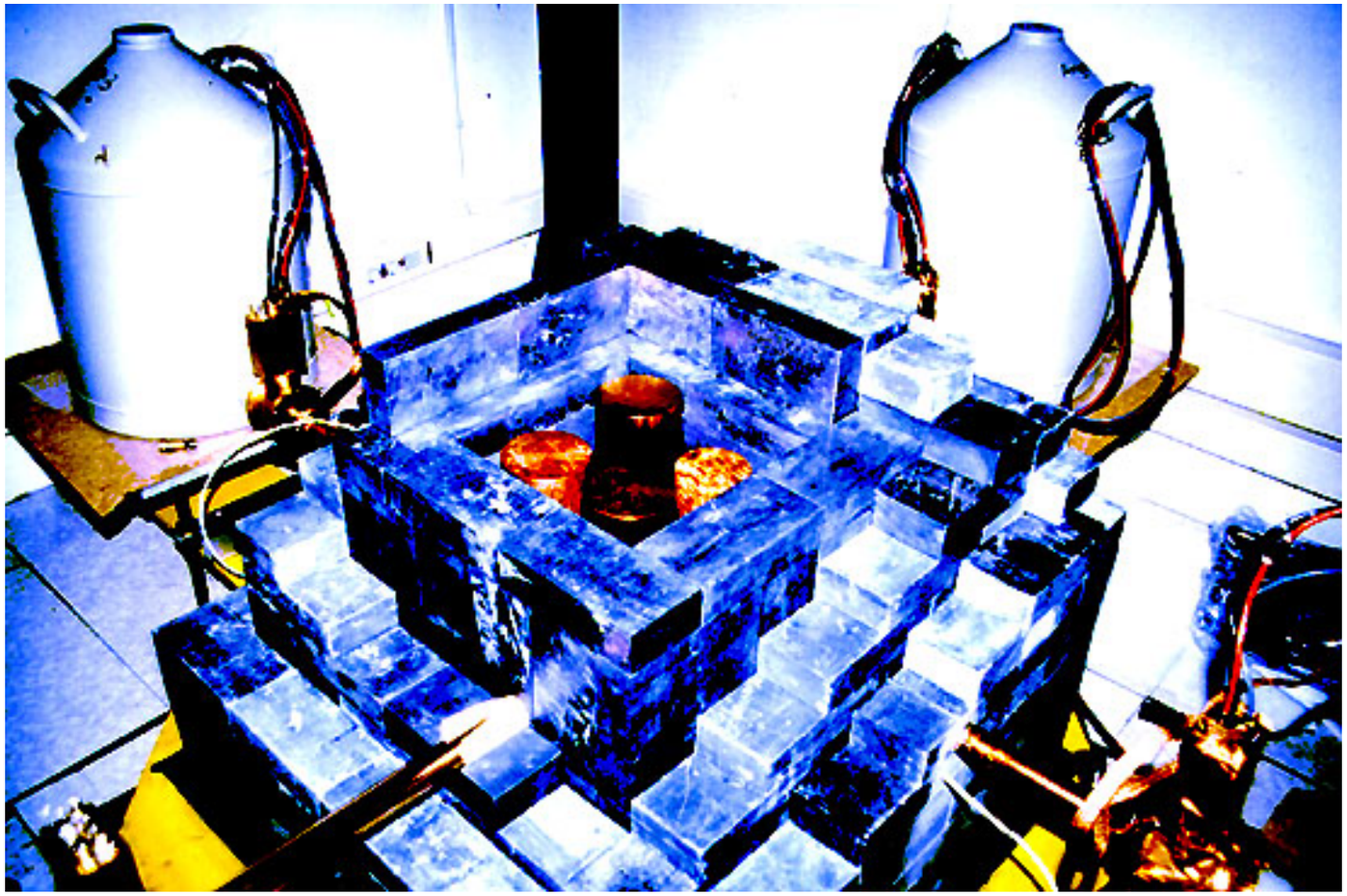

http://www.klapdor-k.de/photo_gallery/photo_gallery.htm

Heidelberg Moscow Results

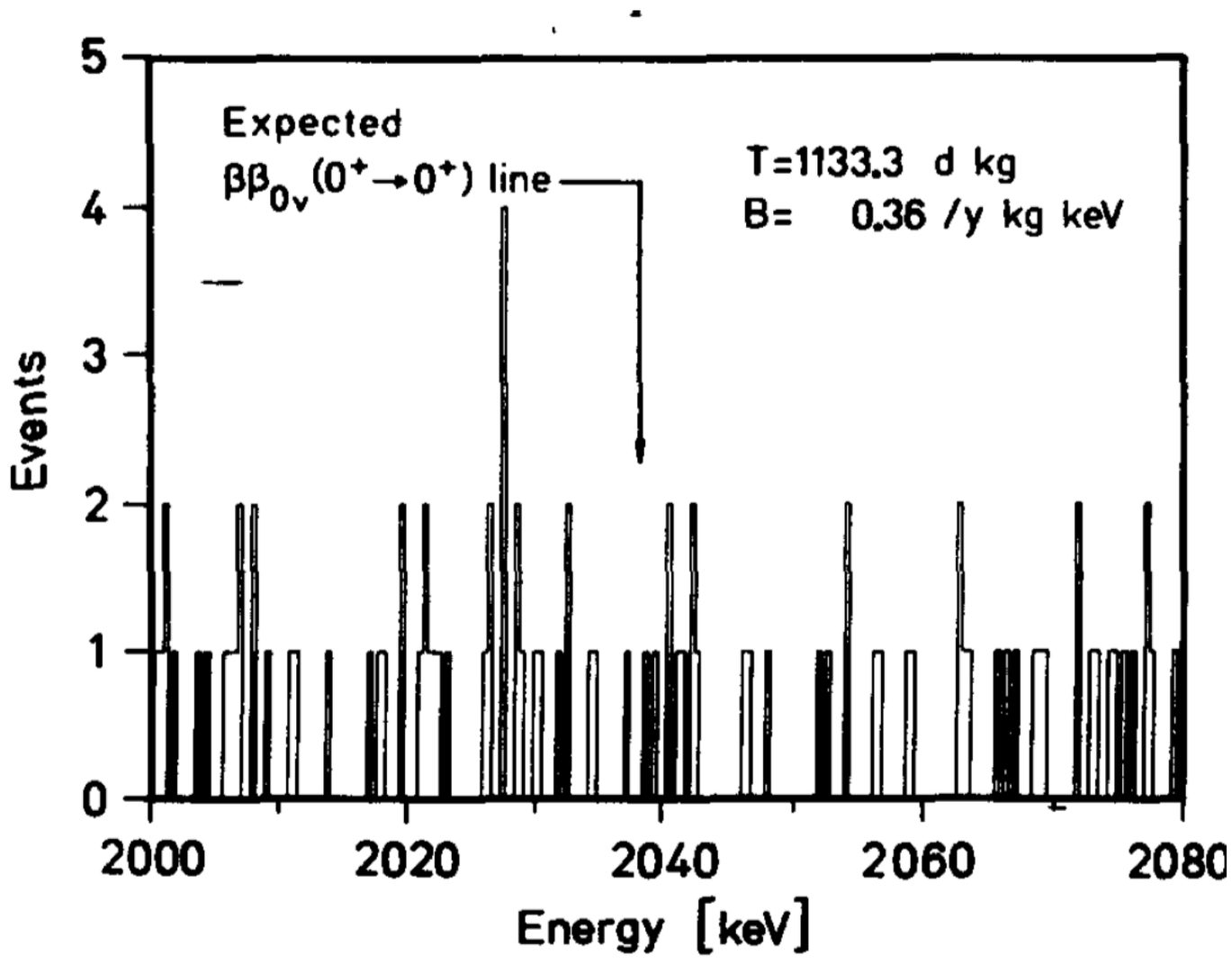

Nuclear Physics B (Proc. Suppl.) 31 (1993) 72–75

Modern Point Contact Detectors

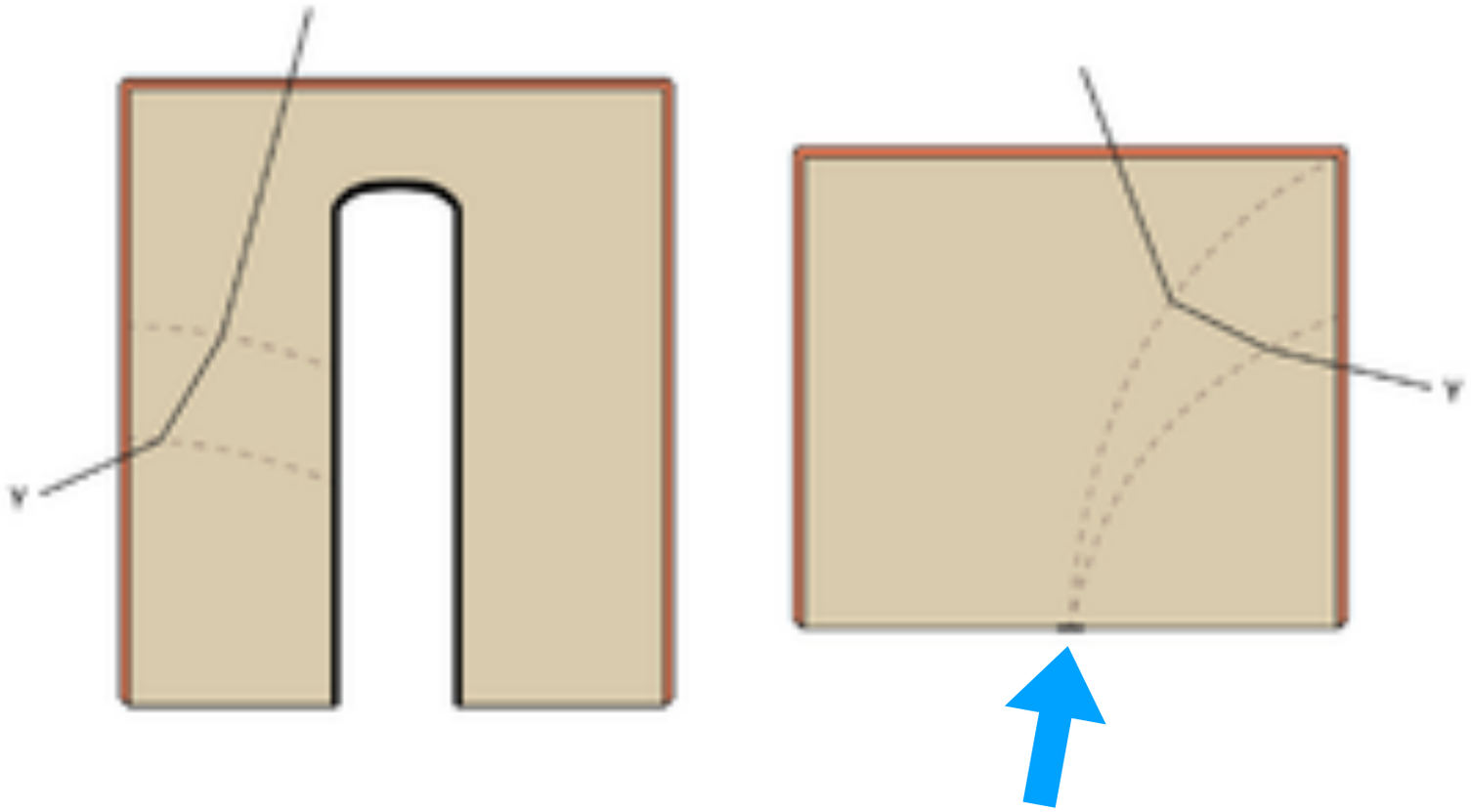

- Cogent was looking for DM with such a point contact detector
- In the search for neutrinoless double beta decay these detectors are now also standard

https://en.wikipedia.org/wiki/MAJORANA

Off Topic: Gerda

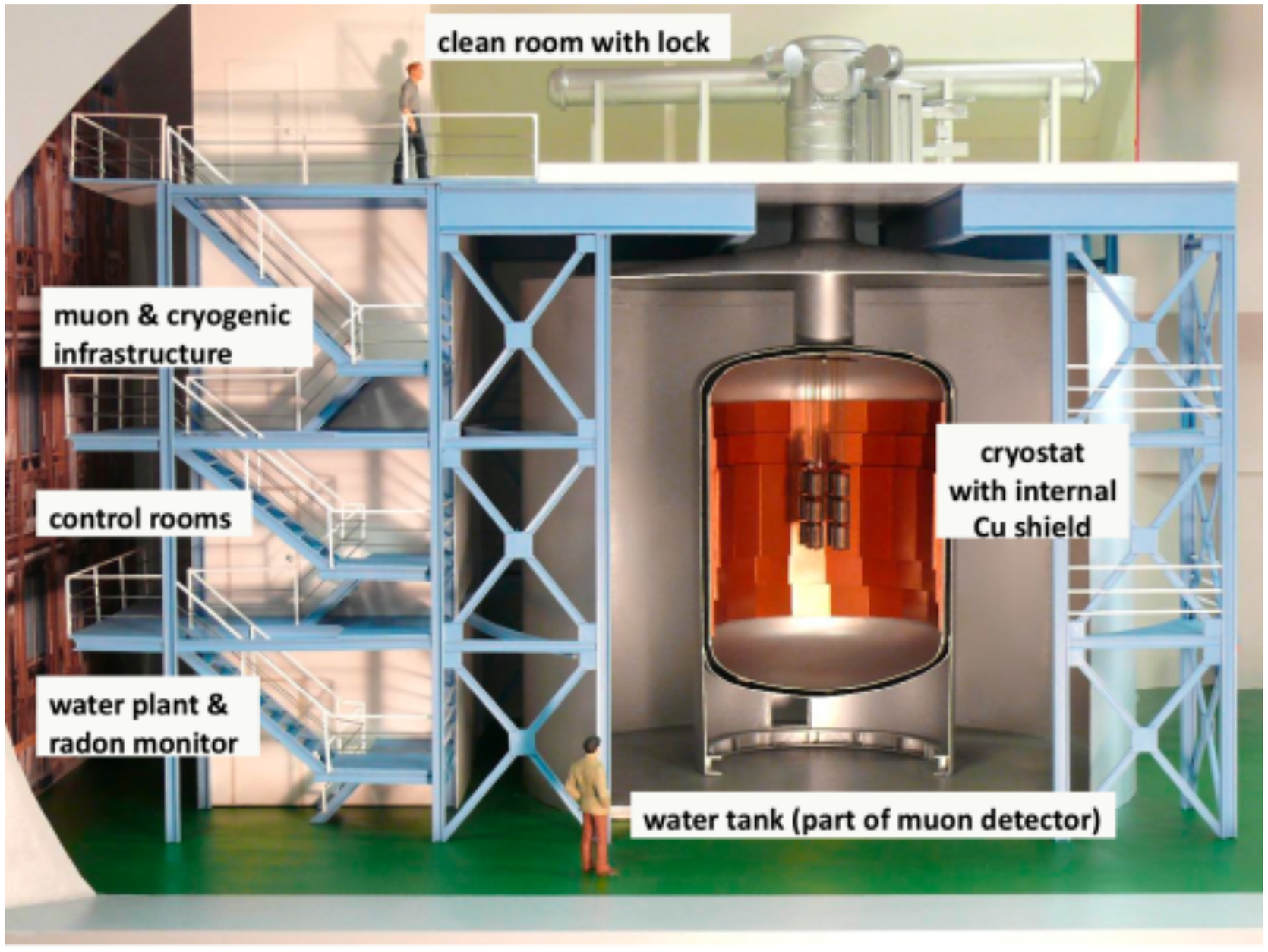

Bolometric Detectors

- These types of detectors allow operation with extremely low thresholds

- They require operational temperatures in the mK range

- The readout collects phonons with a transition edge detector

- There are three main experiments that use this technique:

    - SuperCDMS, Edelweiss and CRESST (and Cuore for 0νββ)

Phonon

- In physics, a phonon is a collective excitation in a periodic, elastic arrangement of atoms or molecules in condensed matter, such as solids and some liquids. Often referred to as a quasiparticle it represents an excited state in the quantum mechanical quantization of the modes of vibrations of elastic structures of interacting particles.

- Phonons play a major role in many of the physical properties of solids, including a material's thermal and electrical conductivities. The study of phonons is an important part of solid state physics.

- The concept of phonons was introduced in 1932 by Russian physicist Igor Tamm. The name phonon comes from the Greek word φωνή (phonē), which translates as sound or voice because long-wavelength phonons give rise to sound.

From Wikipedia, the free encyclopedia

Phonon

- In
  a
  s
  re
  th
- P
  in
  o
- Th
  lg
  (p
  pl

Normal modes of vibration progression through a crystal. The amplitude of the motion has been exaggerated for ease of viewing; in an actual crystal, it is typically much smaller than the lattice spacing.

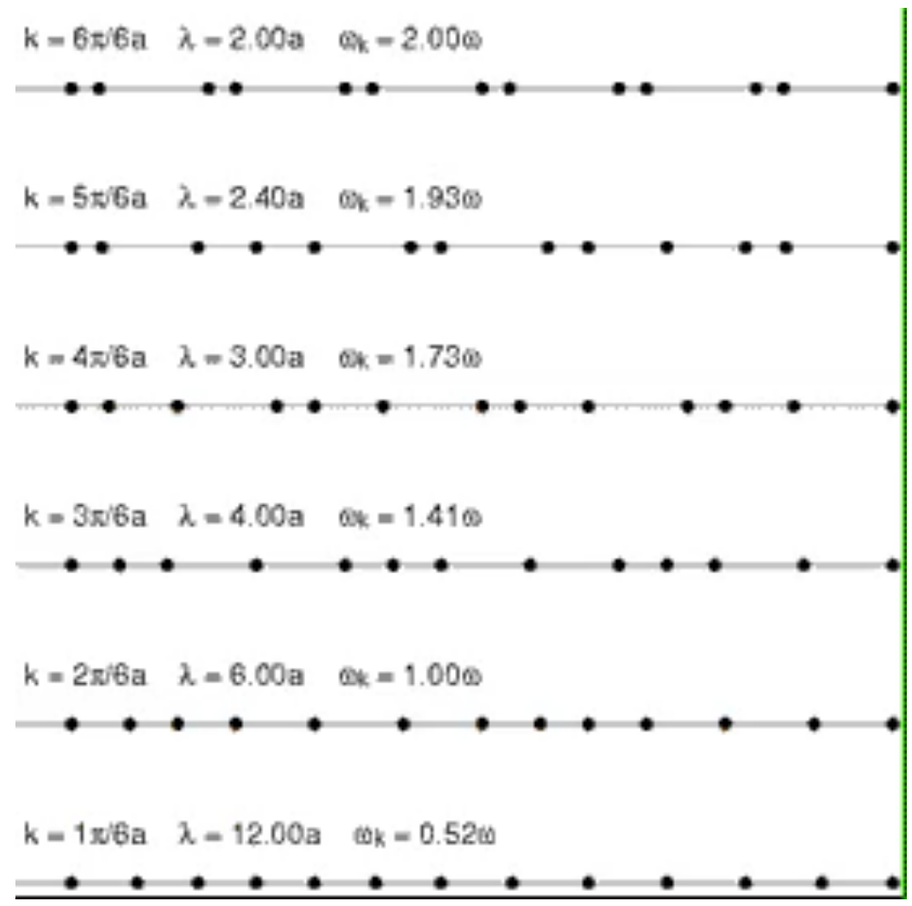

From Wikipedia, the free encyclopedia

CDMS

Thermometer view

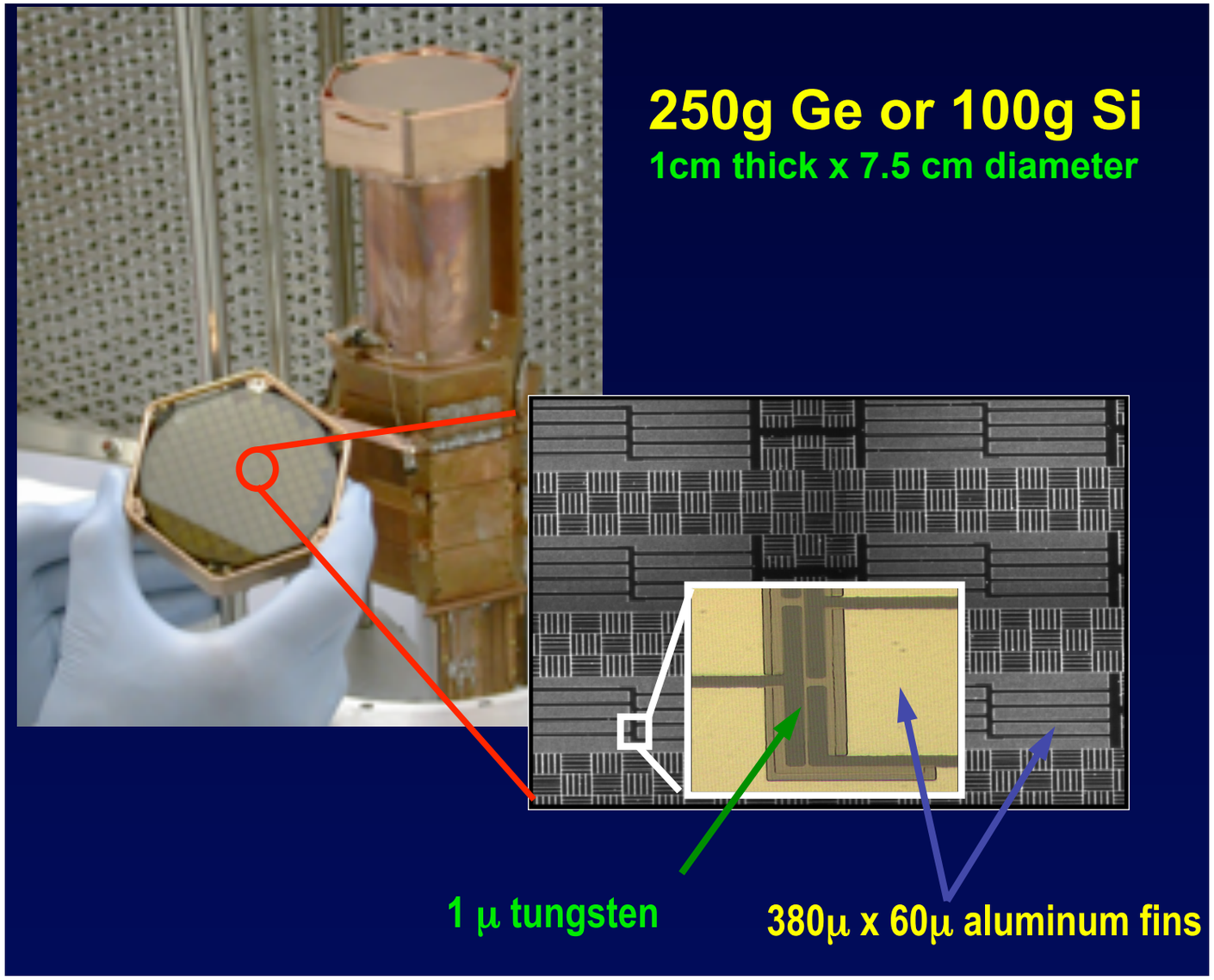

Assembled detector

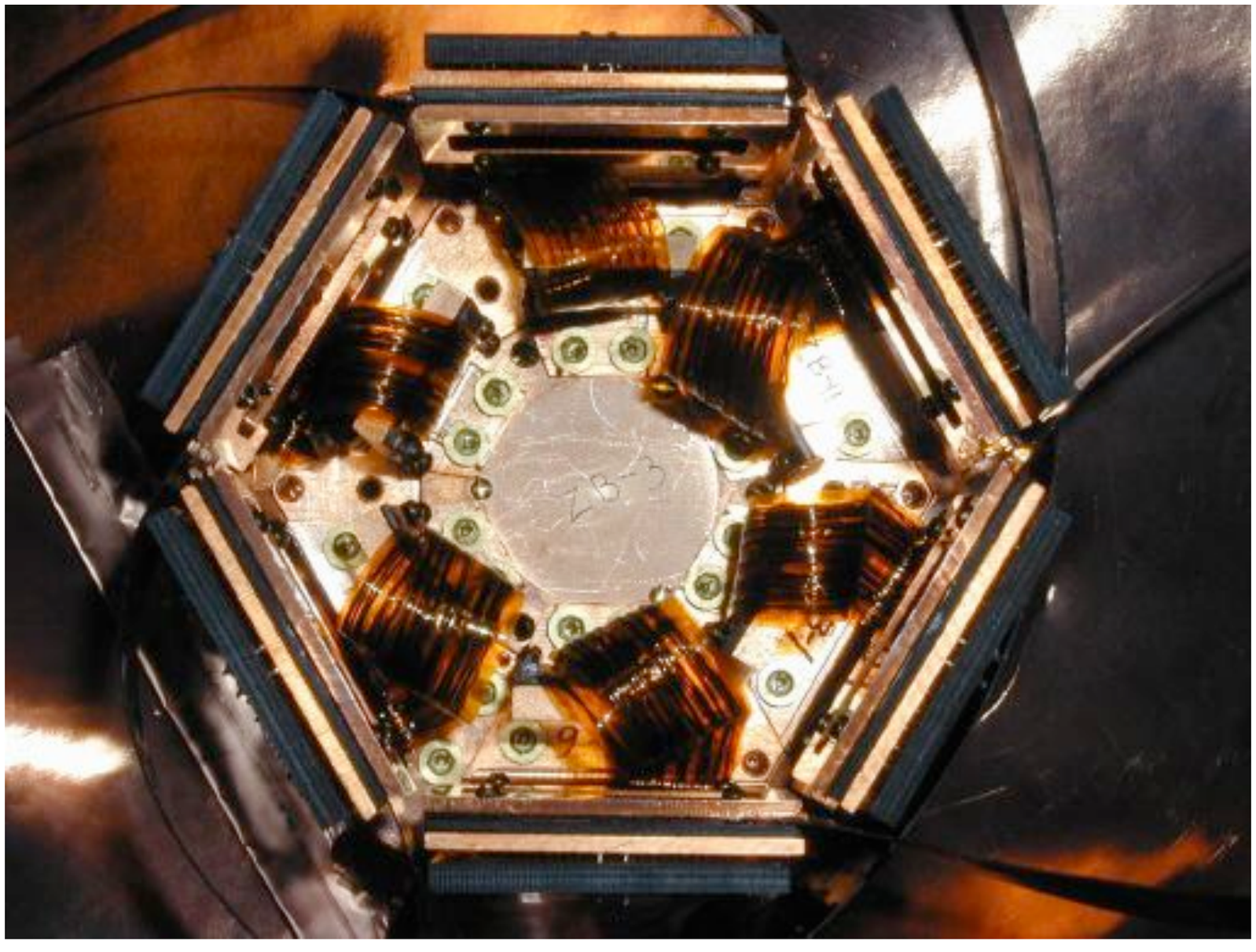

Cryostat view

Detector Principle

- The ionization signal is read out conventionally.
- The phonon signal is acquired with a transition edge thermometer at the surface.

Detector Principle

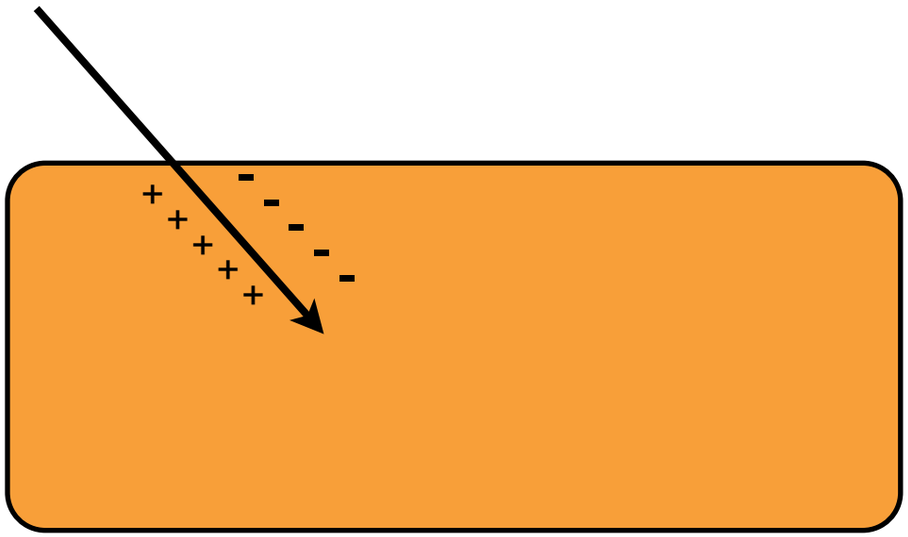

- The ionization signal is read out conventionally.
- The phonon signal is acquired with a transition edge thermometer at the surface.

Detector Principle

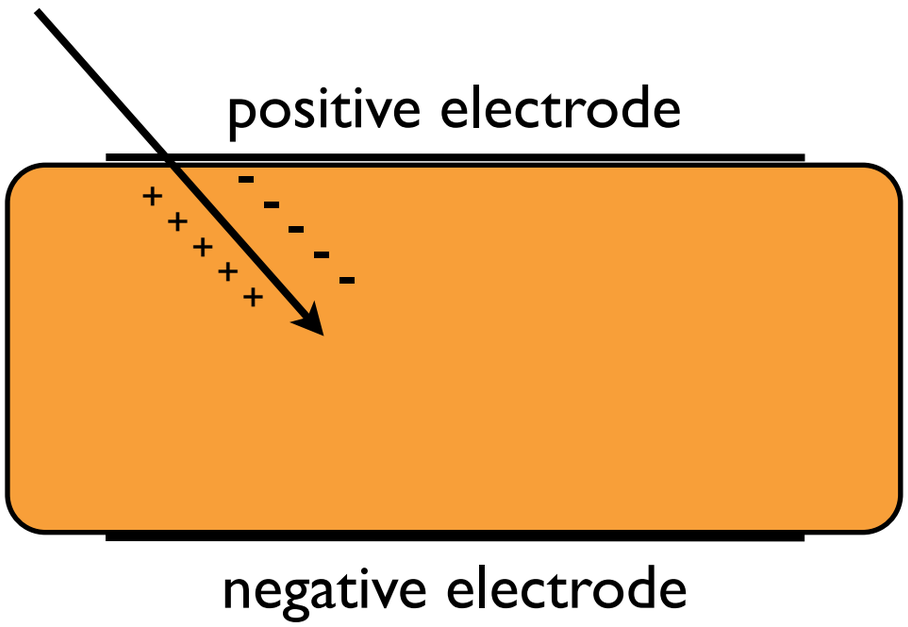

- The ionization signal is read out conventionally.
- The phonon signal is acquired with a transition edge thermometer at the surface.

Detector Principle

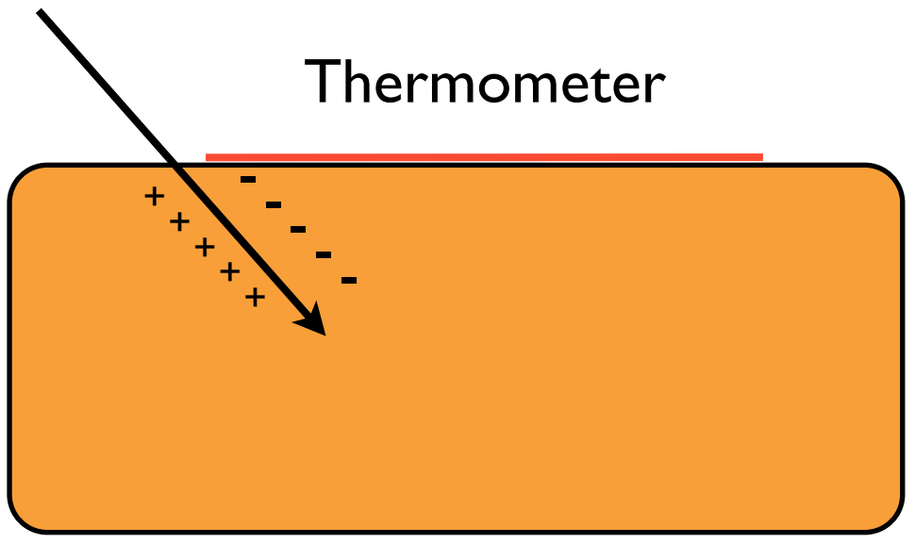

- The ionization signal is read out conventionally.
- The phonon signal is acquired with a transition edge thermometer at the surface.

Detector Principle

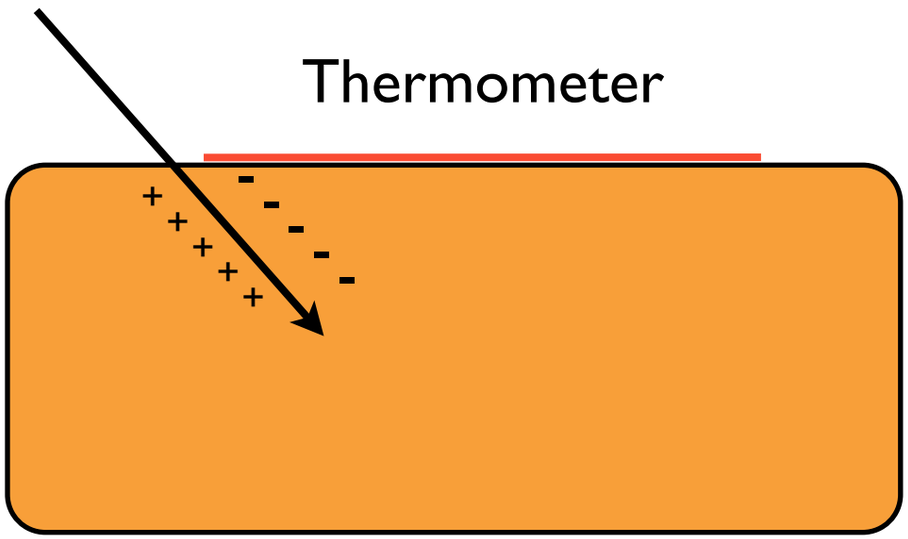

- The ionization signal is read out conventionally.
- The phonon signal is acquired with a transition edge thermometer at the surface.

$$\text{Yield} = \frac{\text{Energy from ionization signal}}{\text{Phonon based energy}}$$

Response

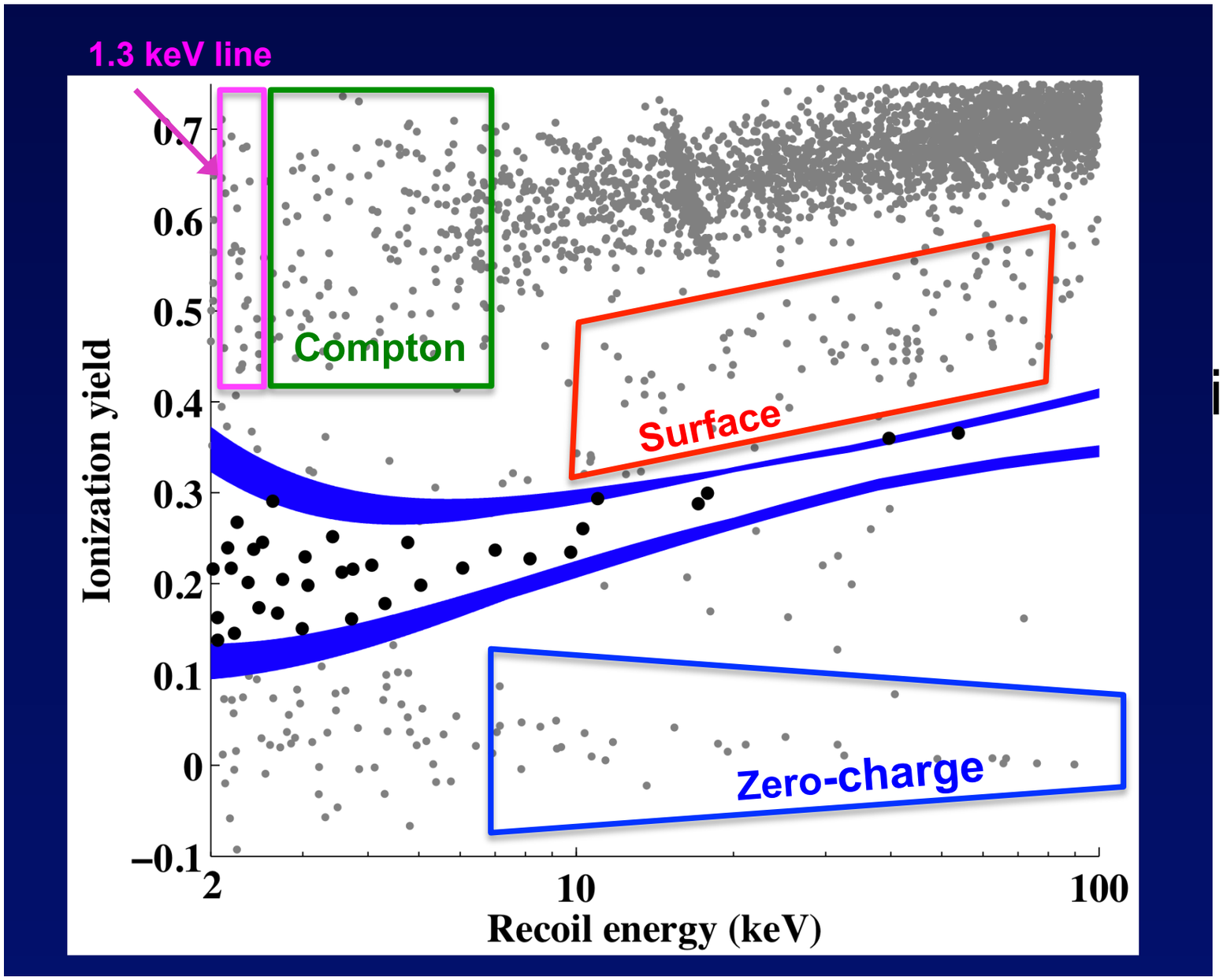

ionizing particles.

Talk: Serfas at UCLA Dark Matter conference 2012

Typical response

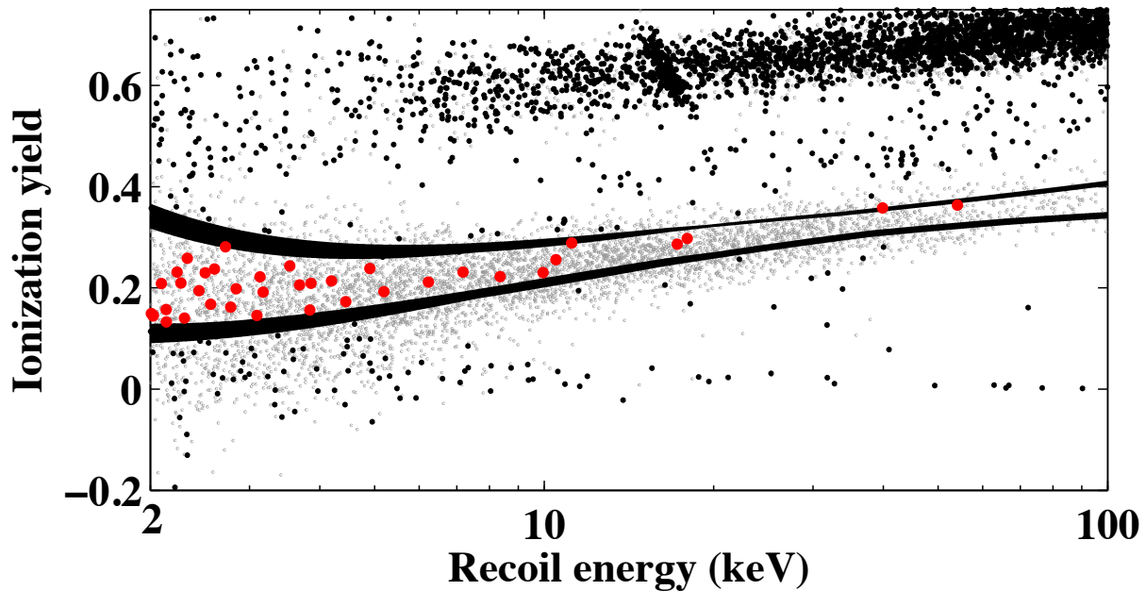

FIG. 2. (color online). Events in the ionization-yield versus recoil-energy plane for T1Z5. Events within the $(+1.25, -0.5)\sigma$ nuclear-recoil band (solid) are WIMP candidates (large dots). Events outside these bands (small, dark dots) pass all selection criteria except the ionization-energy requirement. The widths of the band edges denote variations between data runs. Events from the ^{252}Cf calibration data are also shown (small, light dots). The recoil-energy scale assumes the ionization signal is consistent with a nuclear recoil, causing electron recoils to be shifted to higher recoil energies and lower yields.

Phys.Rev.Lett.106:131302,2011

Top Level View

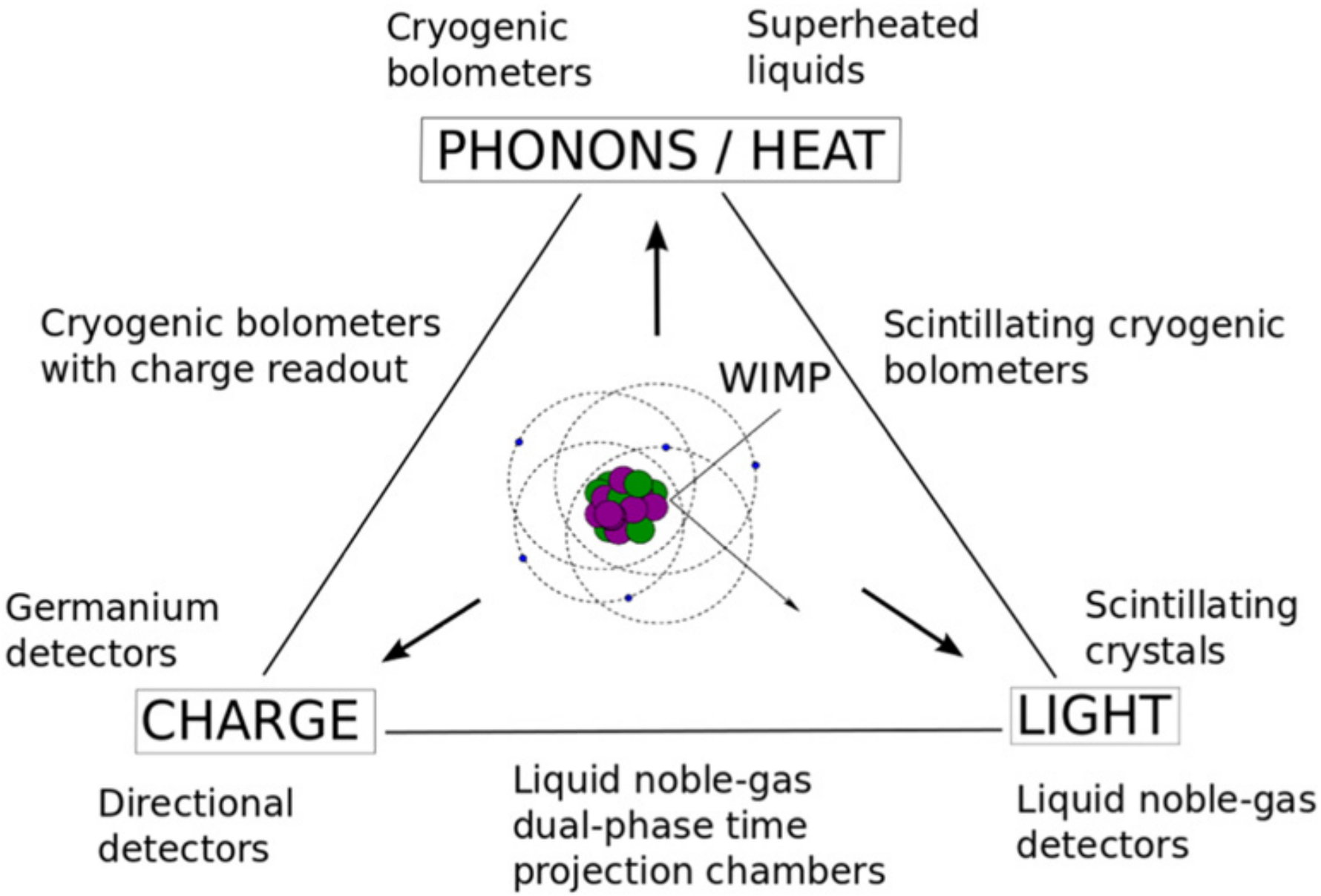

J. Phys. G: Nucl. Part. Phys. 43 (2016) 013001

Top Level View

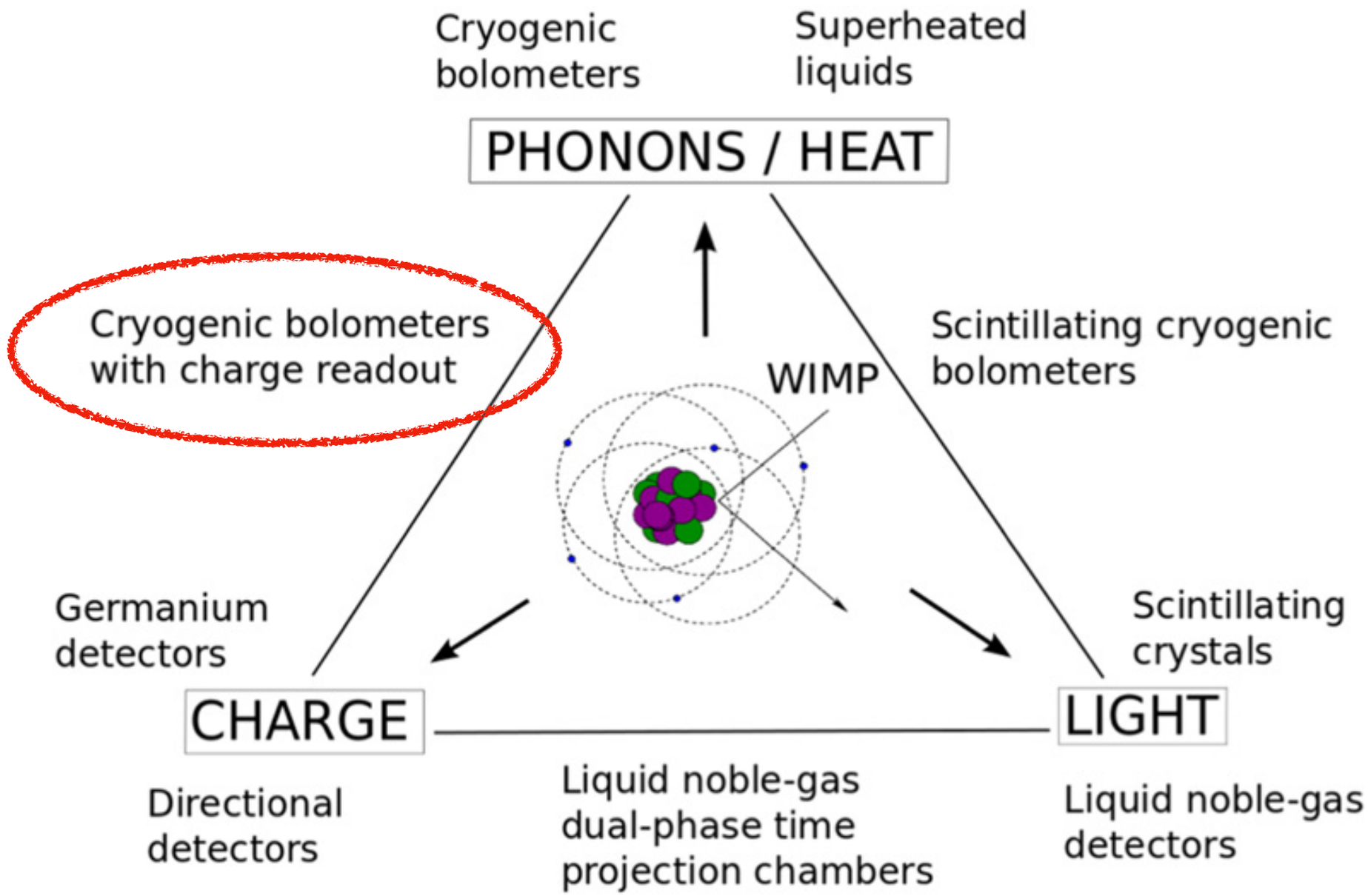

J. Phys. G: Nucl. Part. Phys. 43 (2016) 013001

Edelweiss (Modane)

- Similar detector concept, but different realization.

Pictures from Edelweiss

Edelweiss Cryostat arrangement

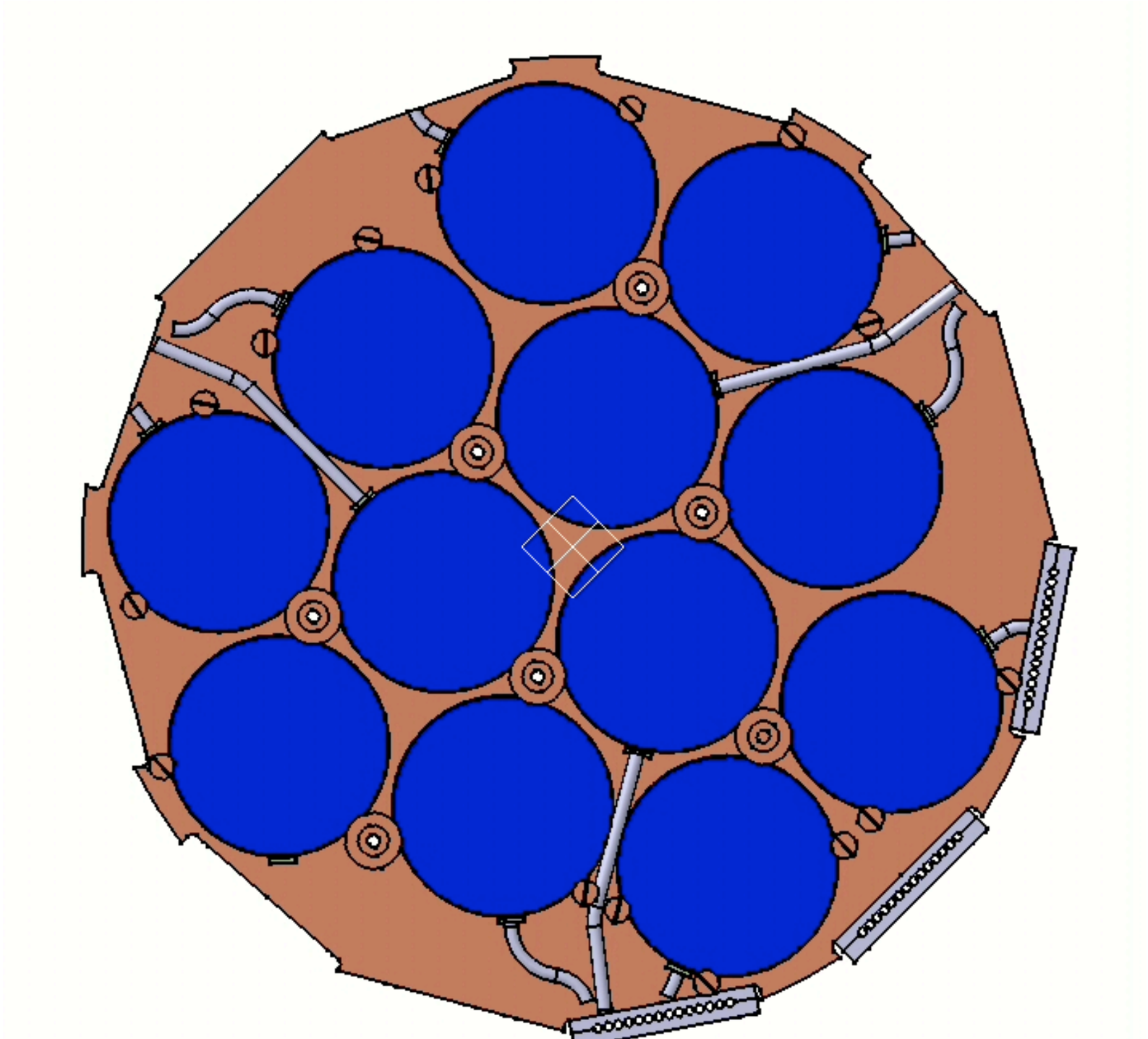

Full System View

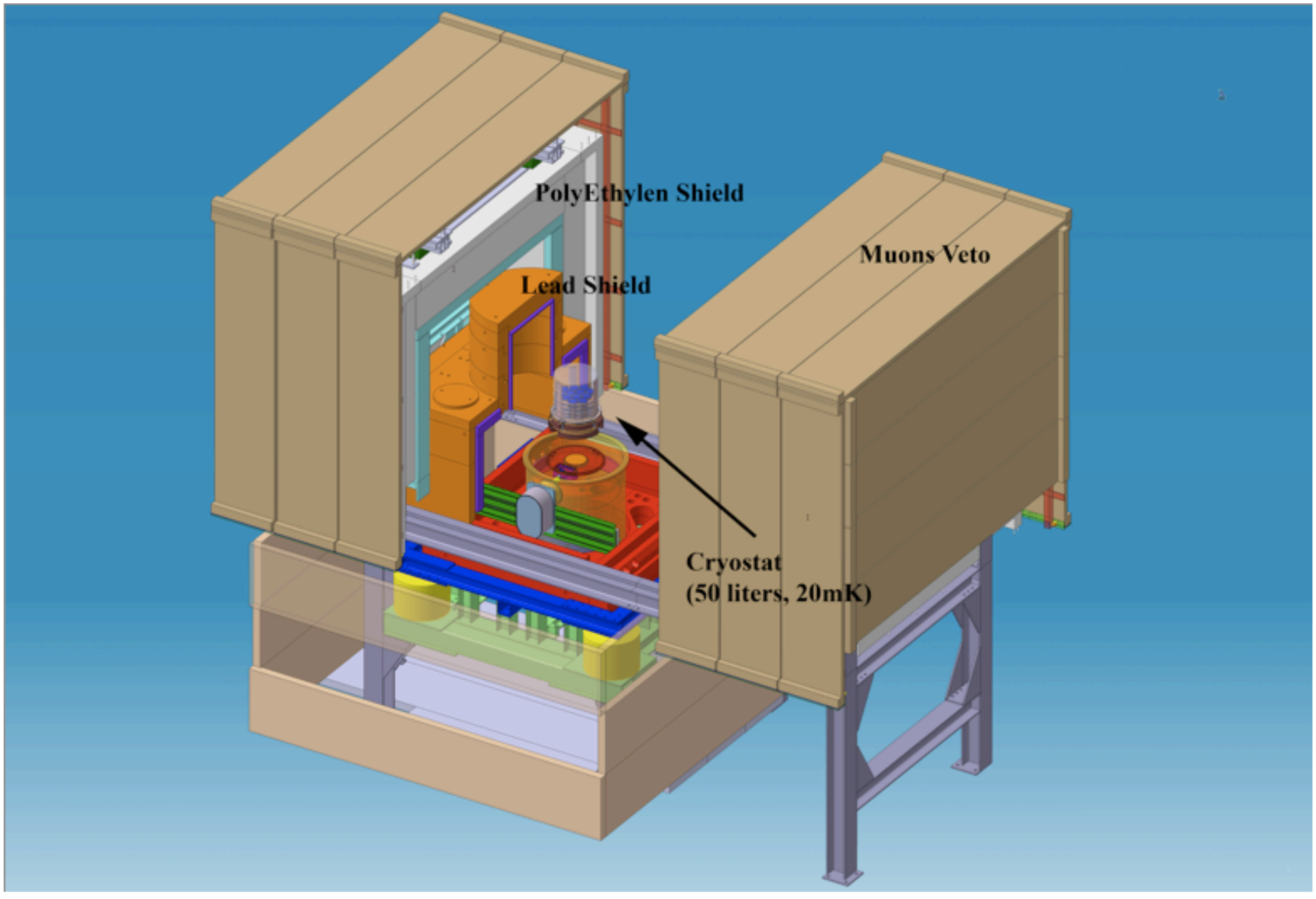

Edelweiss Results

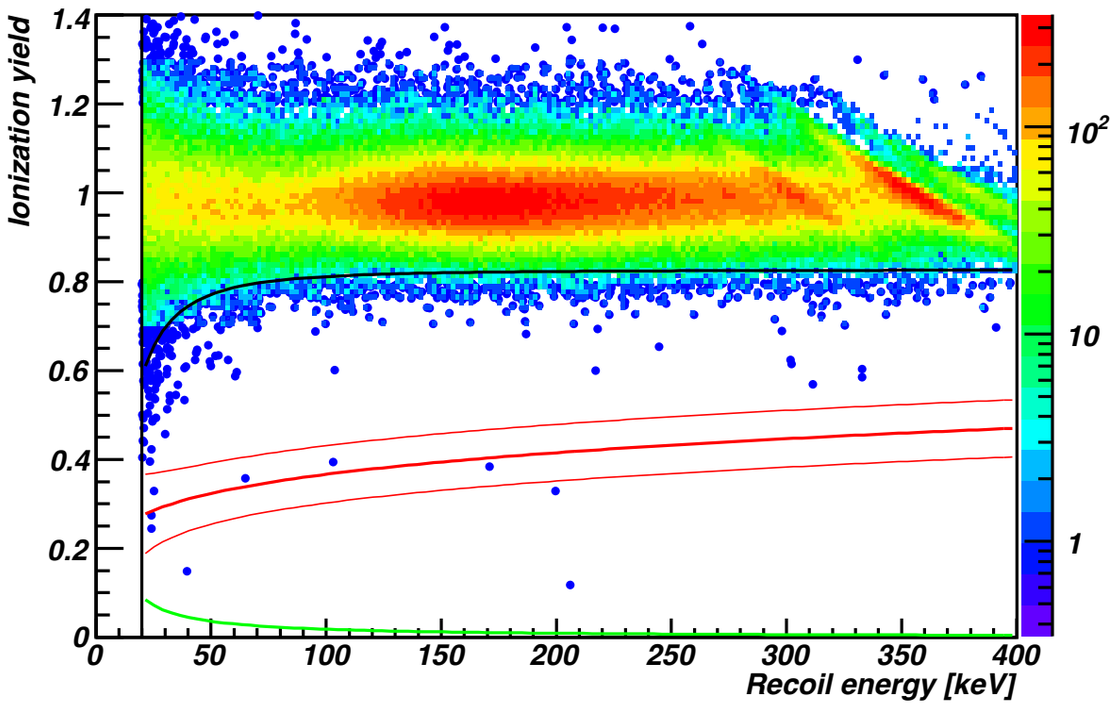

Figure 2: Distribution of the ionization yield versus recoil energy for fiducial events recorded by Ge-ID detectors during all γ-ray calibrations regularly performed with ^{133}Ba sources. The same period selection and quality cuts are applied than in WIMP search. The top line represents the 99.99% lower limit of the electron recoil band for typical noise conditions. The bottom (green) line is the typical ionization threshold, while the 90%CL nuclear recoil region is represented as a red band.

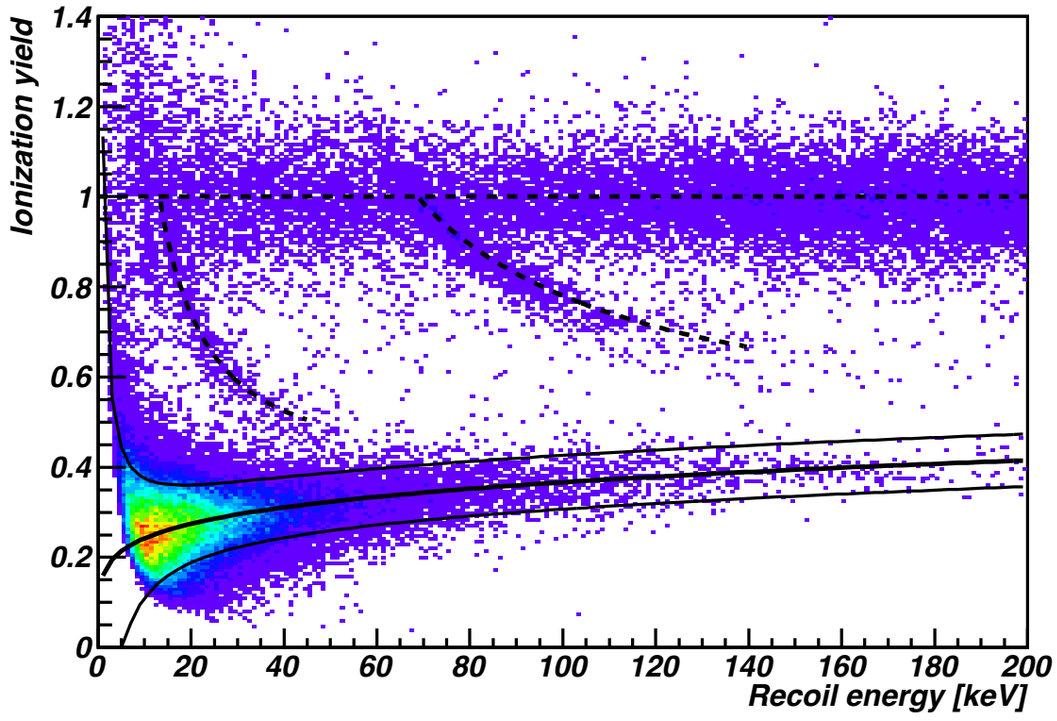

Figure 1: Distribution of the ionization yield versus recoil energy for fiducial events recorded during neutron calibrations for all Ge-ID detectors. The full lines represent the parametrization of Ref. [12] for nuclear recoils and the 90%CL nuclear recoil band. In addition to pure electron and nuclear recoils, inelastic nuclear recoils are visible with associated electromagnetic energies of 13.26 and 68.75 keV, due to the desexcitation of short-lived states of ^{73}Ge created by neutron diffusion (dashed lines).

Collaboration, E., Armengaud, E., Augier, C., Broniatowski, A., Brudanin, V., Censier, B., Chardin, G., et al. (2011, March 21). Final results of the EDELWEISS-II WIMP search using a 4-kg array of cryogenic germanium detectors with interleaved electrodes. *arXiv.org*. doi:10.1016/j.physletb.2011.07.034

WIMP Results

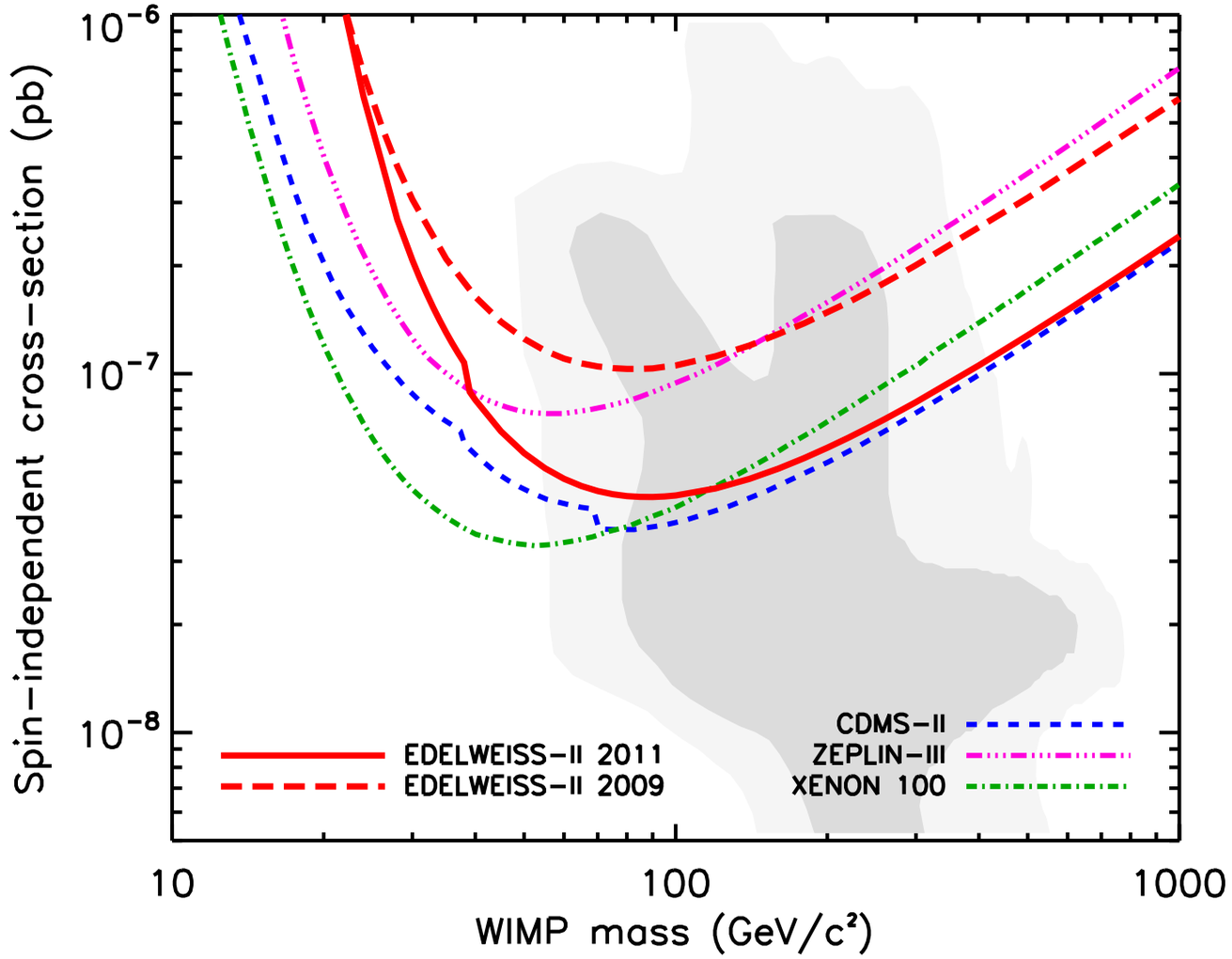

Figure 4: Limits on the cross-section for spin-independent scattering of WIMPs on the nucleon as a function of WIMP mass, derived from the present work, together with the limits from CDMS [19], ZEPLIN [26] and XENON100 [20]. The shaded area correspond to the 68% and 95% probability regions of the cMSSM scan from Ref. [25].

CRESST: Dark Matter Search

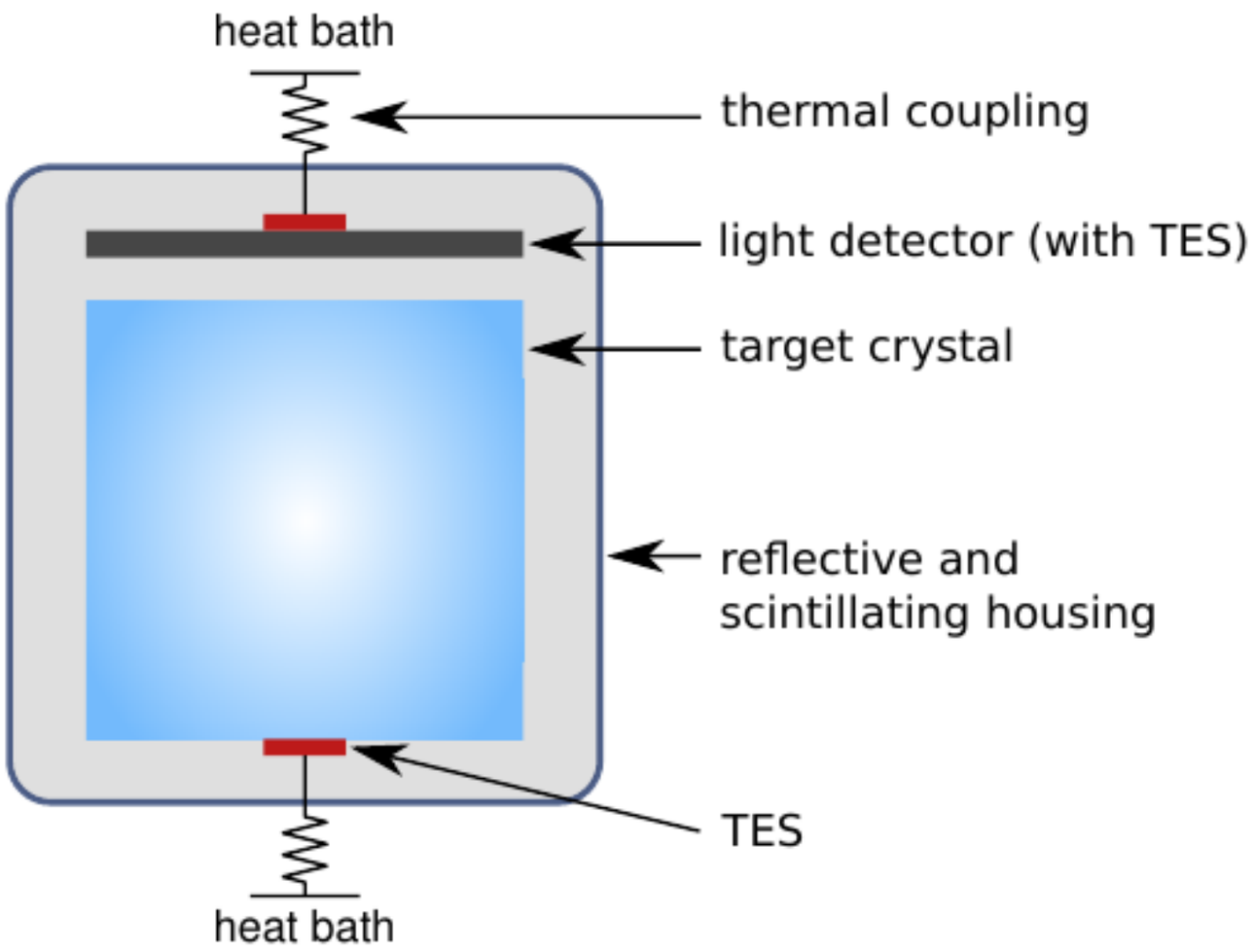

- A slightly different approach is taken here: a crystal that is not a semiconductor, but a scintillator is used as a cryogenic detector

- CRESST uses $CaWO_4$ as active medium

- This medium is transparent and scintillates

www.cresst.de

Detector principle

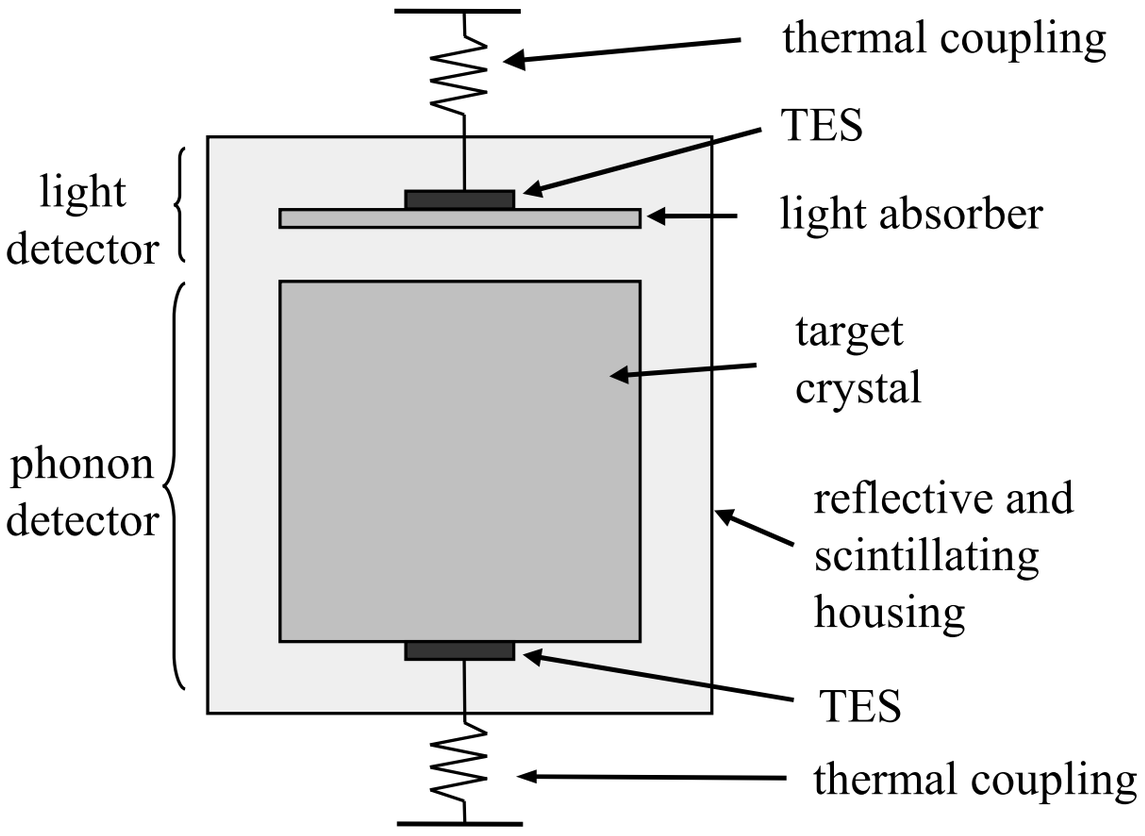

- Scintillation light is captured using a cryodetector. The light on that detector is read out by a thermometer.
- The phonon signal is measured by a thermometer on the detector crystal itself.

- In addition some the elements in contact with the crystal are scintillating to be able to determine the internal contamination. However the clamp holding the crystal was too radioactive in the previous setup.

Angloher, G., Bauer, M., Bavykina, I., Bento, A., Bucci, C., Ciemniak, C., Deuter, G., et al. (2011, September 4). Results from 730 kg days of the CRESST-II Dark Matter Search. *arXiv.org*.

Phase II Detector

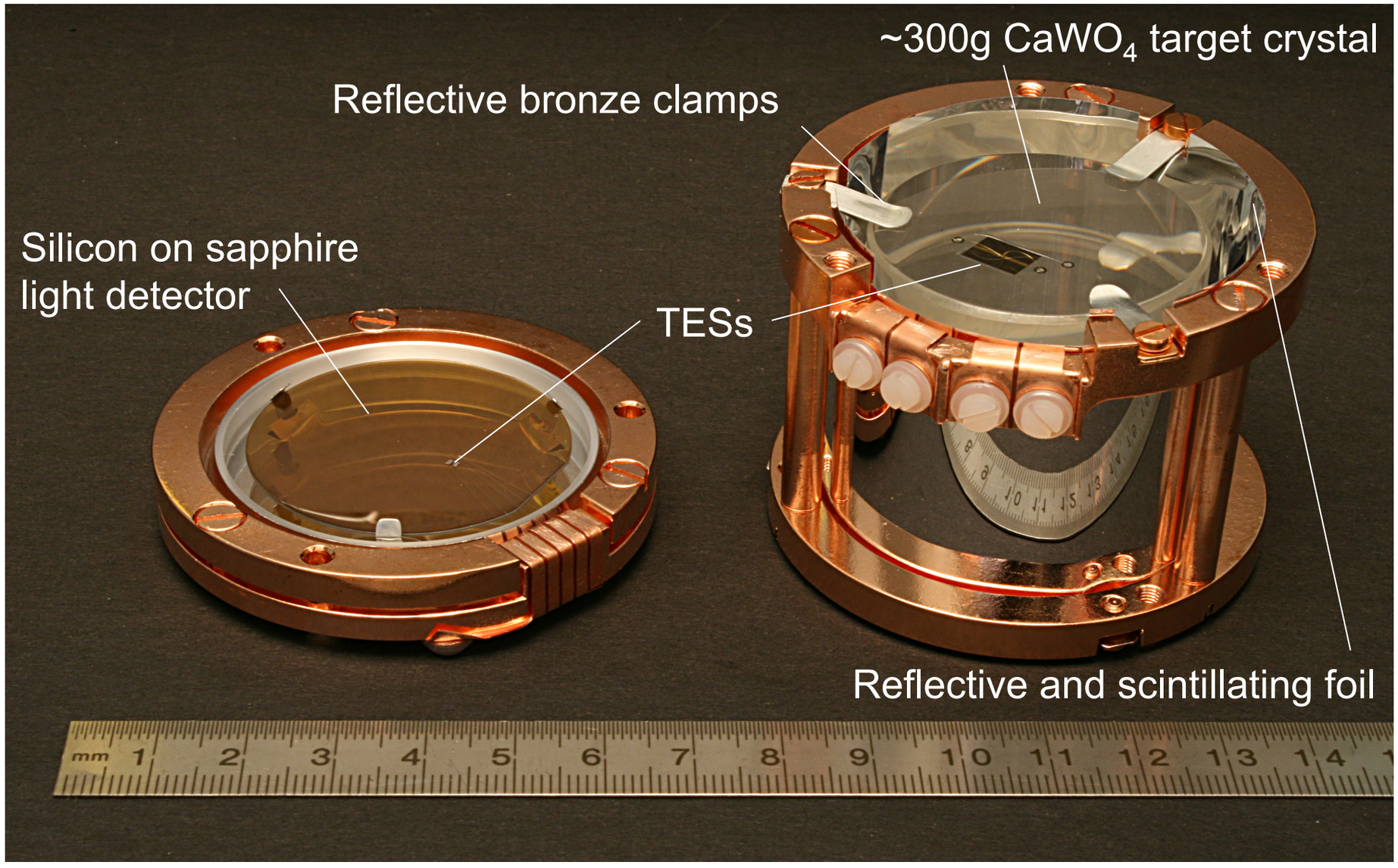

Phase III detector

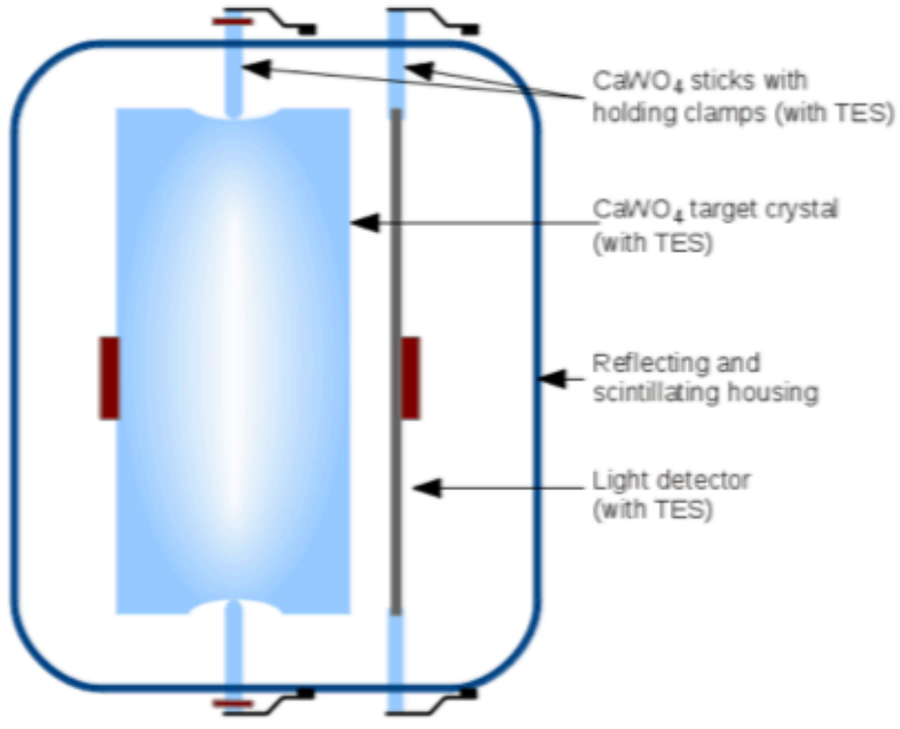

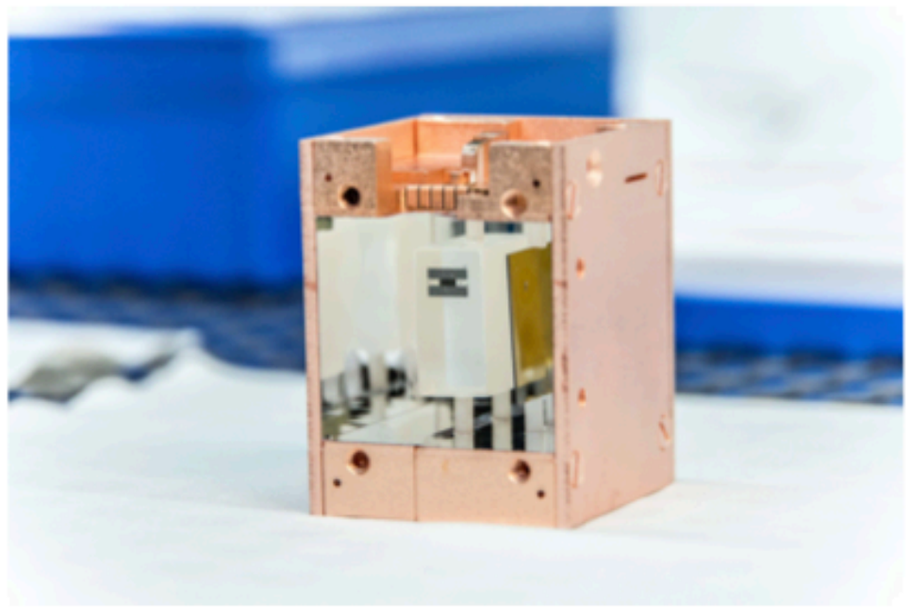

Figure 1. Left: Schematic view of the detector design for CRESST-III modules. Right: Open CRESST-III detector module during mounting in the Gran Sasso facility.

https://arxiv.org/pdf/1711.07692.pdf

CRESST System

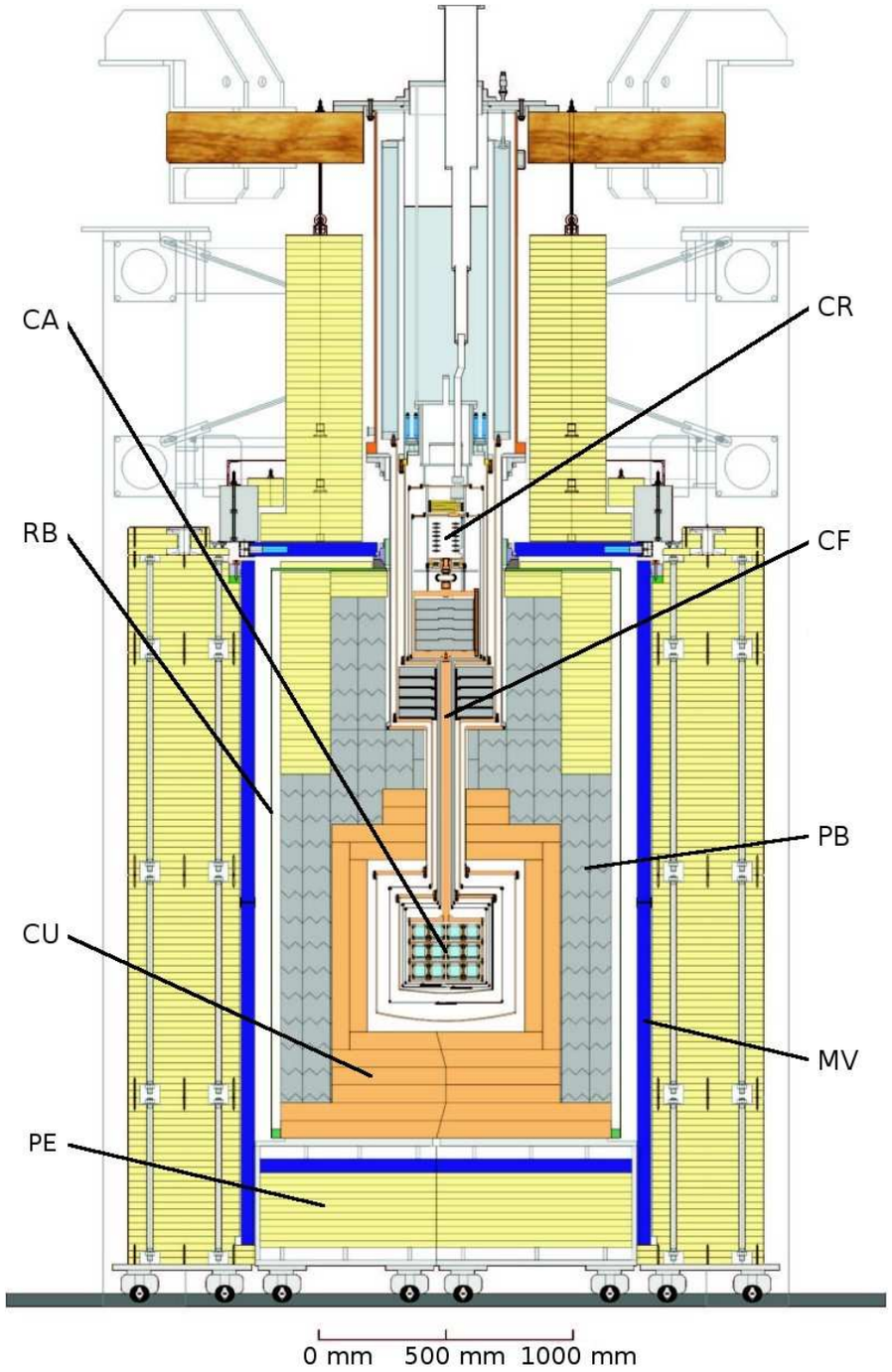

Fig. 4. Schematic drawing of the CRESST setup. A cold finger (CF) links the cryostat (CR) to the experimental volume, where the detectors are arranged in a common support structure, the so-called carousel (CA). This volume is surrounded by layers of shielding from copper (CU), lead (PB), and polyethylene (PE). The copper and lead shieldings are additionally enclosed in a radon box (RB). An active muon veto (MV) tags events which are induced by cosmic radiation.

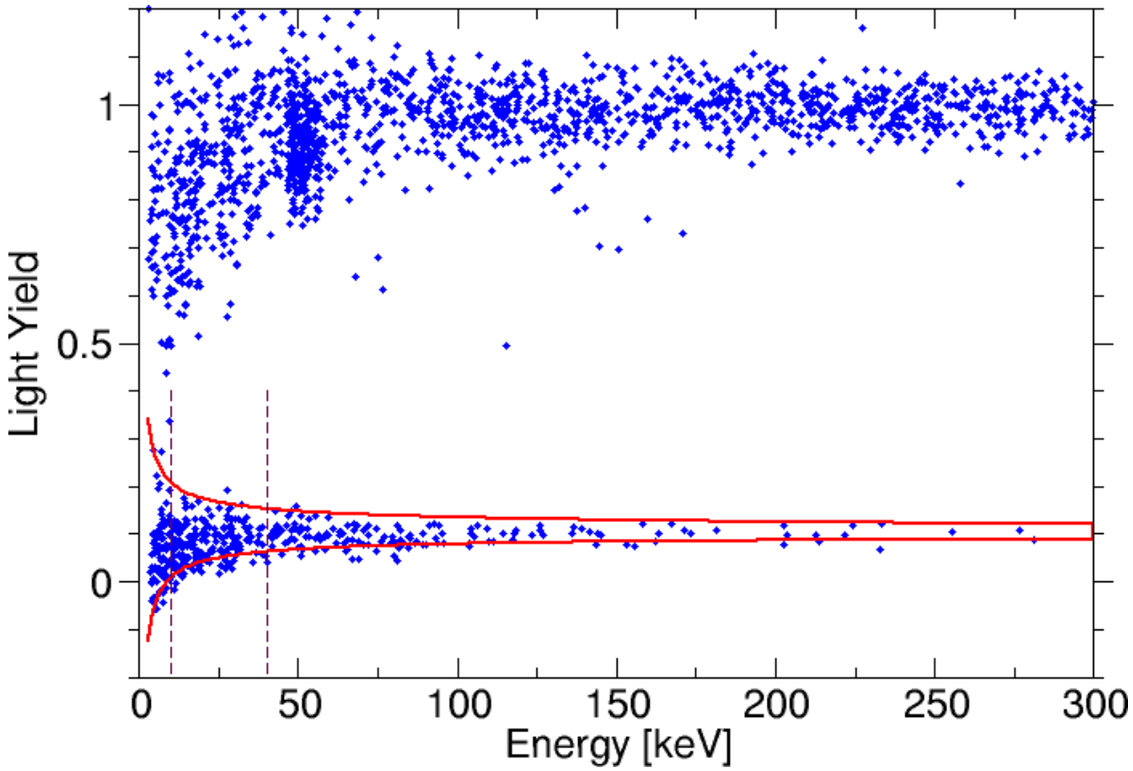

Fig. 5. Data obtained with one detector module in a calibration measurement with an AmBe neutron source, with the source placed outside the lead shielding. The solid red lines mark the boundary of the calculated oxygen recoil band (10 % of events are expected above the upper and 10 % below the lower boundary). The vertical dashed lines indicate the lower and upper energy bounds of the WIMP acceptance region as will be introduced in Section 3.

Cresst III Results

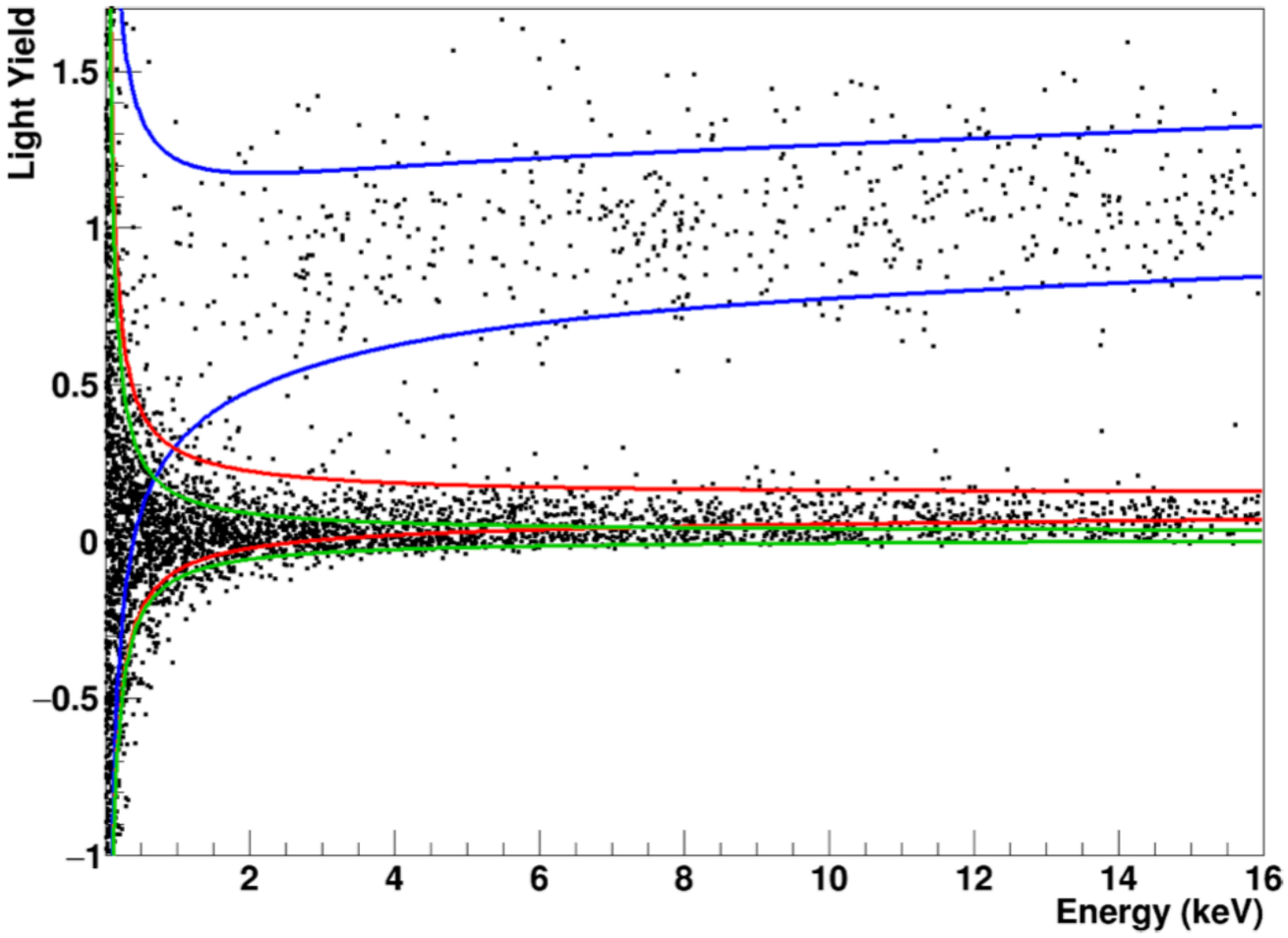

FIG. 3. Neutron calibration data for detector A in the light yield versus energy plane. We fit these data to determine the bands for β/γ-events (blue), nuclear recoils off oxygen (red) and tungsten (green), where the respective lines correspond to the upper and lower 90 % boundaries of the respective band. The band description follows [12].

- Neutron calibration data

https://arxiv.org/pdf/1904.00498.pdf

CRESST III results

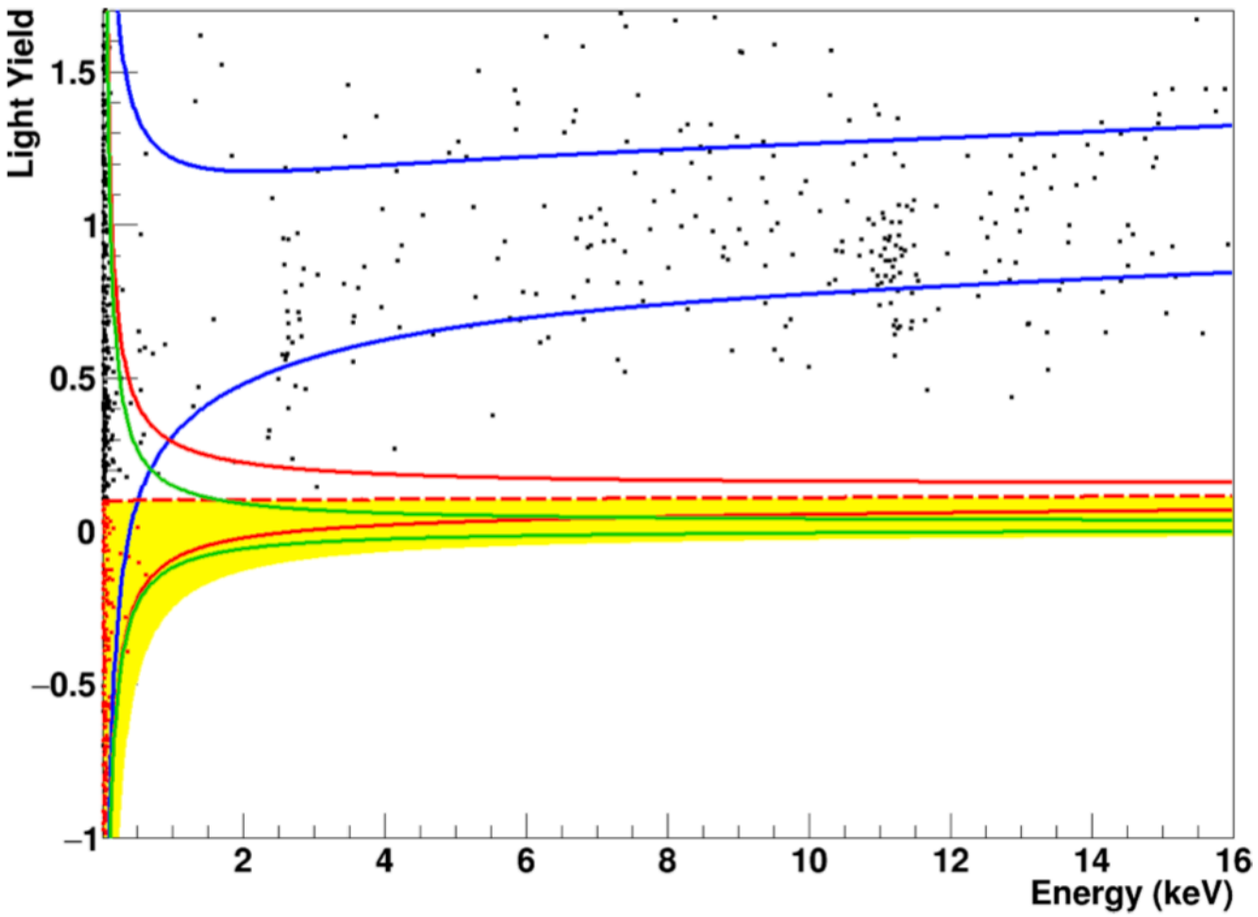

FIG. 5. Light yield versus energy of events in the dark matter dataset, after selection criteria are applied (see section IV 4). The blue band indicates the 90 % upper and lower boundaries of the β/γ-band, red and green the same for oxygen and tungsten, respectively. The yellow area denotes the acceptance region reaching from the mean of the oxygen band (red dashed line) down to the 99.5 % lower boundary of the tungsten band. Events in the acceptance region are highlighted in red. The position of the bands is extracted from the neutron calibration data as shown in figure 3.

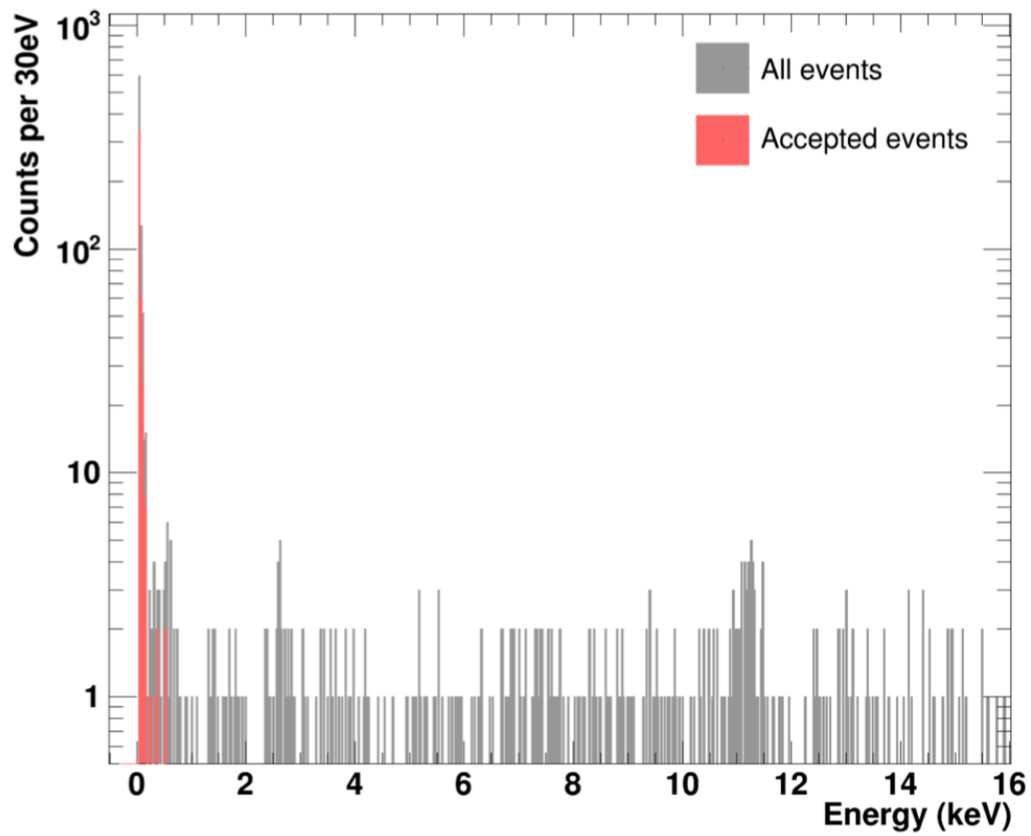

FIG. 6. Energy spectrum of the dark matter dataset with lines visible at 2.6 keV and 11.27 keV originating from cosmogenic activation of ^{182}W [11]. Gray: all events, red: events in the acceptance region (see figure 5).

https://arxiv.org/pdf/1904.00498.pdf

CRESST III Exclusion Limits

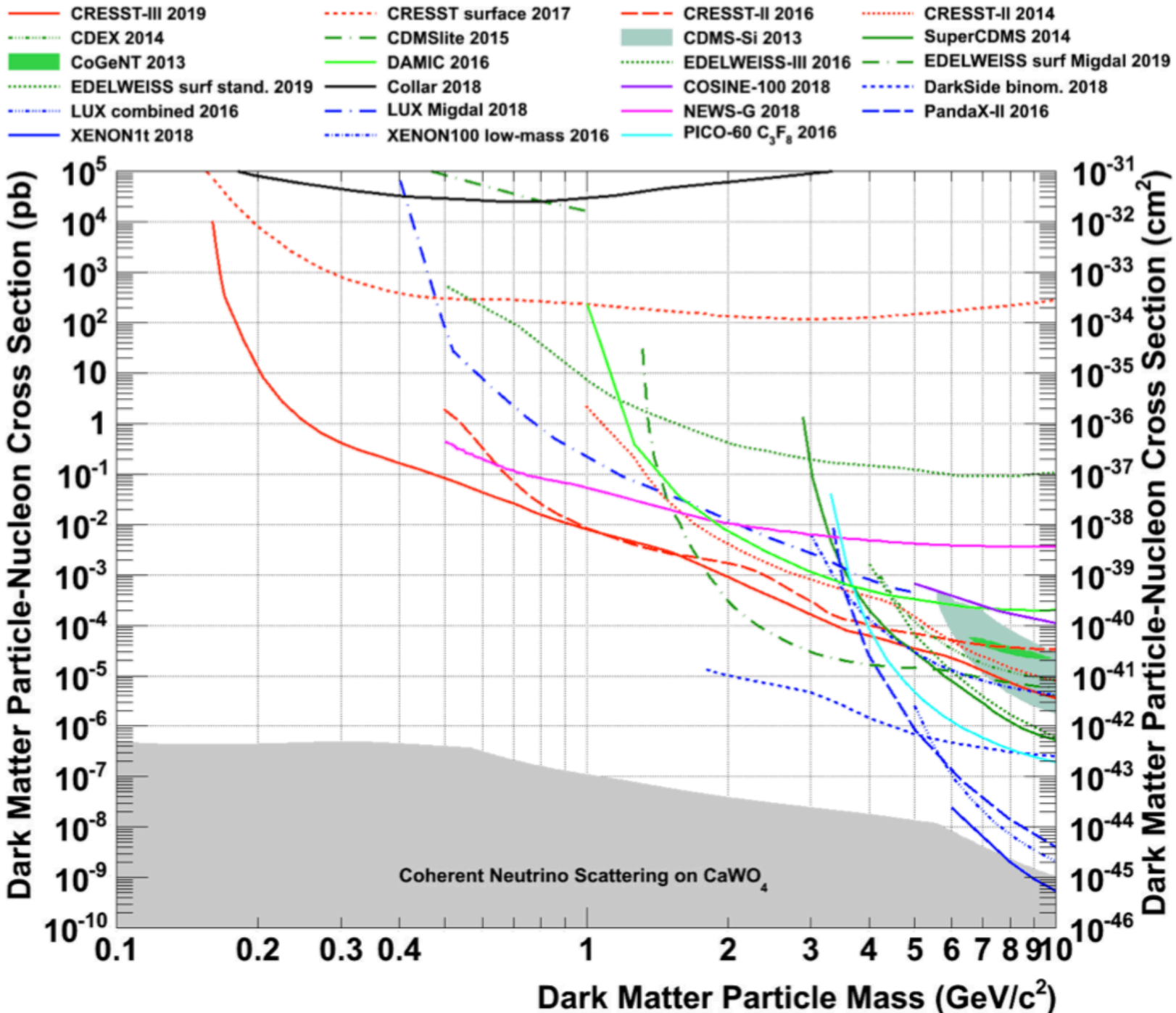

https://arxiv.org/pdf/1904.00498.pdf

Liquid Noble DM Searches

- Argon and xenon are ideal targets for large scale dark matter searches:
    - High scintillation light yield
    - Great transparency for scintillation light
    - Low intrinsic backgrounds (xenon), purification possible (to remove Kr, Rn, Ar)
    - Pulse shape discrimination possible (argon) to suppress electron recoil events
- CHEAP (when compared to bolometric detectors)

Detector Types

- For argon, TPC type detectors and single phase argon detectors have been used

- For xenon TPC type detectors are now leading the world in sensitivity (and have for many years)

- Argon: ArDM, DEAP, DarkSide

- Xenon: Lux, Xenon xT, LZ, Panda-X

Xenon TPC

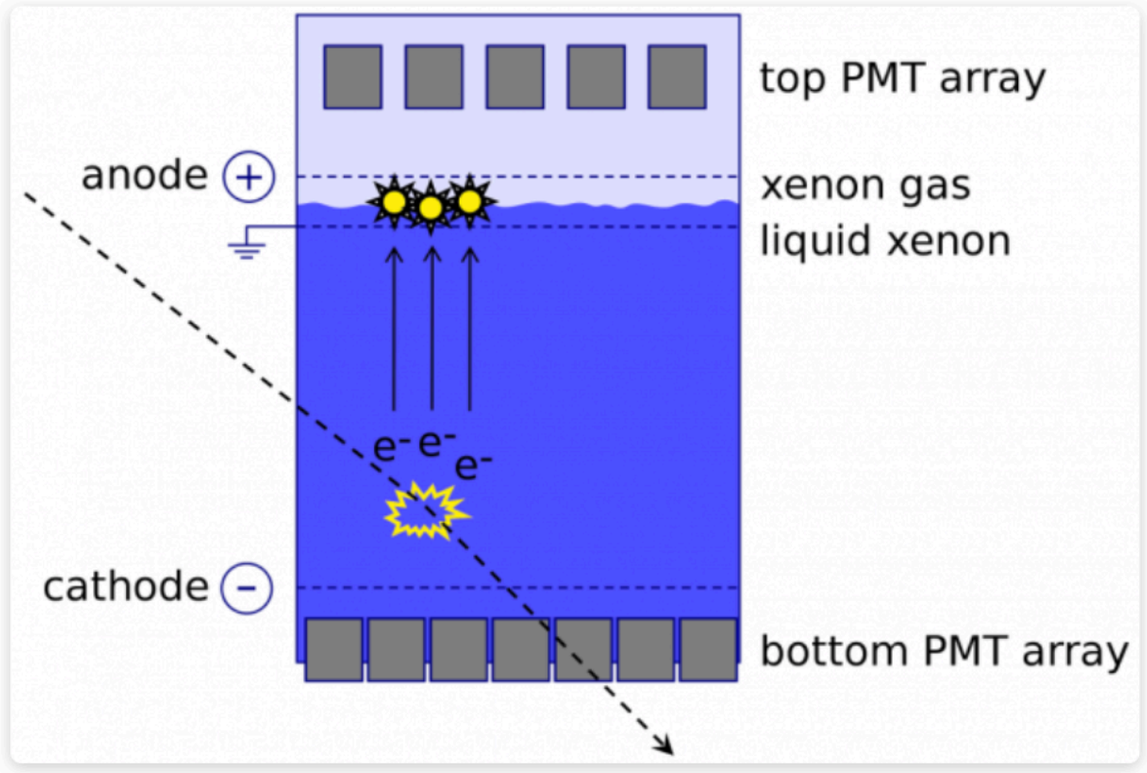

Schema of the XENON experiment: any particle interaction in the liquid xenon (blue) yields two signals: a prompt flash of light, and a delayed charge signal. Together, these two signals give away the energy and position of the interaction as well as the type of the interacting particle. (Schema: The XENON collaboration/Rafael Lang)

DANIEL
Tyvek

Xenon 1T Results

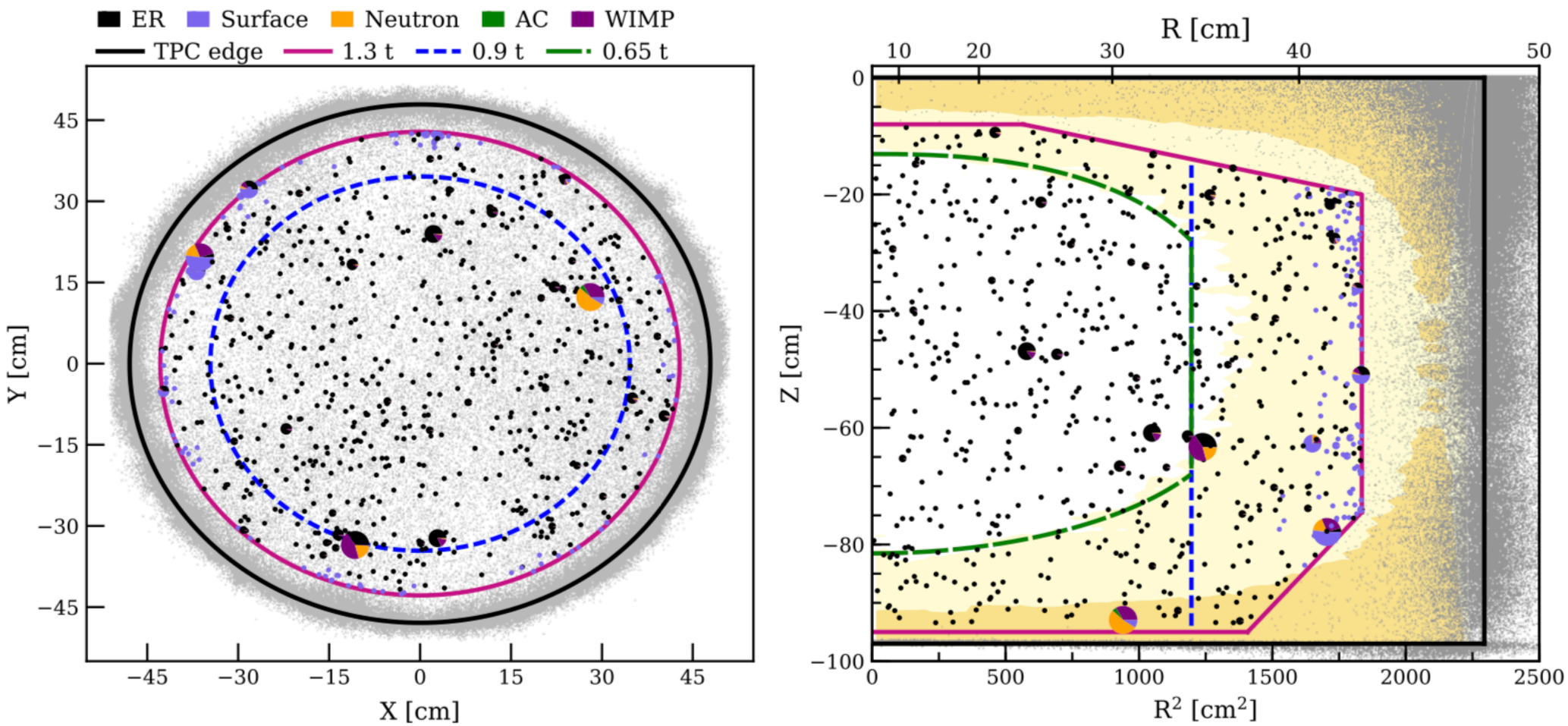

FIG. 2. Spatial distributions of DM search data. Events that pass all selection criteria and are within the fiducial mass are drawn as pie charts representing the relative probabilities of the background and signal components for each event under the best-fit model (assuming a 200 GeV/c^2 WIMP and a resulting best-fit $\sigma_{\mathrm{SI}} = 4.7 \times 10^{-47}$ cm^2) with the color code given in the legend. Small charts (mainly single-colored) correspond to unambiguously background-like events, while events with larger WIMP probability are drawn progressively larger. Gray points are events reconstructed outside the fiducial mass. The TPC boundary (black line), the 1.3 tons fiducial mass (magenta), the maximum radius of the reference 0.9 ton mass (blue dashed), and the 0.65 ton core mass (green dashed) are shown. Yellow shaded regions display the 1σ (dark) and 2σ (light) probability density percentiles of the radiogenic neutron background component for SR1.

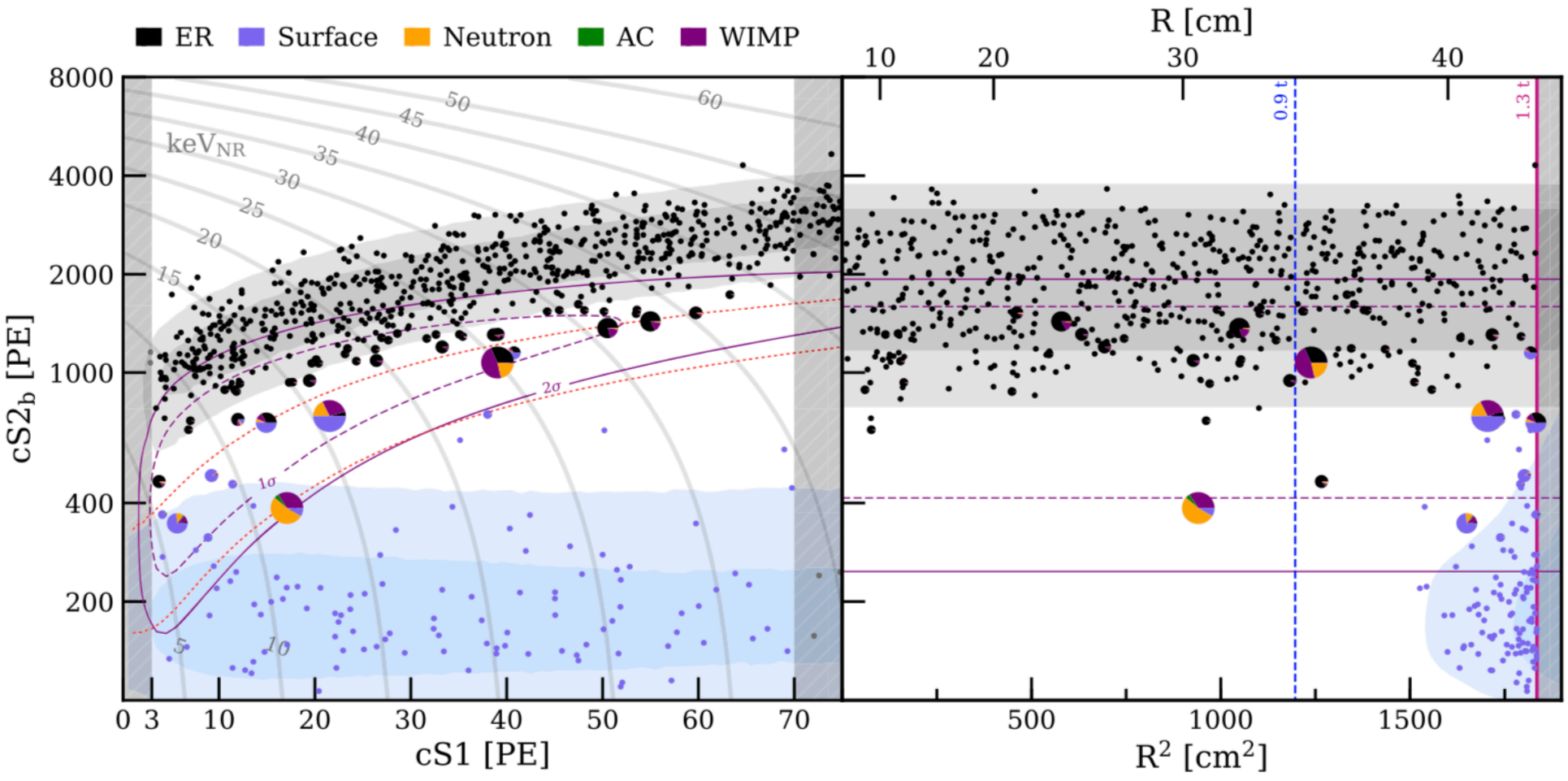

FIG. 3. DM search data in the 1.3 tons fiducial mass distributed in the (c$S1$, c$S2_b$) (left) and (R^2, c$S2_b$) (right) parameter spaces with the same marker descriptions as in Fig. 2. Shaded regions are similar to Fig. 2, showing the projections in each space of the surface (blue) and ER (gray) background components for SR1. The 1σ (purple dashed) and 2σ (purple solid) percentiles of a 200 GeV/c^2 WIMP signal are overlaid for reference. Vertical shaded regions are outside the ROI. The NR signal reference region (left, between the two red dotted lines) and the maximum radii (right) of the 0.9 ton (blue dashed) and 1.3 tons (magenta solid) masses are shown. Gray lines show isoenergy contours in NR energy.

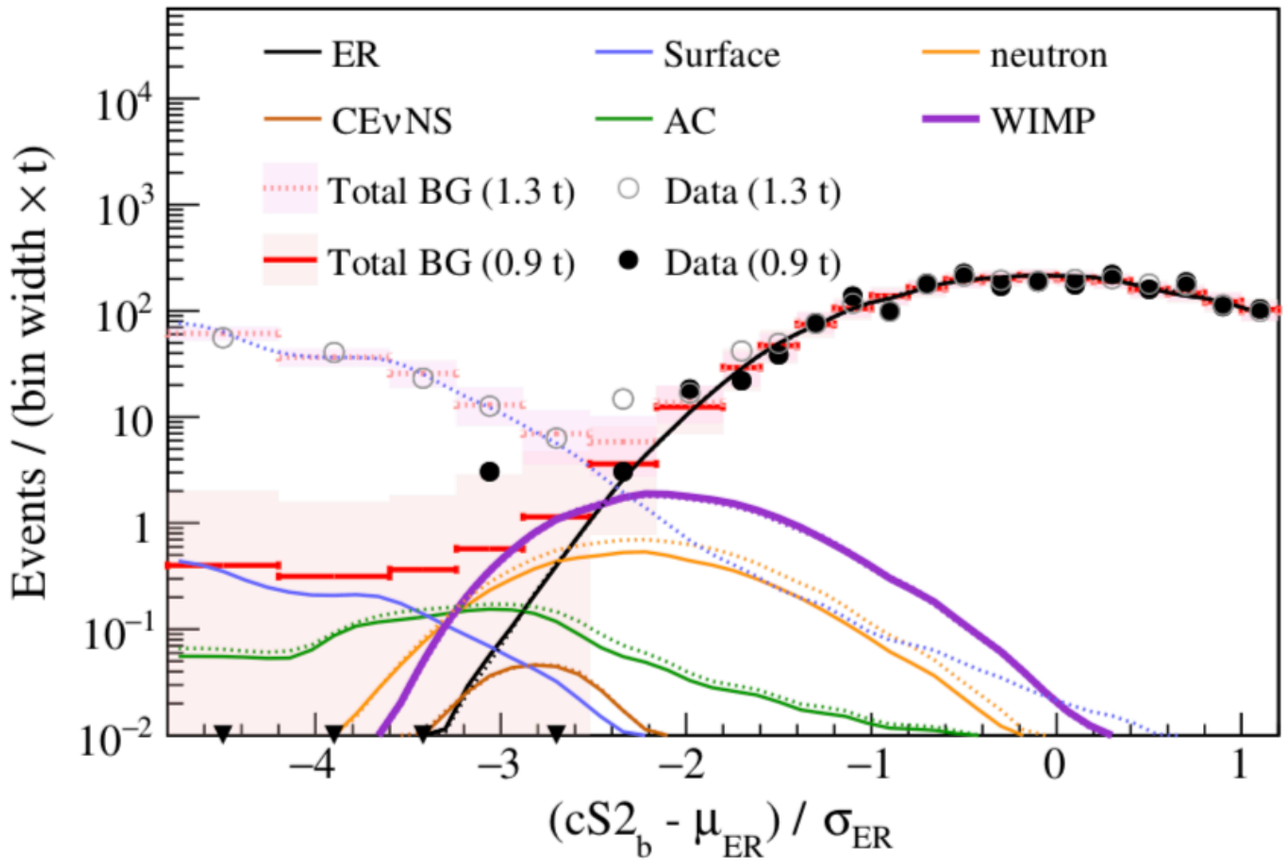

FIG. 4. Background and 200 GeV/c^2 WIMP signal best-fit predictions, assuming $\sigma_{SI} = 4.7 \times 10^{-47}$ cm^2, compared to DM search data in the 0.9 ton (solid lines and markers) and 1.3 tons (dotted lines and hollow markers) masses. The horizontal axis is the projection along the ER mean (μ_{ER}), shown in Fig. 3, normalized to the ER 1σ quantile (σ_{ER}). Shaded bands indicate the 68% Poisson probability region for the total BG expectations.

Xenon 1T Exclusion Plot

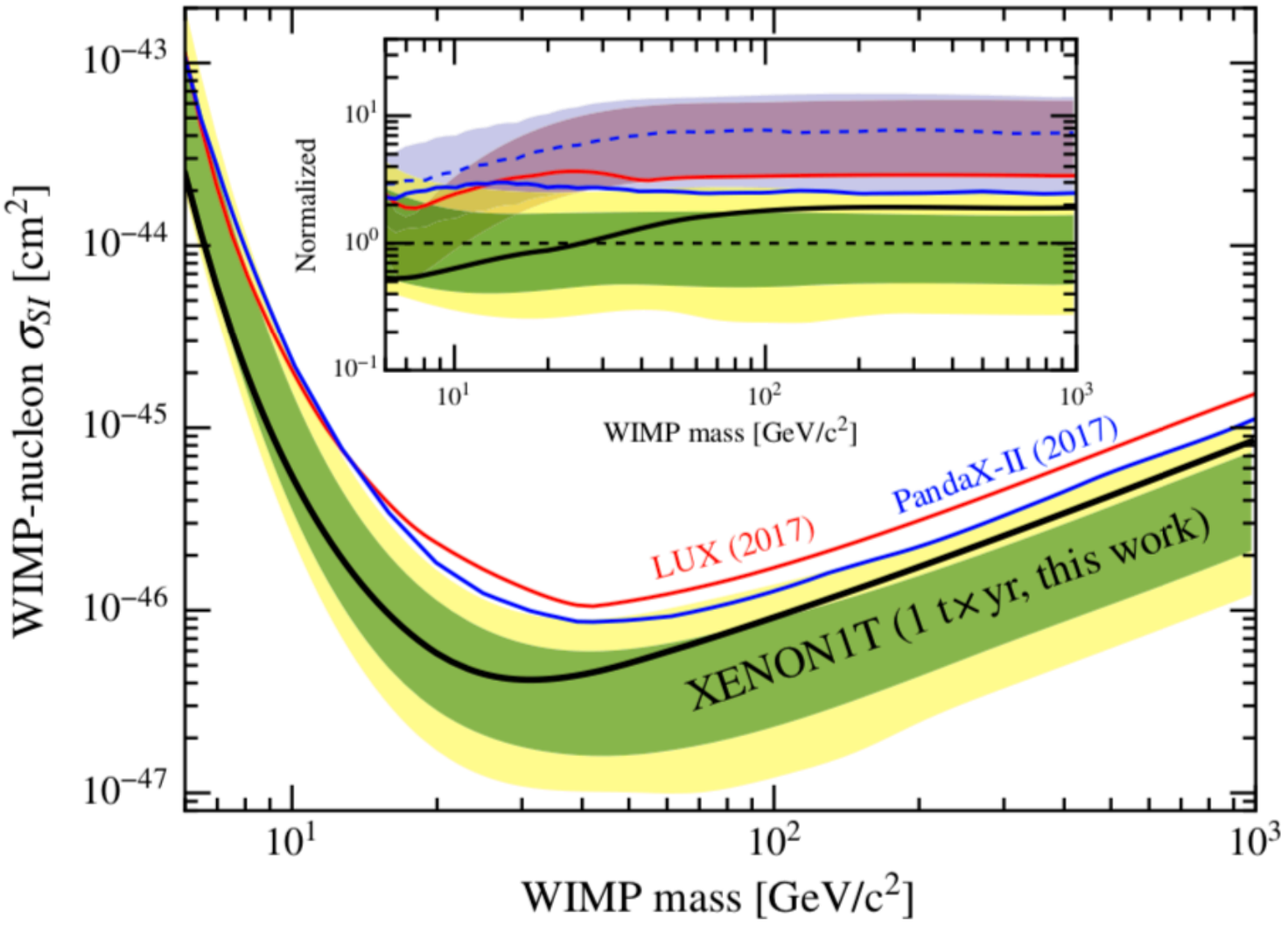

FIG. 5. 90% confidence level upper limit on σ_{SI} from this work (thick black line) with the 1σ (green) and 2σ (yellow) sensitivity bands. Previous results from LUX [6] and PandaX-II [7] are shown for comparison. The inset shows these limits and corresponding $\pm 1\sigma$ bands normalized to the median of this work's sensitivity band. The normalized median of the PandaX-II

DEAP 3600

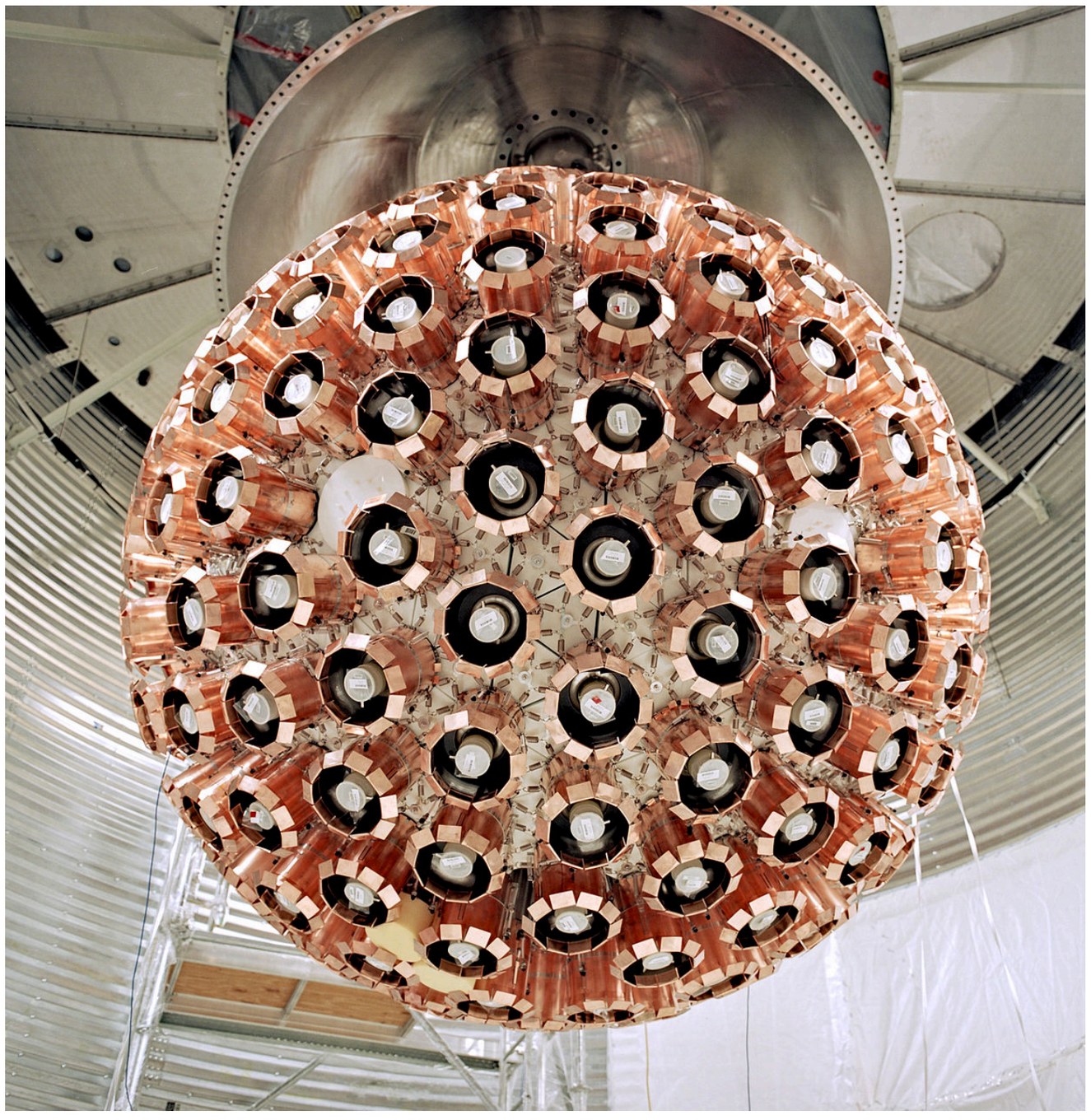

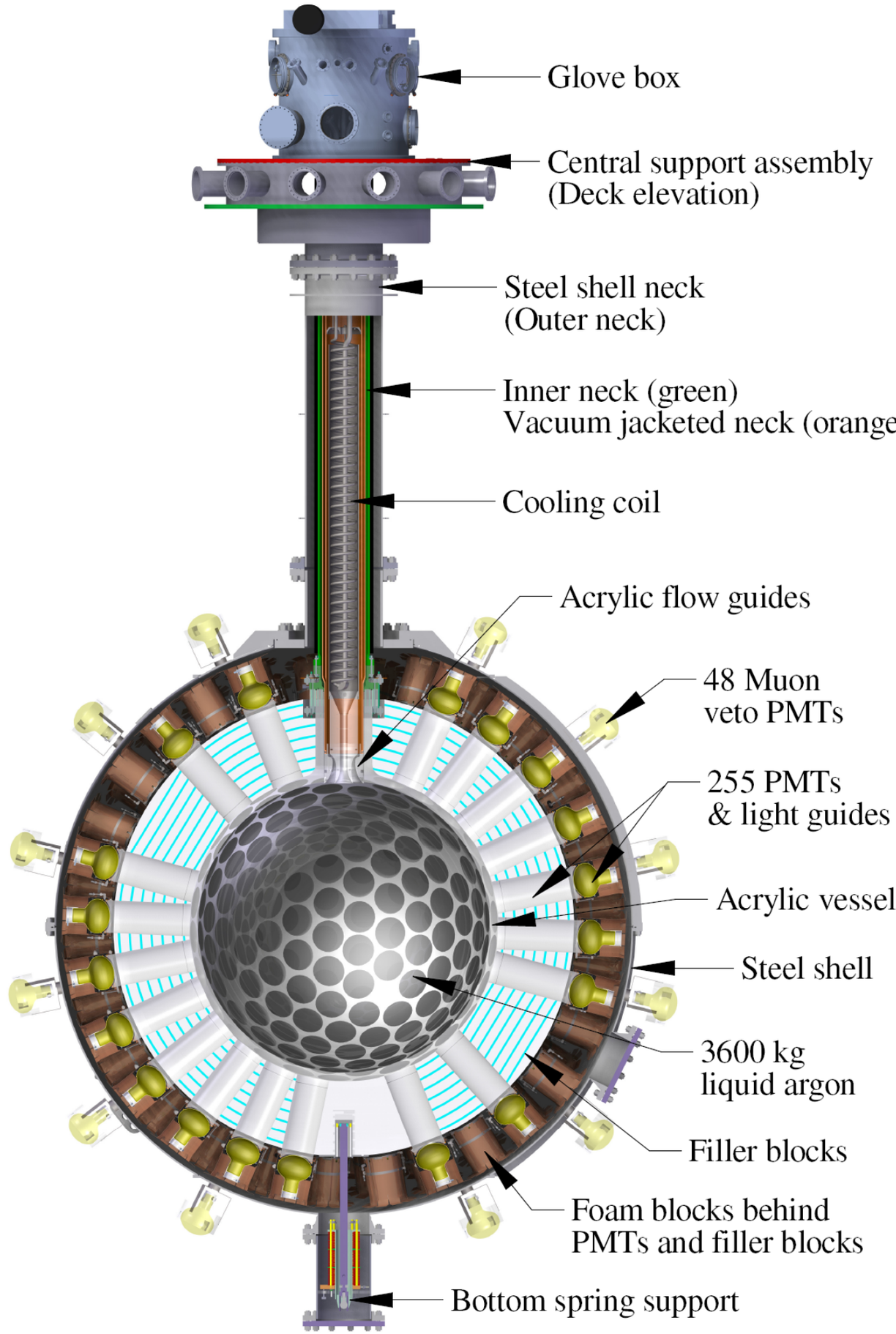

SOLID EDGE ACADEMIC COPY

Pulse Shape Discrimination

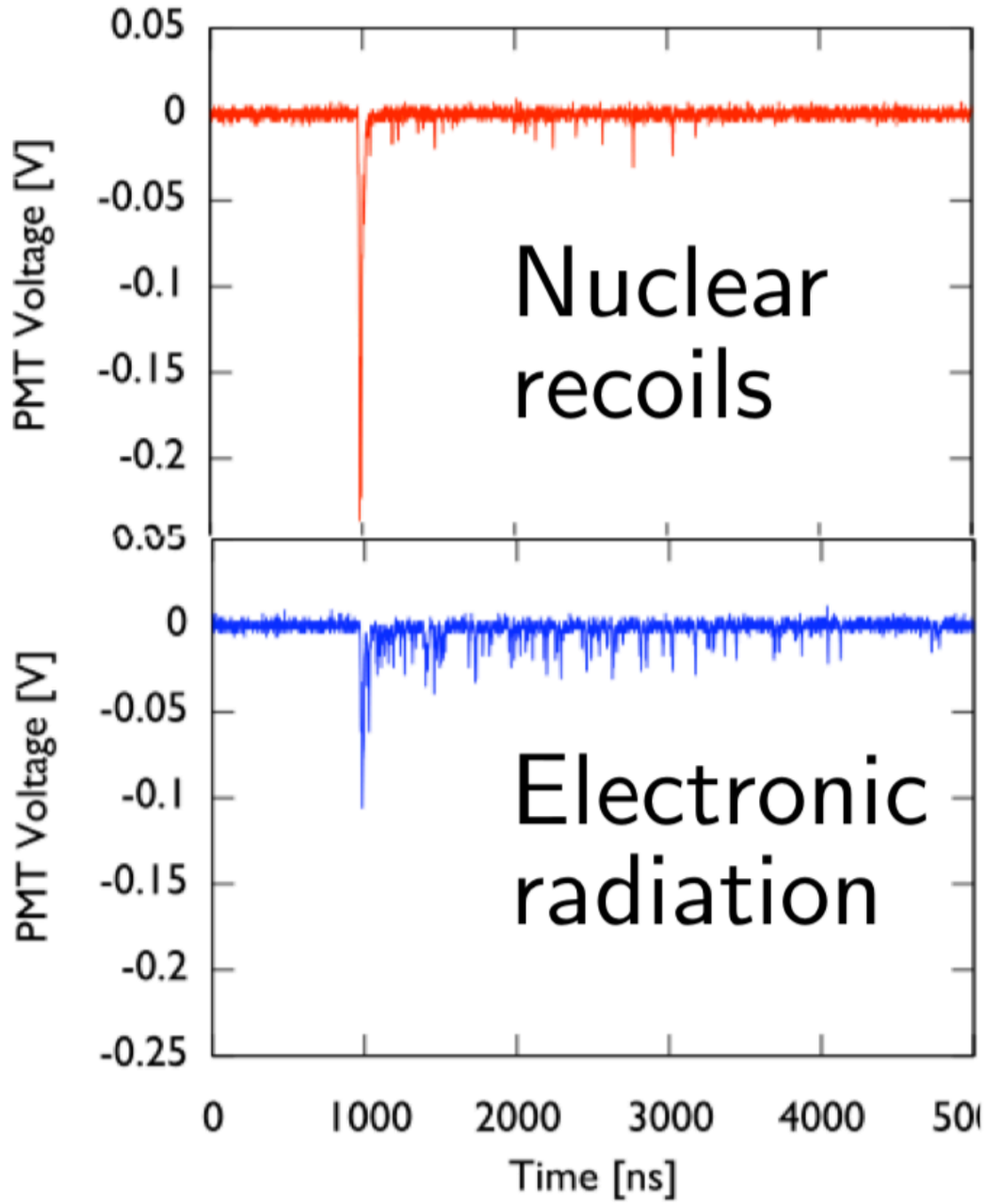

$$\frac{\text{Singlets}}{\text{Triplets}} = 3$$

$$\frac{\text{Singlets}}{\text{Triplets}} = 0.3$$

http://deap3600.ca/Contents/presentations/DEAP-3600TAUP2015Beltran.pdf

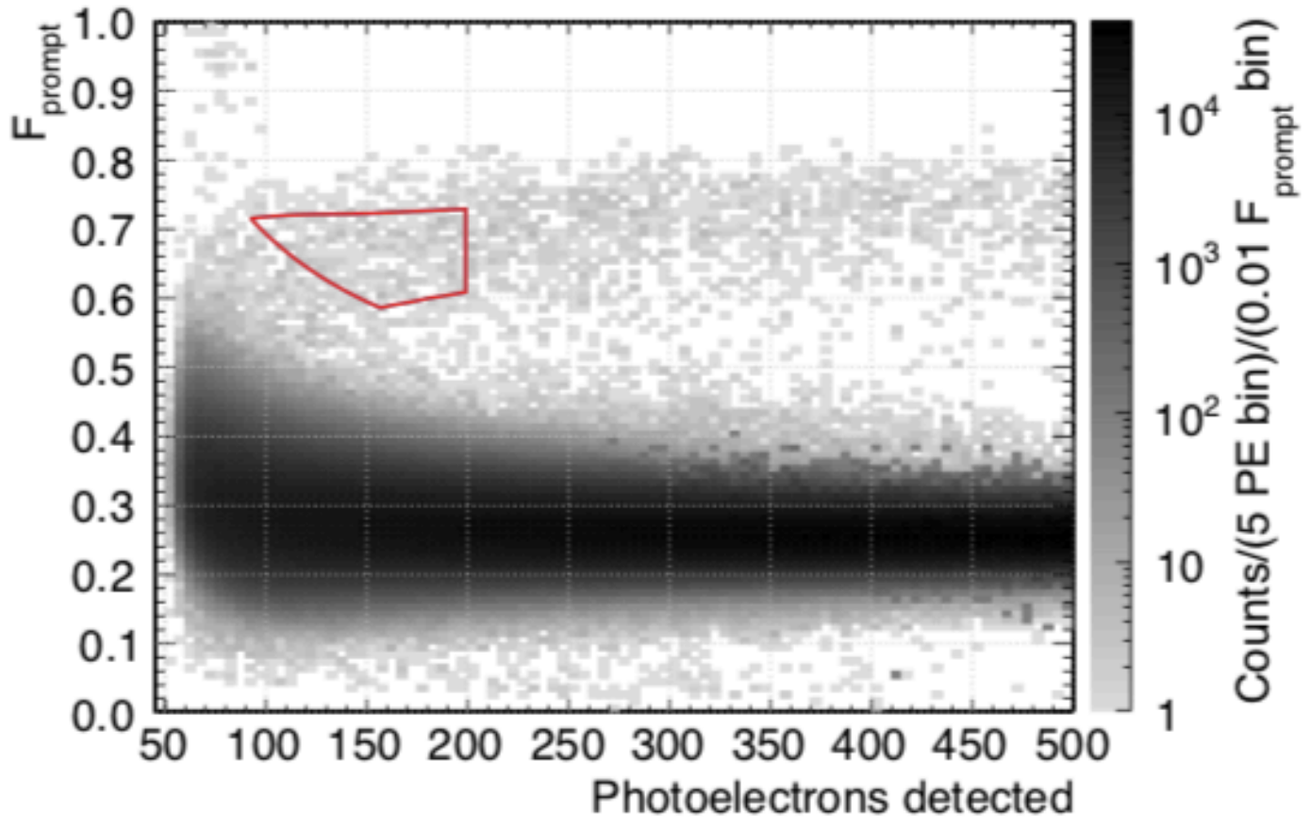

FIG. 8. F_{prompt} vs. PE distribution for data taken with an AmBe neutron source near the equator of the stainless steel shell. The WIMP-search ROI is shown in red. Separation can be seen between the NR band ($F_{prompt}\sim0.7$) and ER band ($F_{prompt}\sim0.3$). Events in the prescaled region (ER band with PE$\gtrsim$300) are weighted with a correction factor of 100, corresponding to the prescale factor. Note that multiple neutron scatters and pileup with Cherenkov and ER signals bias the NR spectrum away from the expected distribution for pure single-scatter NRs and populate the region between both bands.

https://arxiv.org/abs/1902.04048

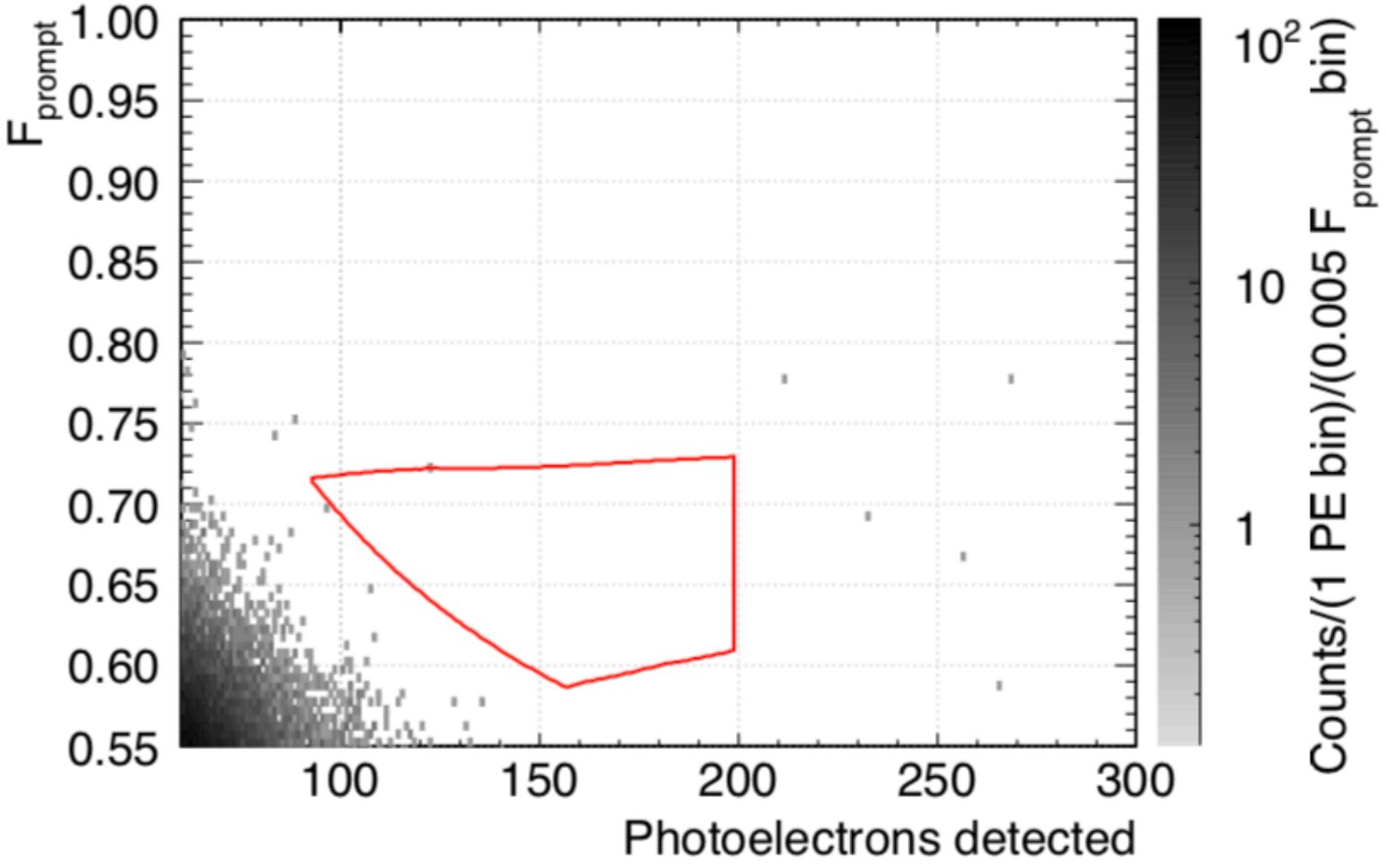

FIG. 22. Observed F_{prompt} vs. PE distribution after all cuts. The region of interest is shown in red.

- Omitting a very complex analysis that took years to put together to remove events from Cherenkov radiation in the acrylic and events from the neck region

https://arxiv.org/abs/1902.04048

DEAP 3600 Exclusion Plot

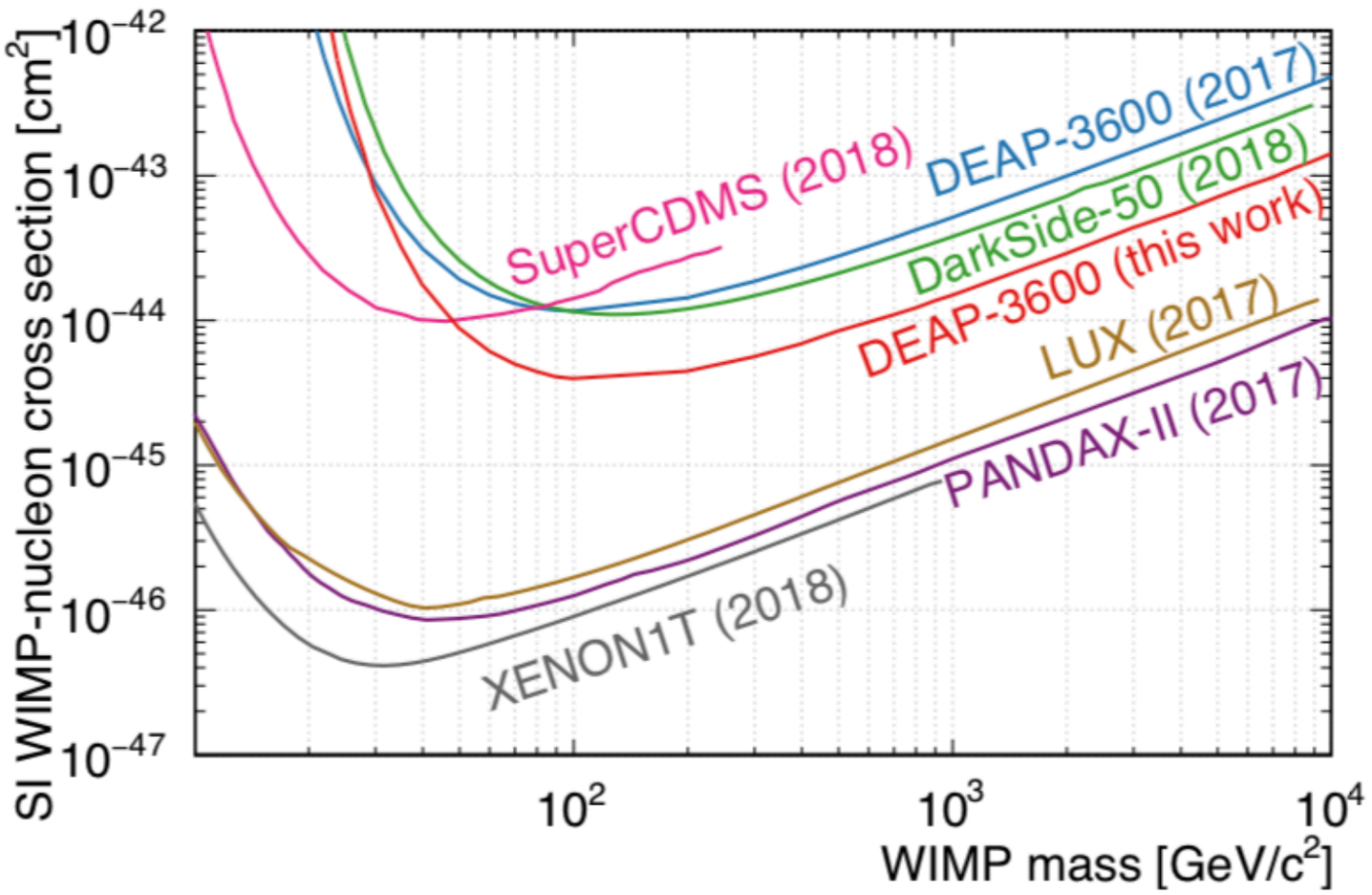

FIG. 24. 90% confidence upper limit on the spin-independent WIMP-nucleon cross sections based on the analysis presented in this paper (blue), compared to other published limits, including our previous limit [6], SuperCDMS [45], DarkSide-50 [7], LUX [46], PANDAX-II [47], and XENON1T [5].

https://arxiv.org/abs/1902.04048

SuperCDMS lite

- The Neganov-Trofimov-Luke (NTL) effect uses a higher bias voltage across a germanium detector to induce secondary electron-hole pair creation in the detector (analogous to gas amplification in a proportional counter)

- This effect allows to operate the detector as lower thresholds, while loosing the recoil discrimination

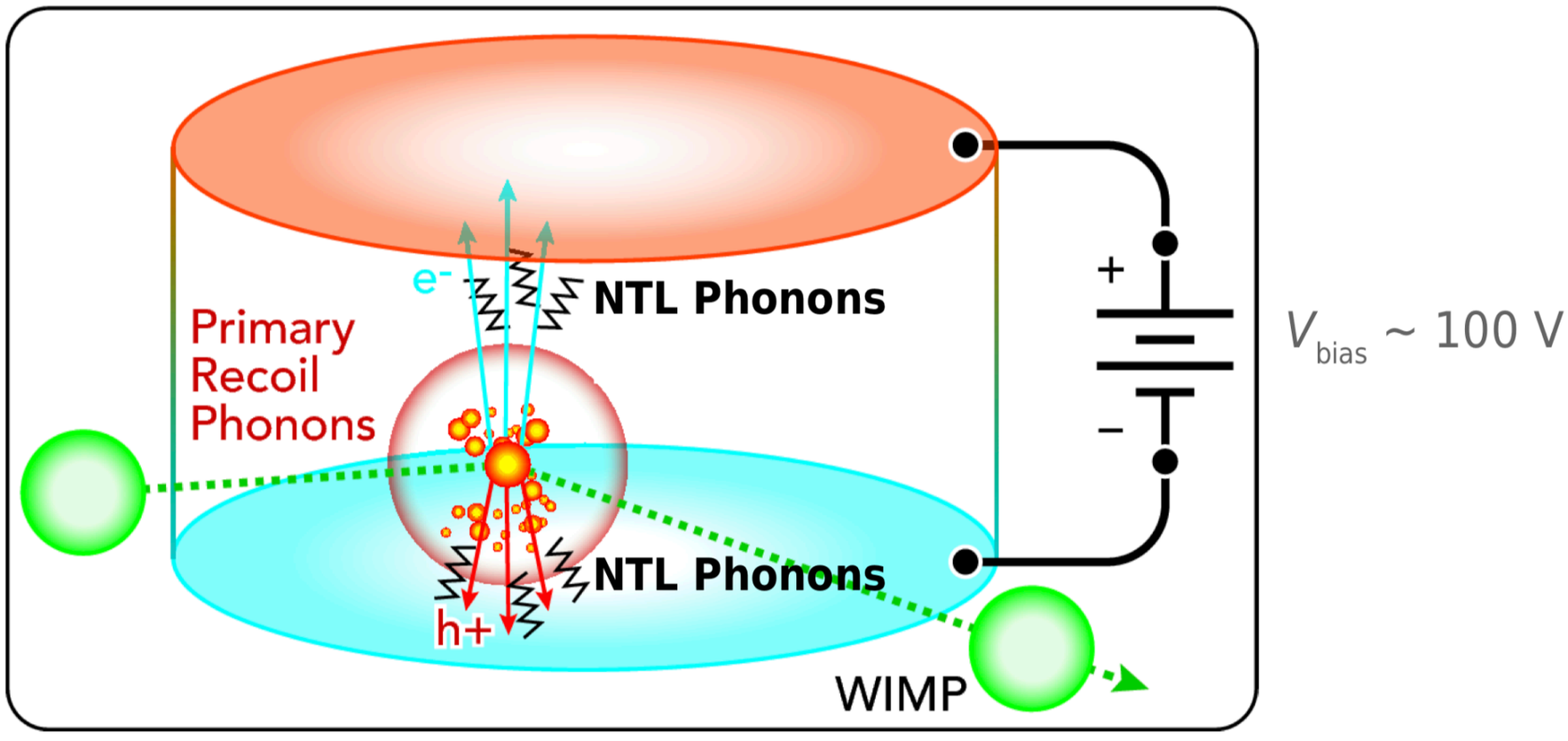

SuperCDMS Lite Result

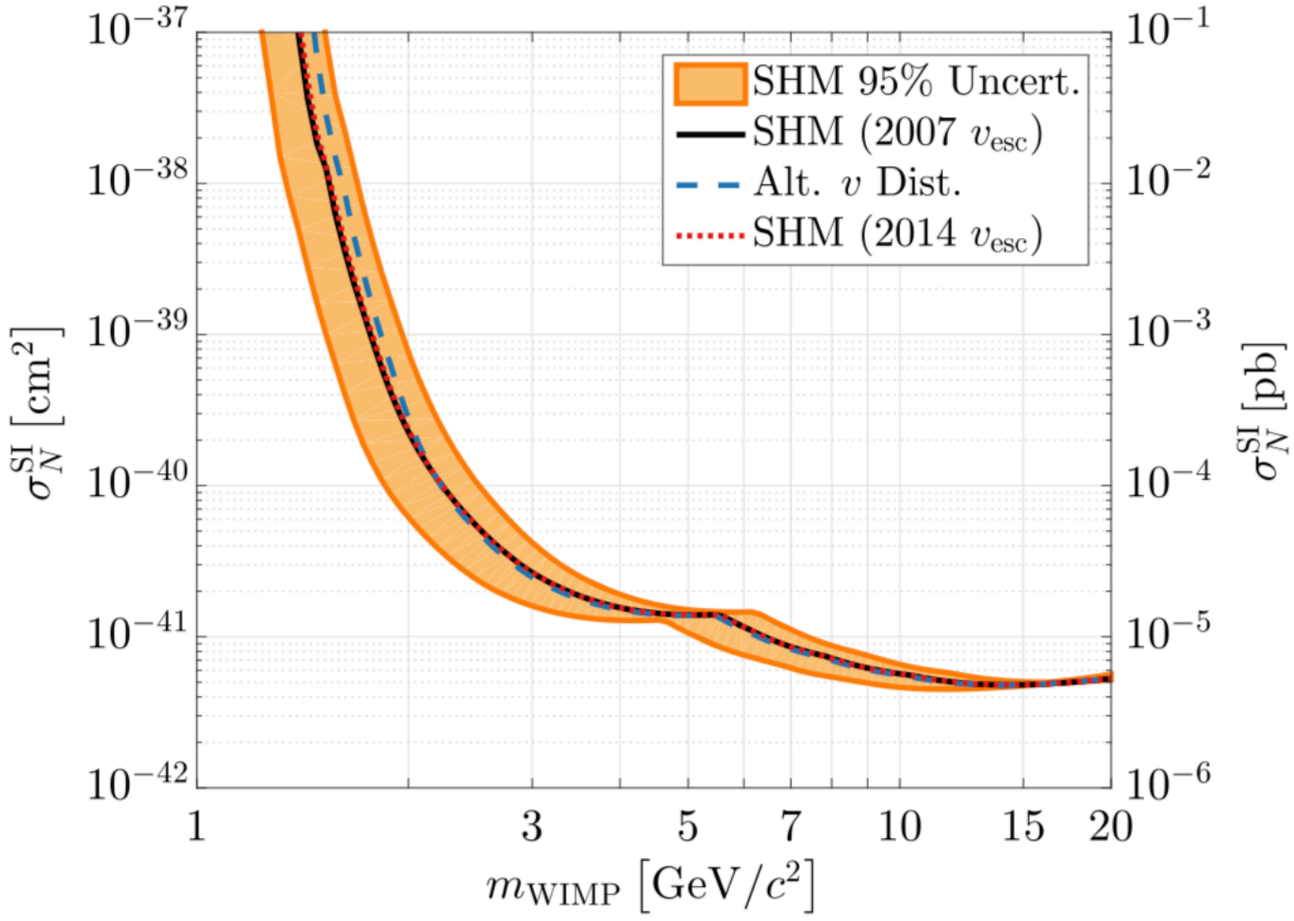

FIG. 31. The 95% (orange) uncertainty band on the best-fit Run 2 spin-independent limit (black solid) due to the uncertainties in the most probable WIMP velocity (v_0) and the Galactic escape velocity ($v_{\rm esc}$) used in the SHM. The 2014 RAVE survey $v_{\rm esc}$ distribution is sampled, and thus the best-fit curve substituting the 2014 median value into the SHM is given for consistency (red dotted). The black and red-dotted curves are the same as in Fig. 29, where an enlargement at low WIMP mass is given. The best-fit limit computed using the alternative velocity distribution of Eq. (26) is also presented (blue dashed).

- This is an analysis of the data from a single detector, operated at higher voltage with an exposure of 76kg d in two runs

- Pulse fitting, fiducial cuts, noise reduction, optimal filtering, time filtering needs to be applied to the data

PHYSICAL REVIEW D 97, 022002 (2018)

SuperCDMS

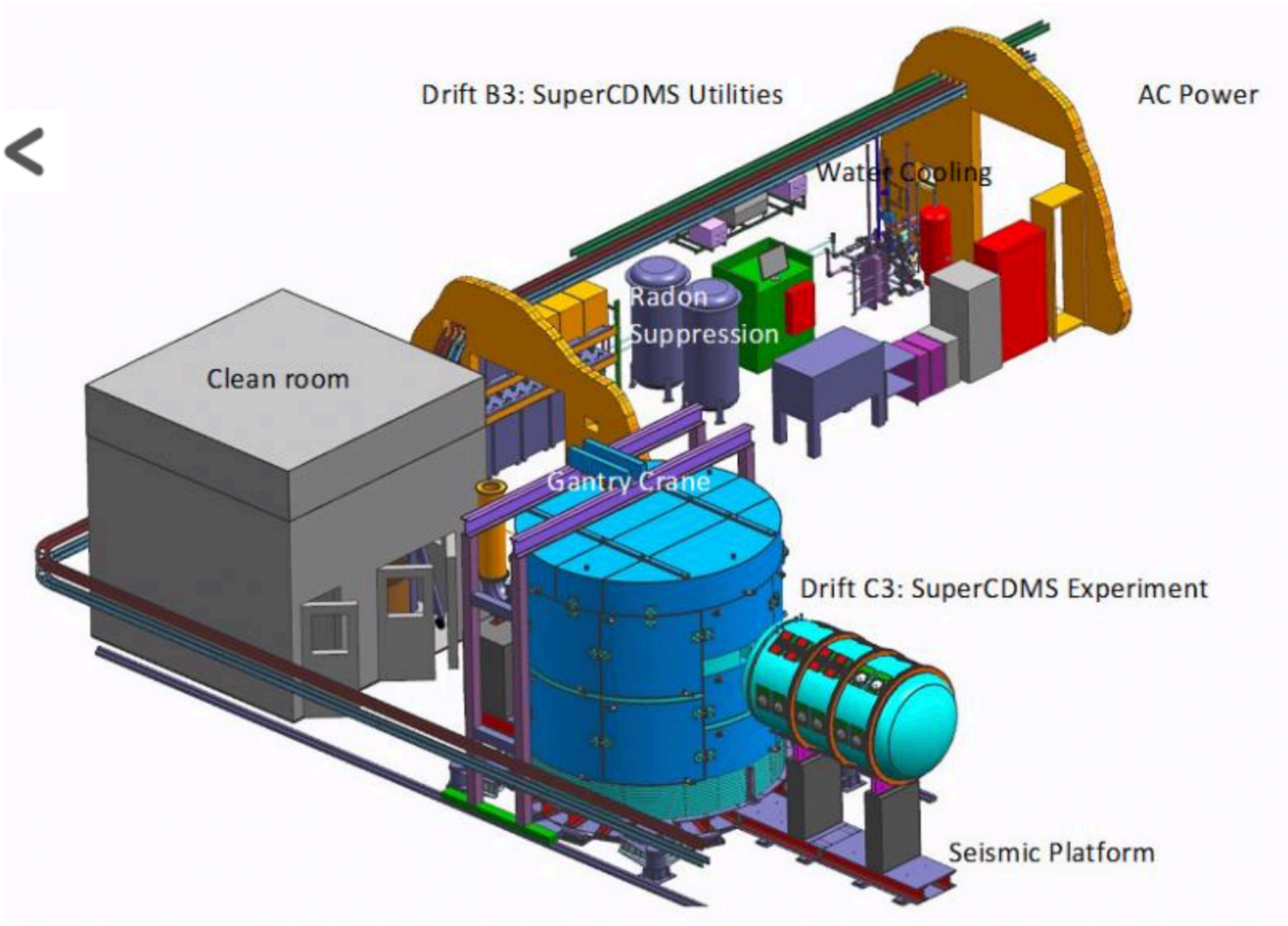

Model of the SuperCDMS SNOLAB experiment as it will be located in the deep underground laboratory at SNOLAB.

SuperCDMS projected Sensitivity

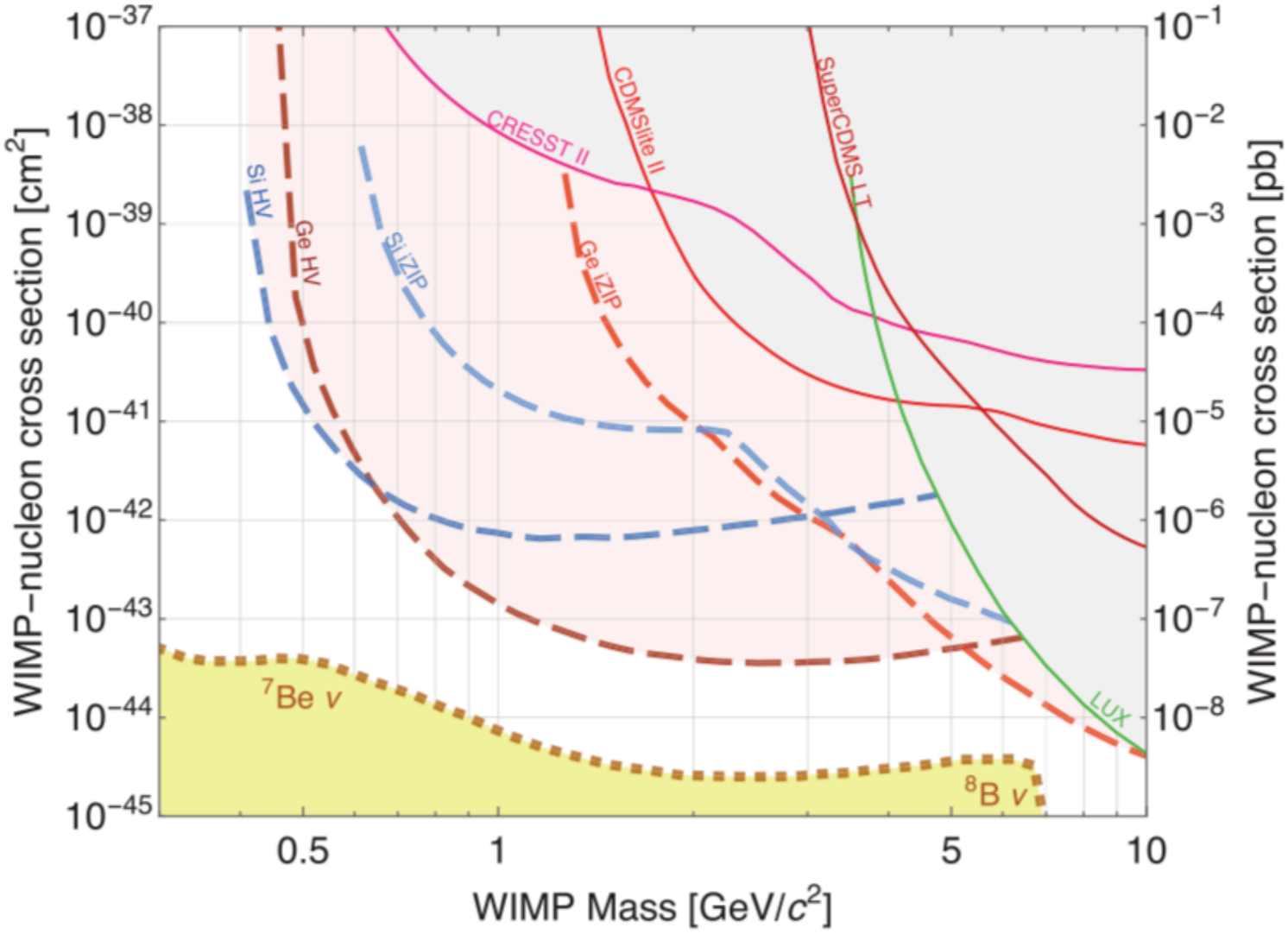

FIG. 8. Projected exclusion sensitivity for the SuperCDMS SNOLAB direct detection dark matter experiment. The vertical axis is the spin-independent WIMP-nucleon cross section under standard halo assumptions [47], and the horizontal axis is the WIMP mass, where WIMP is used to mean any low-mass particle dark matter candidate. The blue dashed curves represent the expected sensitivities for the Si HV and iZIP detectors and the red dashed curves the expected sensitivities of the Ge HV and iZIP detectors. These sensitivity limits are determined using the optimum interval method [48,49], which does not incorporate any knowledge of the specific disposition and source of background events observed during the experimental operation. The solid lines are the current experimental exclusion limits in the low-mass region, from the CRESST-II [50], SuperCDMS [4,5] and LUX [51] experiments. The dotted orange line is the dark matter discovery limit from Ref. [52], which represents the cross section at which the interaction rate from dark matter particles becomes comparable to the solar neutrino coherent elastic scattering rate.

Spin Dependent Searches

- Atoms with a large unpaired spin couple to WIMPs that prefer interactions to WIMPs that also carry spin

- Preferred atoms are ^{3}He and ^{19}F

  Interaction is driven by the nuclear physics form factors:

$$\Lambda = (1/J)[a_p\langle S_p\rangle + a_n\langle S_n\rangle]$$

Dark Matter Bubble Chamber: PICO

- PICO uses C3F8 as active fluid (boiling point -45°C). The chambers typically operate at 30psi and +16°C

- Bubble chambers are threshold detectors: they provide no information abou $\Lambda = (1/J)[a_p\langle S_p\rangle + a_n\langle S_n\rangle]$ particle, except that it was above the threshold energy

- Bubble chambers for dark matter searches are operated such that electron recoils (and hence MIPS) are not causing a bubble to form

- Alpha backgrounds are removed by their different acoustic properties

Dark Matter Bubble Chamber

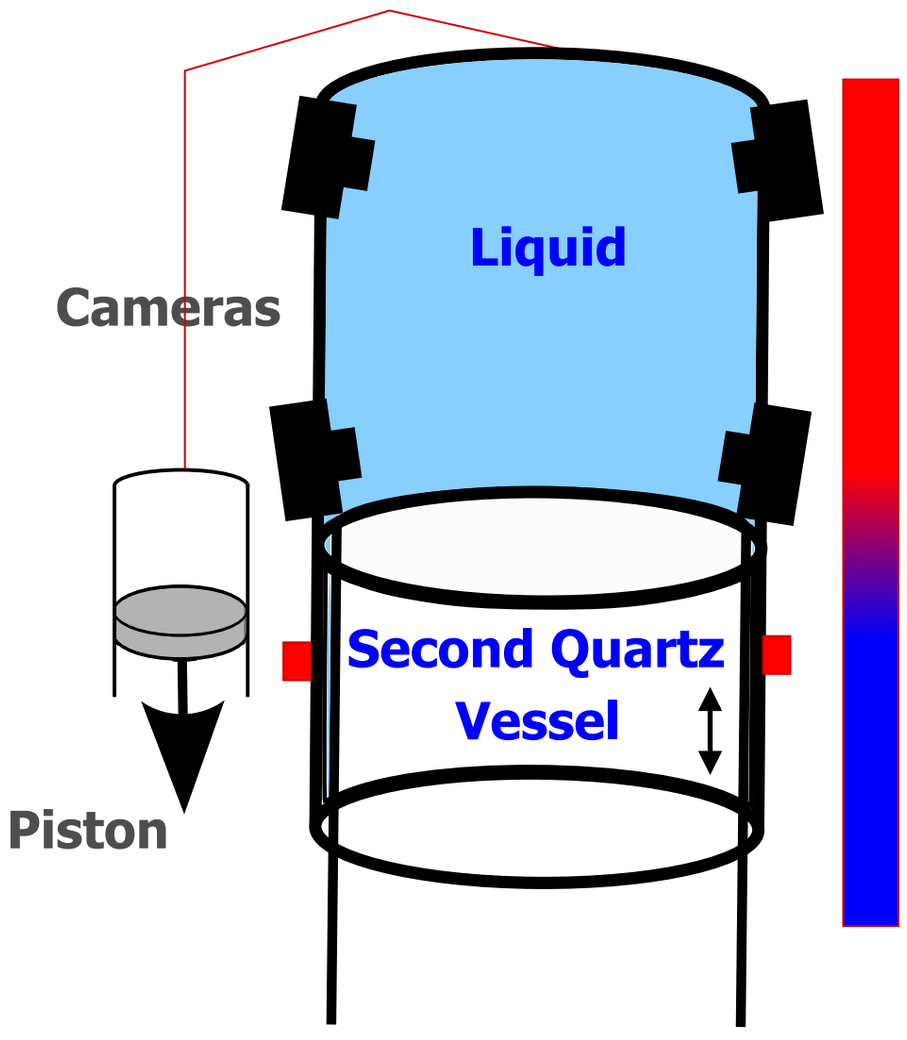

- Any bubble chamber has:
  - optical system with camera, lights
  - expansion system, piston, temperature control

PICO uses acoustic background discrimination

PICO 40L - “Right Side Up”

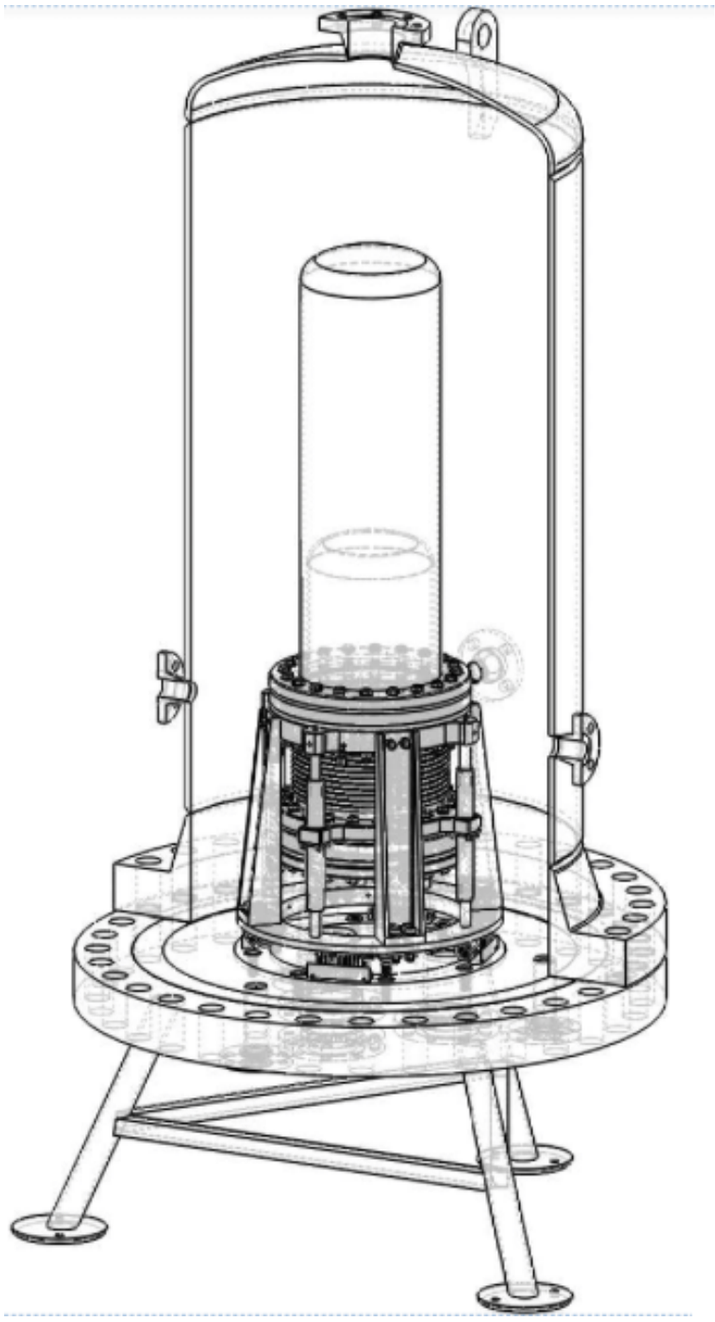

- To eliminate the water as source of background events, an inverted chamber without any buffer liquid was developed

- This chamber will be deployed at SNOLAB in 2017 to explore the ultimate sensitivity of a 40 litre chamber

- This design also incorporates various improvements based on the PICO 60 operational experience

PICO 40L

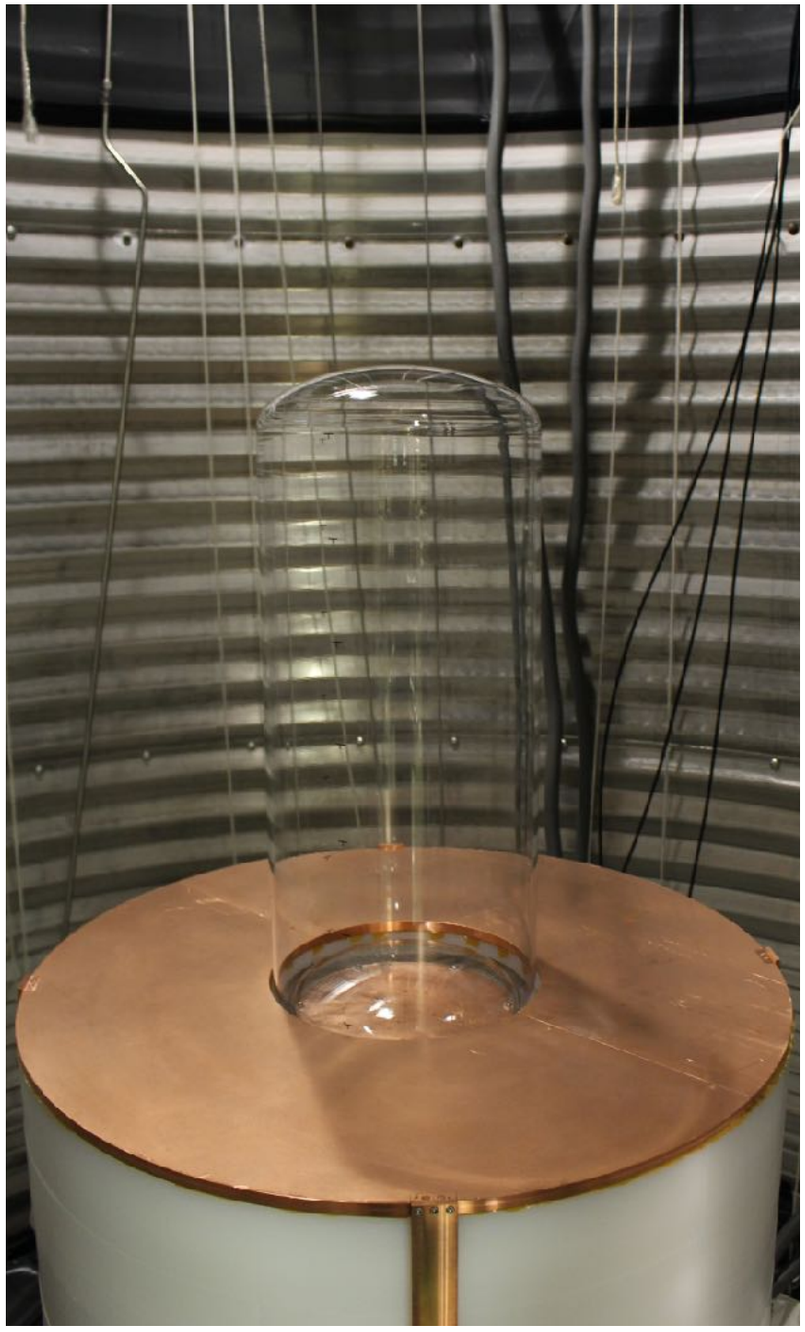

- This new detector saw the first bubble this week!
- If things work according to plan this will be 10x better than previous PICO bubble chambers in terms of background

PICO 60 Results

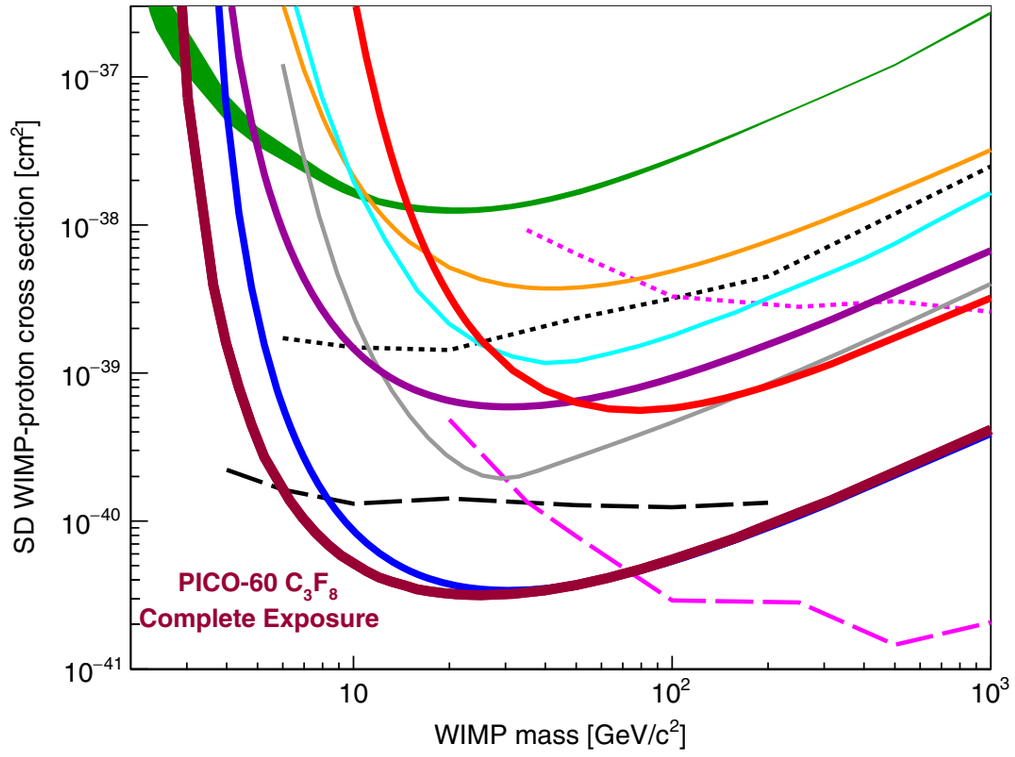

FIG. 7. The 90% C.L. limit on the SD WIMP-proton cross section from the profile likelihood analysis of the PICO-60 C_3F_8 combined blind exposure plotted in thick maroon, along with limits from the first blind exposure of PICO-60 C_3F_8 (thick blue) [6], as well as limits from PICO-60 CF_3I (thick red) [7], PICO-2L (thick purple) [33], PICASSO (green band) [34], SIMPLE (orange) [35], XENON1T (gray) [36], PandaX-II (cyan) [37], IceCube (dashed and dotted pink) [38], and SuperK (dashed and dotted black) [39,40]. The indirect limits from IceCube and SuperK assume annihilation to τ leptons (dashed) and b quarks (dotted). Additional limits, not shown for clarity, are set by LUX [41] (comparable to PandaX-II) and by ANTARES [42,43] (comparable to IceCube).

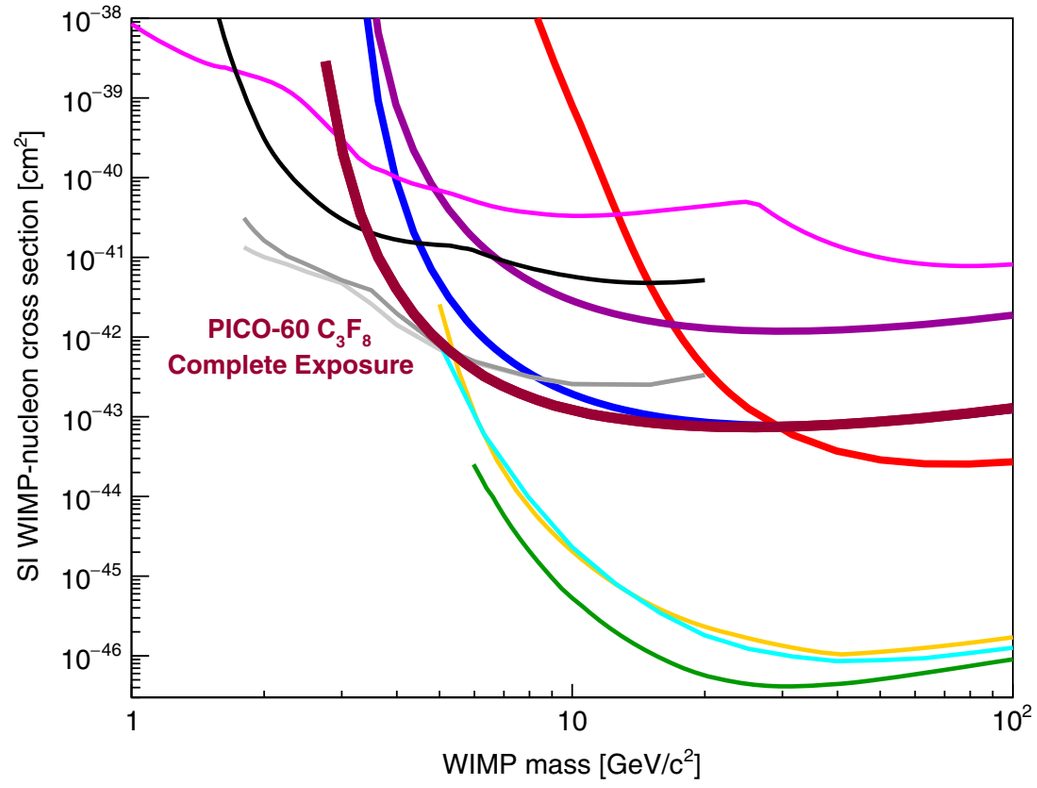

FIG. 8. The 90% C.L. limit on the SI WIMP-nucleon cross section from the profile likelihood ratio analysis of the PICO-60 C_3F_8 combined blind exposure plotted in thick maroon, along with limits from the first blind exposure of PICO-60 C_3F_8 (thick blue) [6], PICO-60 CF_3I (thick red) [7], PICO-2L (thick purple) [33], DarkSide-50 low-mass (gray) [44], XENON1T (green) [45], LUX (yellow) [46], PandaX-II (cyan) [47], CDMSlite (black) [48], and CRESST-II (magenta) [49]. Additional limits, not shown for clarity, are set by PICASSO [34], XENON100 [50], SuperCDMS [51], CDMS-II [52], and Edelweiss-III [53].

Next Up: PICO 500

- PICO 500 will explore the ultimate sensitivity of a low background bubble chamber
- It will be located at SNOLAB
- The bubble chamber technology is ready for an experiment of this scale

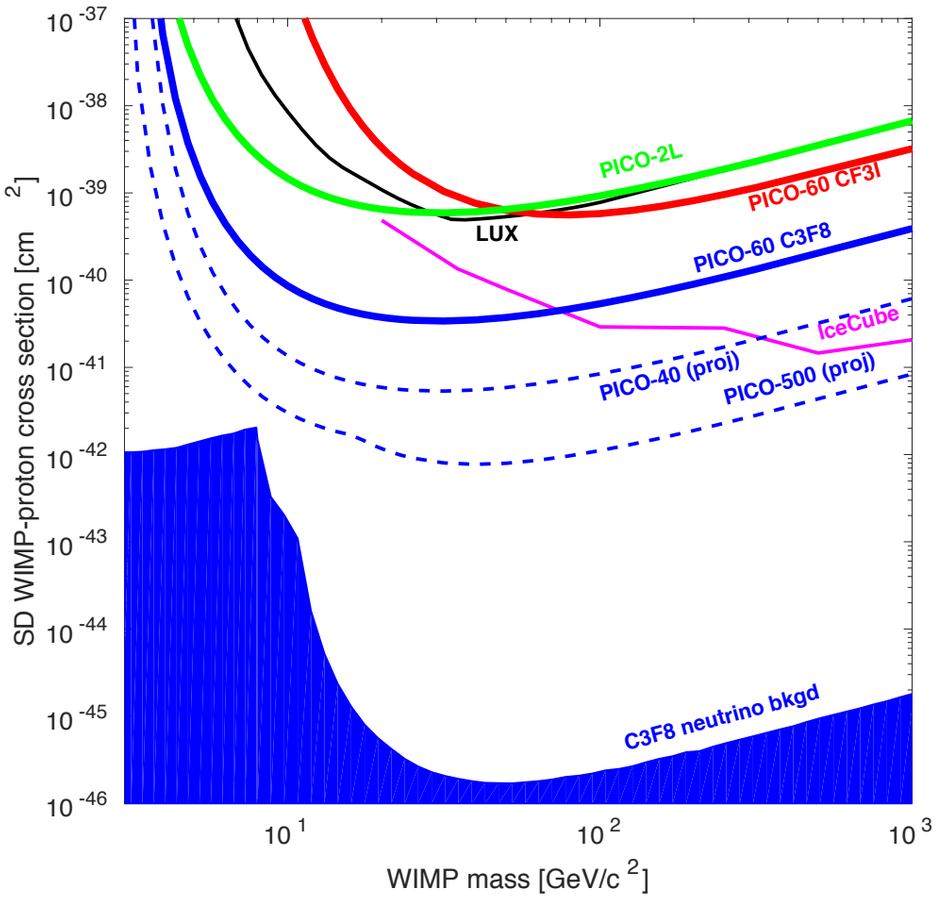

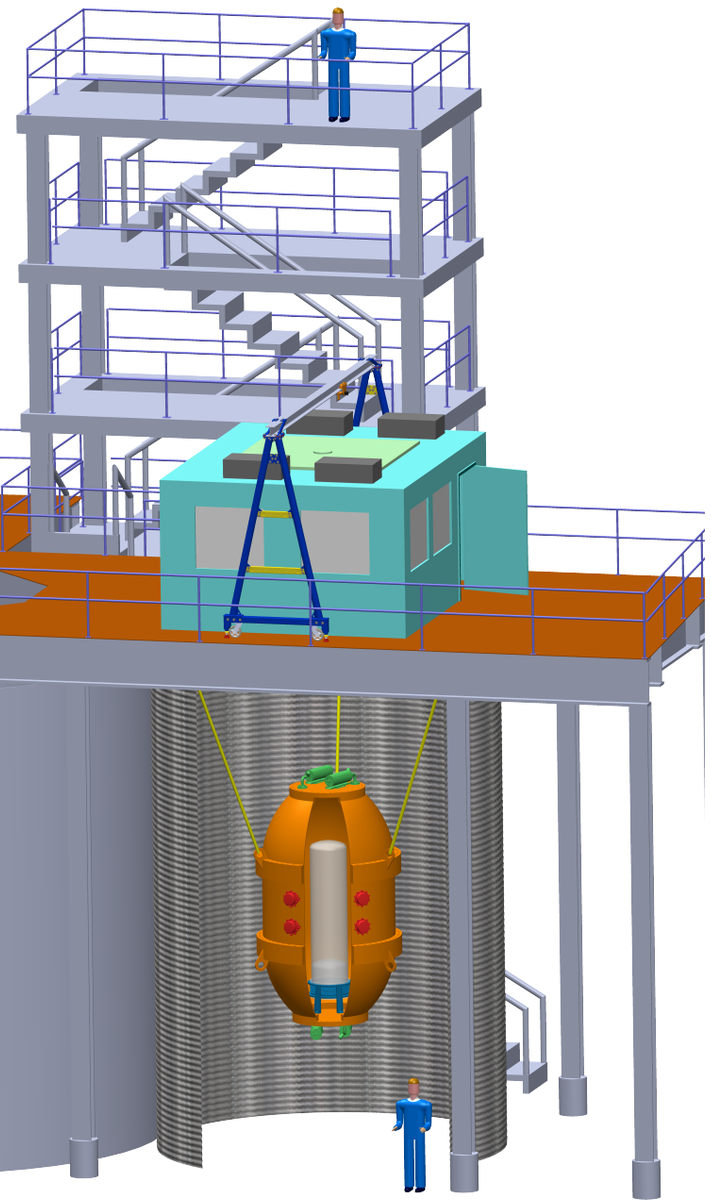

Summary

- No direct detection of dark matter yet!

Directional Dark Matter Searches

- Several groups are building chamber that reconstruct the direction of the primary particle by detecting the track direction of the nuclear recoil

- This will help to overcome the solar neutrino coherent neutrino nucleus scattering limit (“neutrino floor”)

Drift Experiment

- Gaseous detector filled with CS_2
- In a gaseous detector in principle, resolutions in the µm range are possible

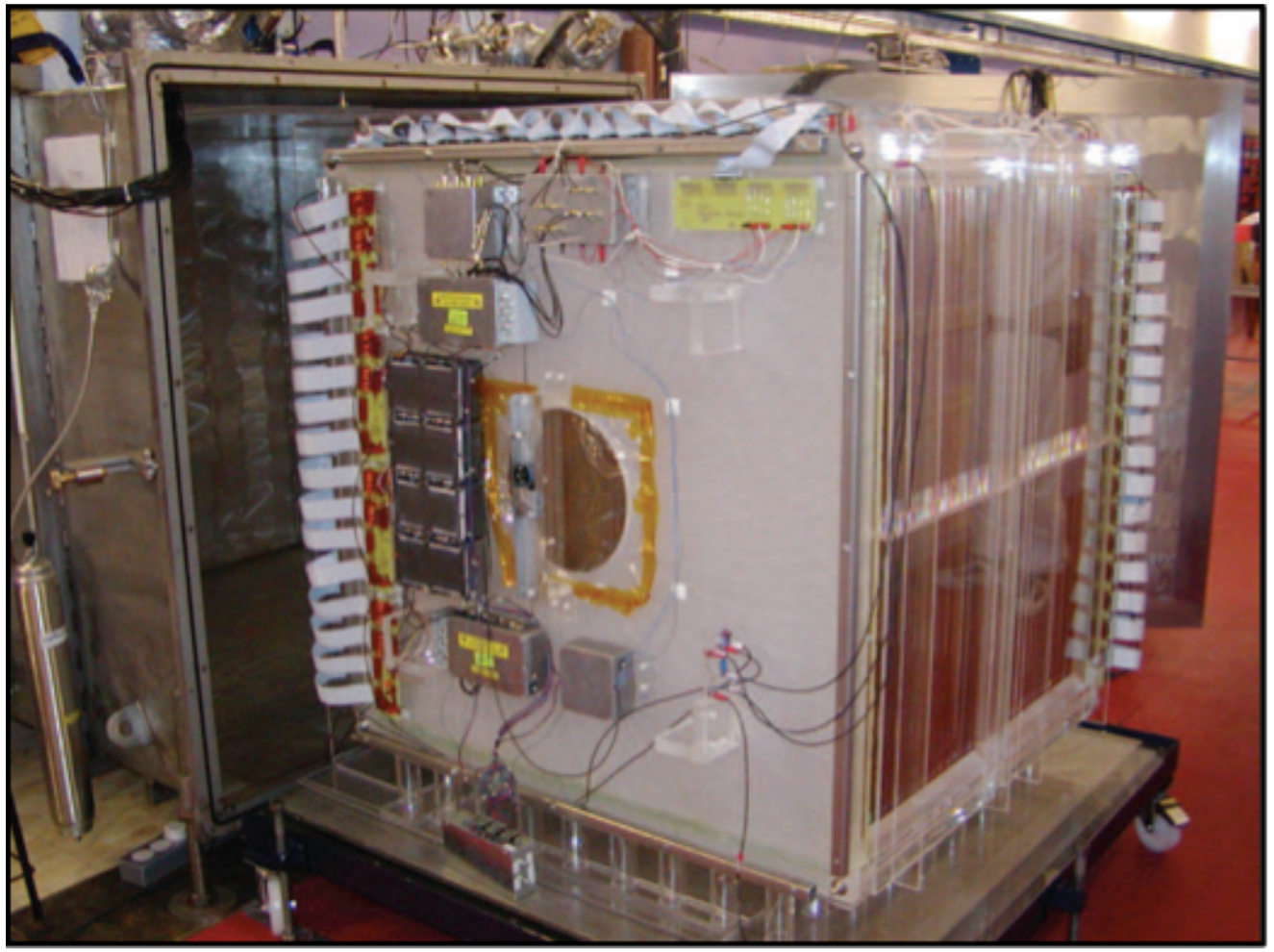

Proof of Principle

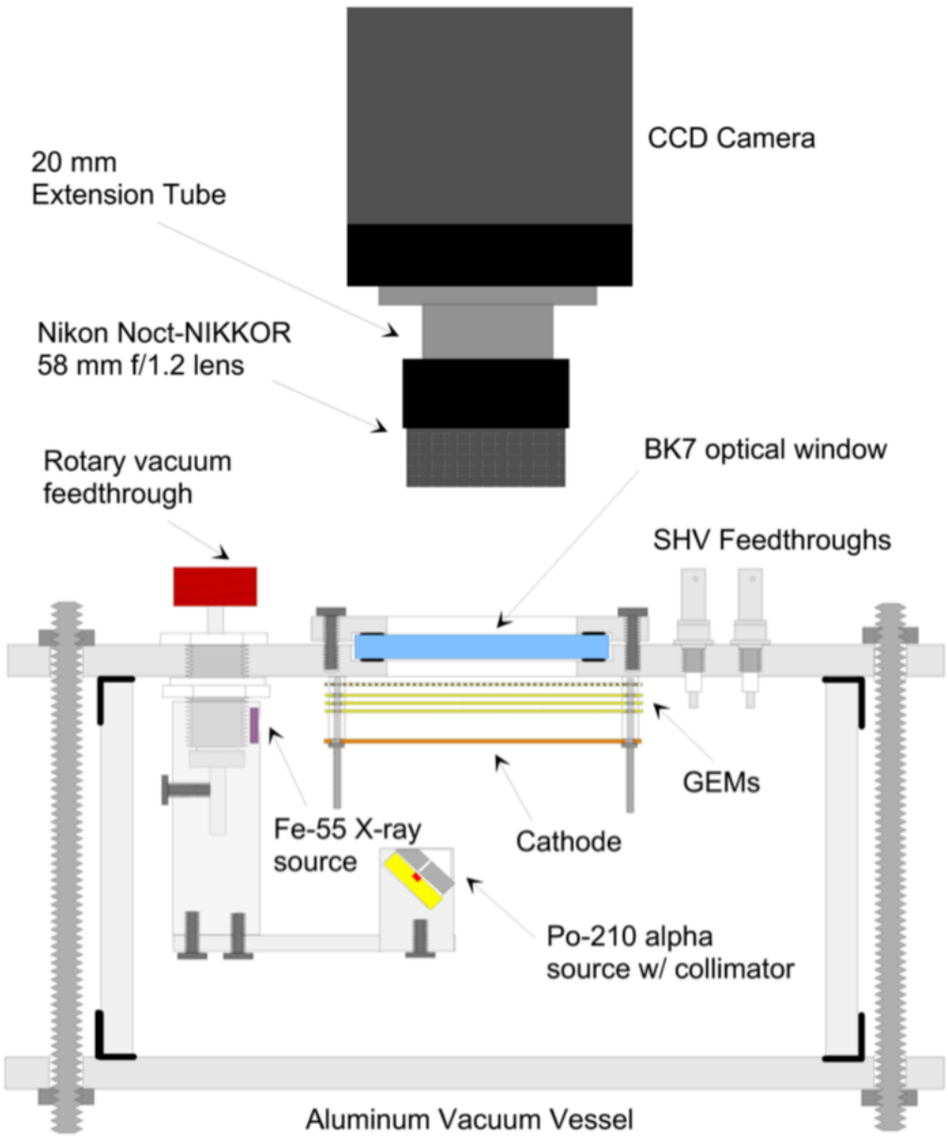

(a) CCD detector

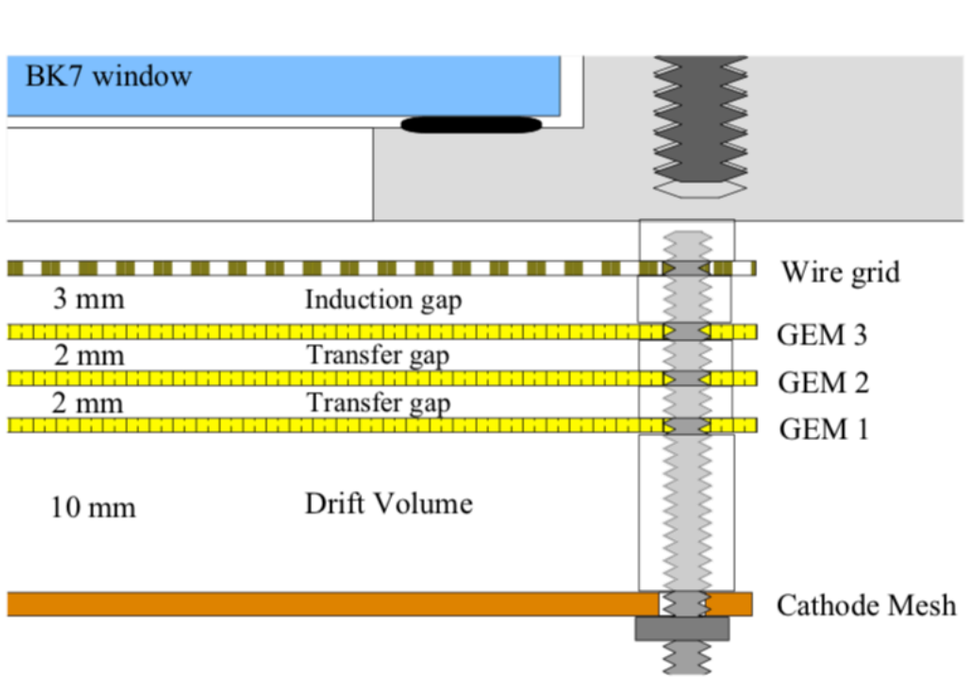

(b) Detection region

https://arxiv.org/pdf/1510.02170.pdf

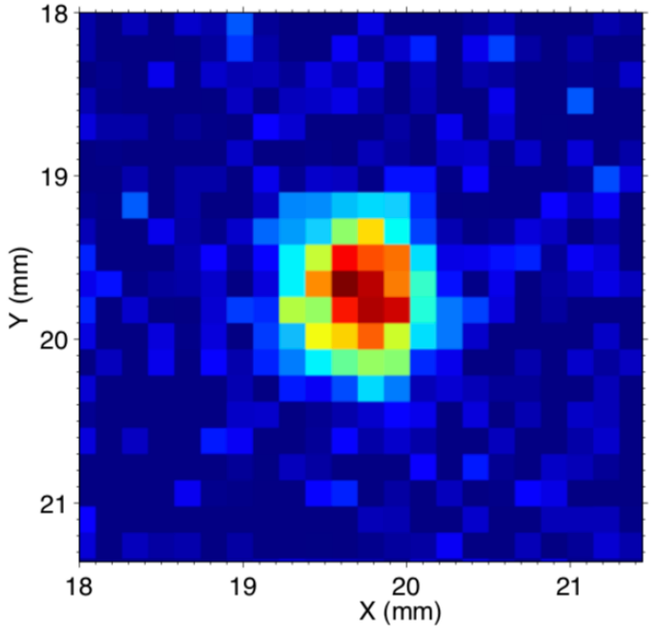

(a) 28 keVr (~ 13 keVee) nuclear recoil

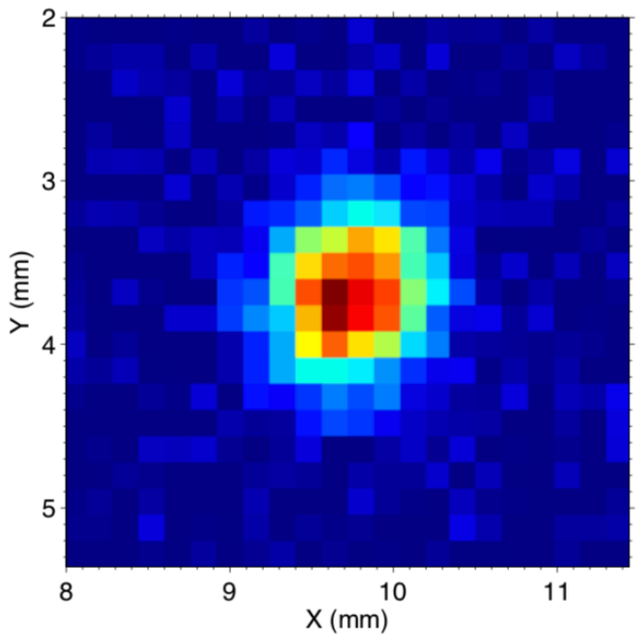

(b) 53 keVr (~ 28 keVee) nuclear recoil

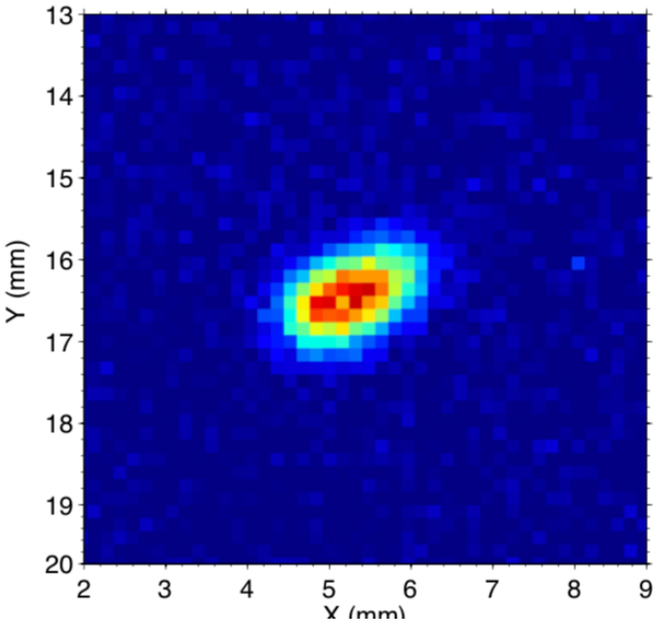

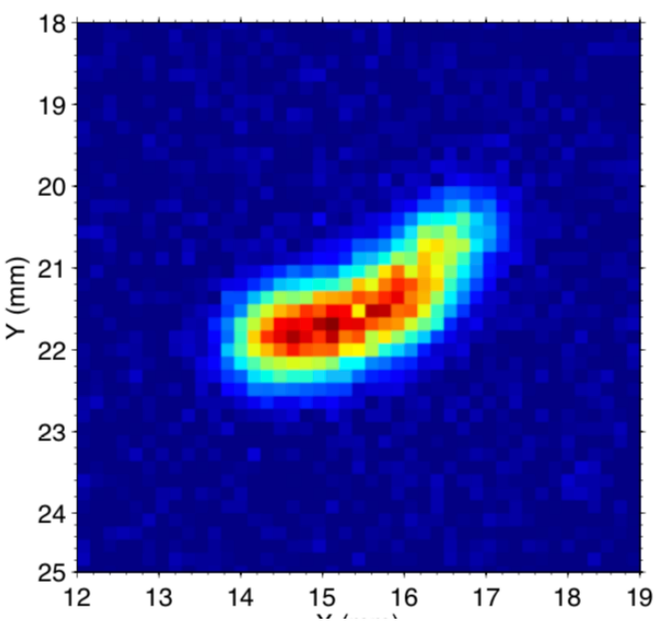

- Pure CF_4 detector TPC @ 100Torr
- Shown are nuclear recoils 28, 53, 104 and 214 keV nuclear recoil energy
- Recorded with a gas amplifying stage and a CCD camera

https://arxiv.org/pdf/1510.02170.pdf

The future of dark matter searches

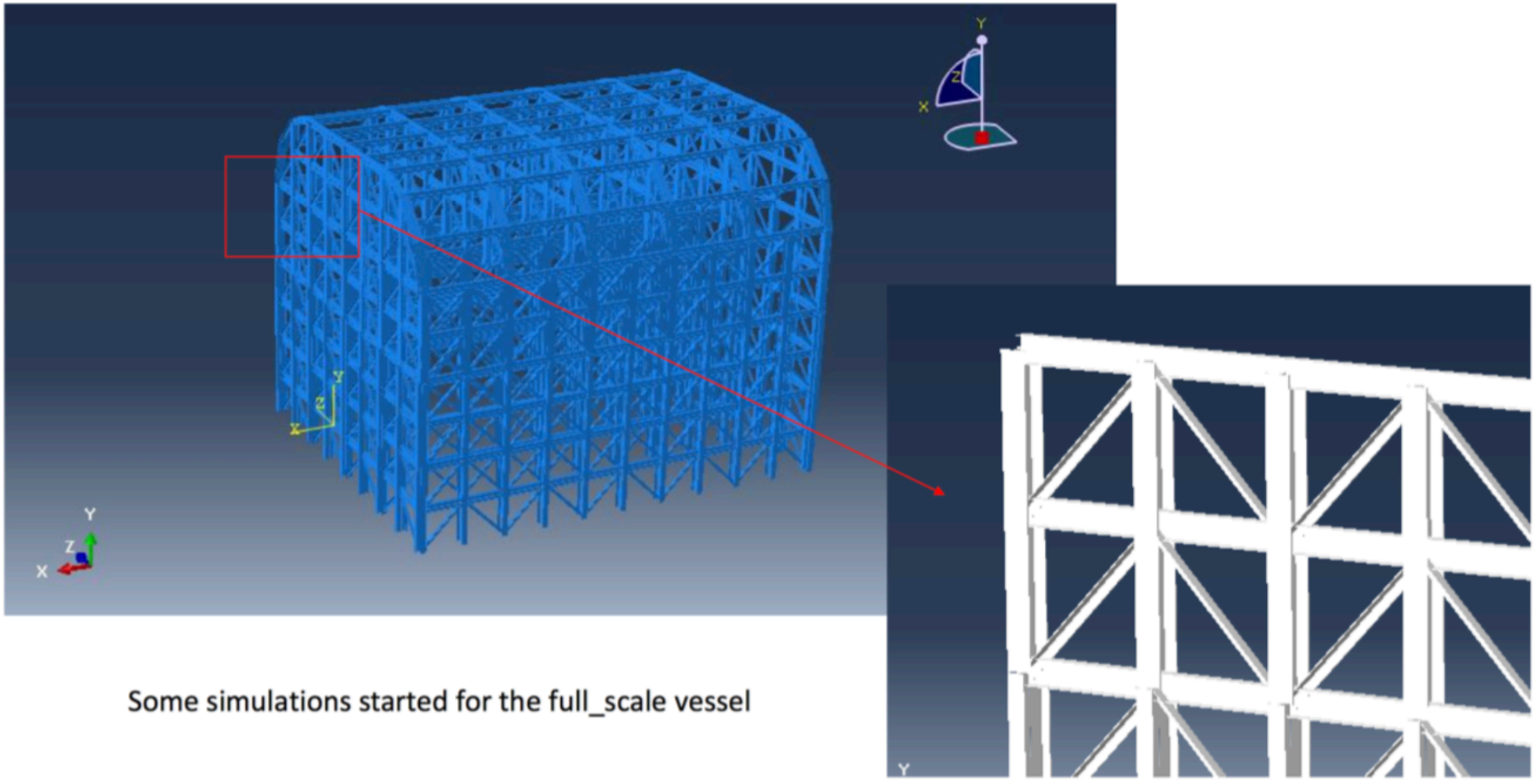

Some simulations started for the full_scale vessel

- Planning started towards a 100m^3 detector

Annual Modulation

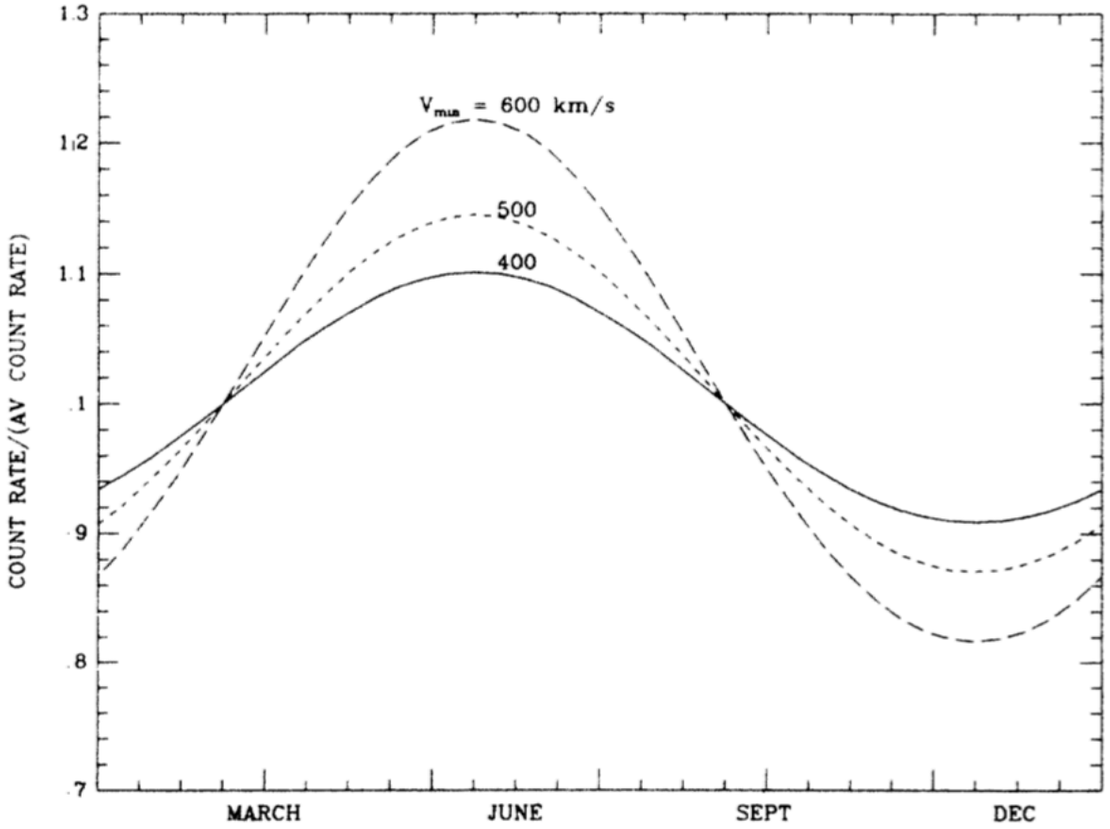

FIG. 7. Modulation of dark-matter signal in the detector due to the motion of the Earth around the Sun. Expected count rate/(averaged count rate) is plotted for different months of the year. This modulation effect can be used to enhance background subtraction.

- Predicted in 1987 by K Freese et al.
- Modulation comes from the motion of the earth through the galactic dark matter halo and therefore from the change of relative velocity

Phys. Rev. D **33**, 3495 – Published 15 June 1986

Dama/Libra

- DAMA/Libra uses NaI(Tl) crystals at the Gran Sasso laboratory

- DAMA has been running since 2003 and reported an annual modulation in their lowest energy bins

- The reported significance of the modulation is in excess of 9.3σ

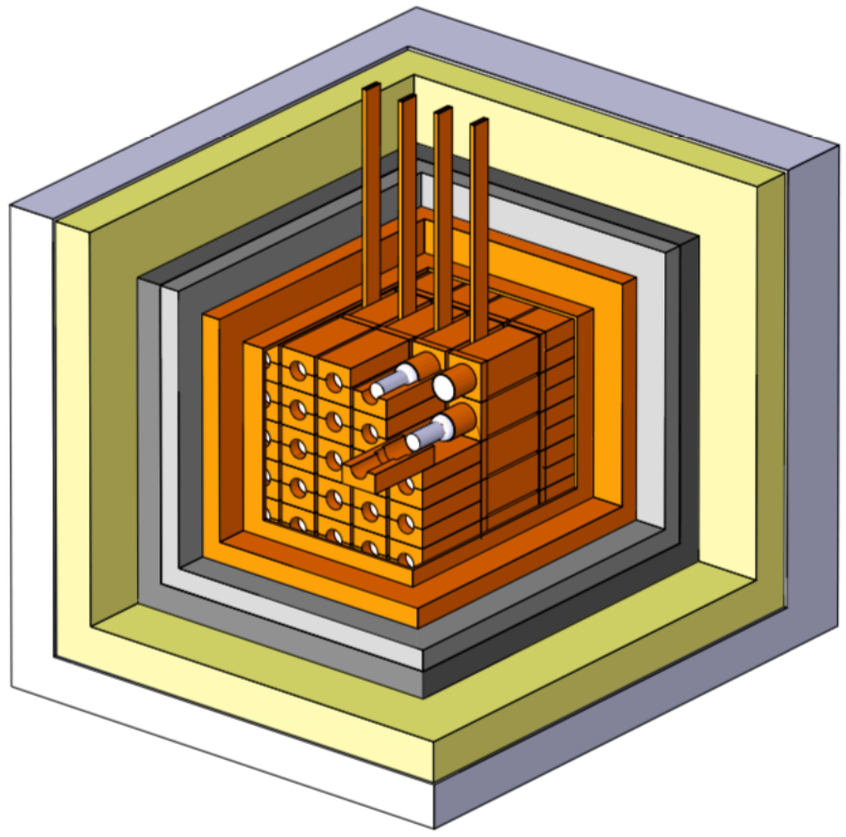

Fig. 1 Schematic view of the DAMA/LIBRA apparatus. The 25 highly radiopure NaI(Tl) crystal scintillators (5-rows by 5-columns matrix), housed in the sealed copper box continuously maintained in High Purity Nitrogen atmosphere, within low-radioactive passive shield are visible. Mostly outside the installation, the DAMA/LIBRA apparatus is also almost fully surrounded by about 1 m concrete made of the Gran Sasso rock. The copper guides of the calibration system are also shown. For details see Ref. [1]

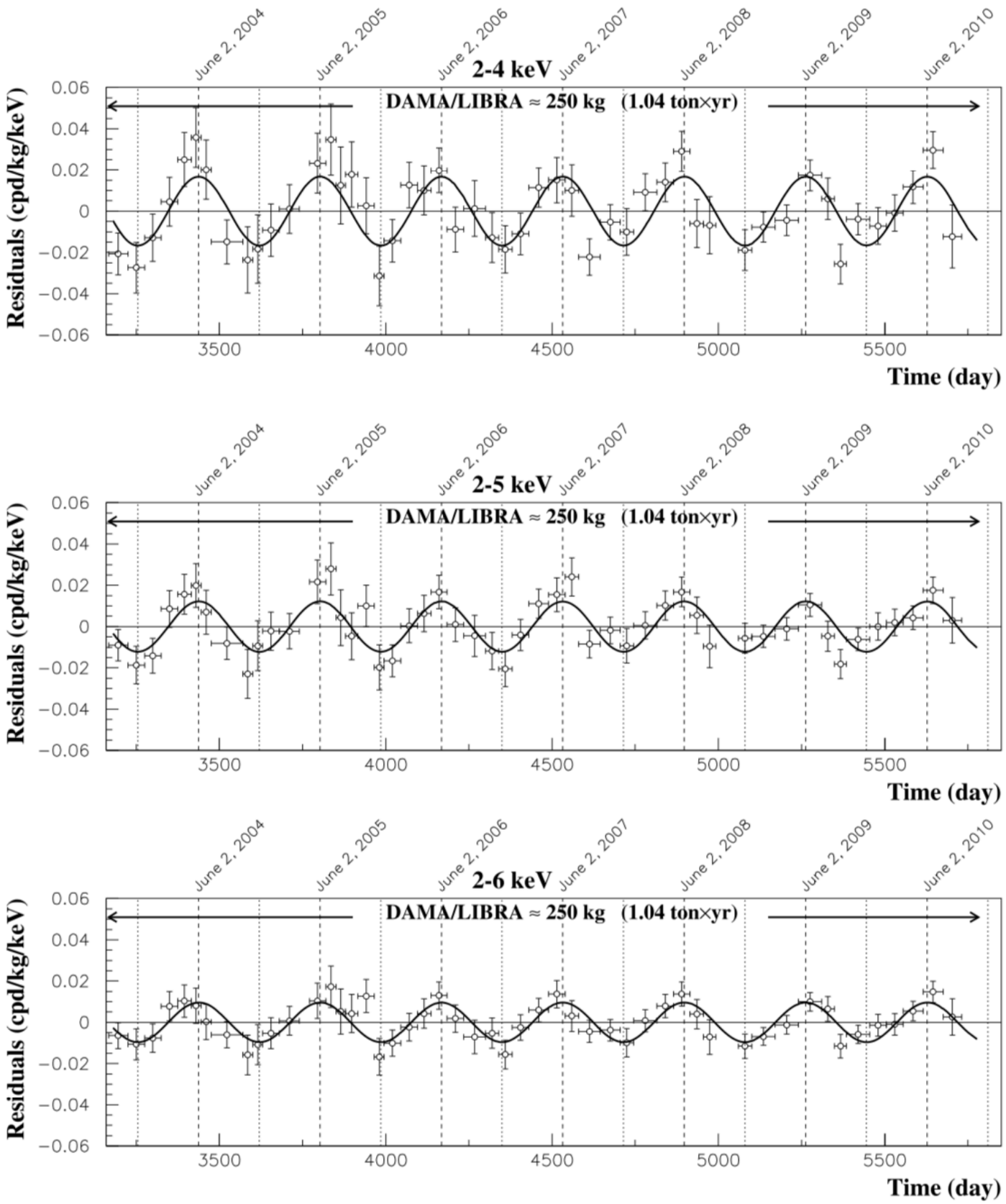

Fig. 2 Experimental residual rate of the *single-hit* scintillation events measured by DAMA/LIBRA–phase1 in the (2–4), (2–5) and (2–6) keV energy intervals as a function of the time. The time scale is maintained the same of the previous DAMA papers for coherence. The data points present the experimental errors as *vertical bars* and the associated time bin width as *horizontal bars*. The superimposed curves are the cosinusoidal functions behaviours $A\cos\omega(t-t_0)$ with a period $T=\frac{2\pi}{\omega}=1$ yr, a phase $t_0=152.5$ day (June 2nd) and modulation amplitudes, A, equal to the central values obtained by best fit on the data points of the entire DAMA/LIBRA–phase1. The *dashed vertical lines* correspond to the maximum expected for the DM signal (June 2nd), while the *dotted vertical lines* correspond to the minimum

Energy distribution

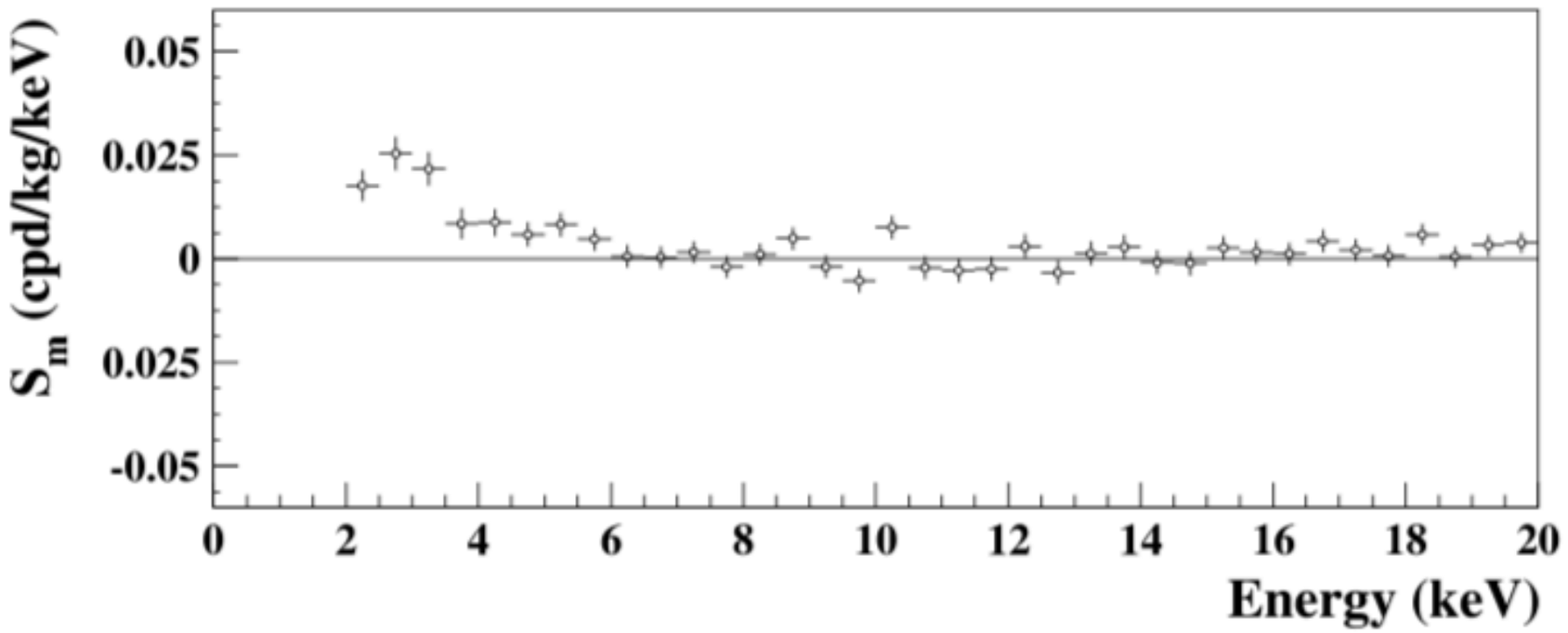

Fig. 8 Energy distribution of the S_m variable for the total cumulative exposure 1.33 ton × yr. The energy bin is 0.5 keV. A clear modulation is present in the lowest energy region, while S_m values compatible with zero are present just above. In fact, the S_m values in the (6–20) keV energy interval have random fluctuations around zero with χ^2 equal to 35.8 for 28 degrees of freedom (upper tail probability of 15 %)

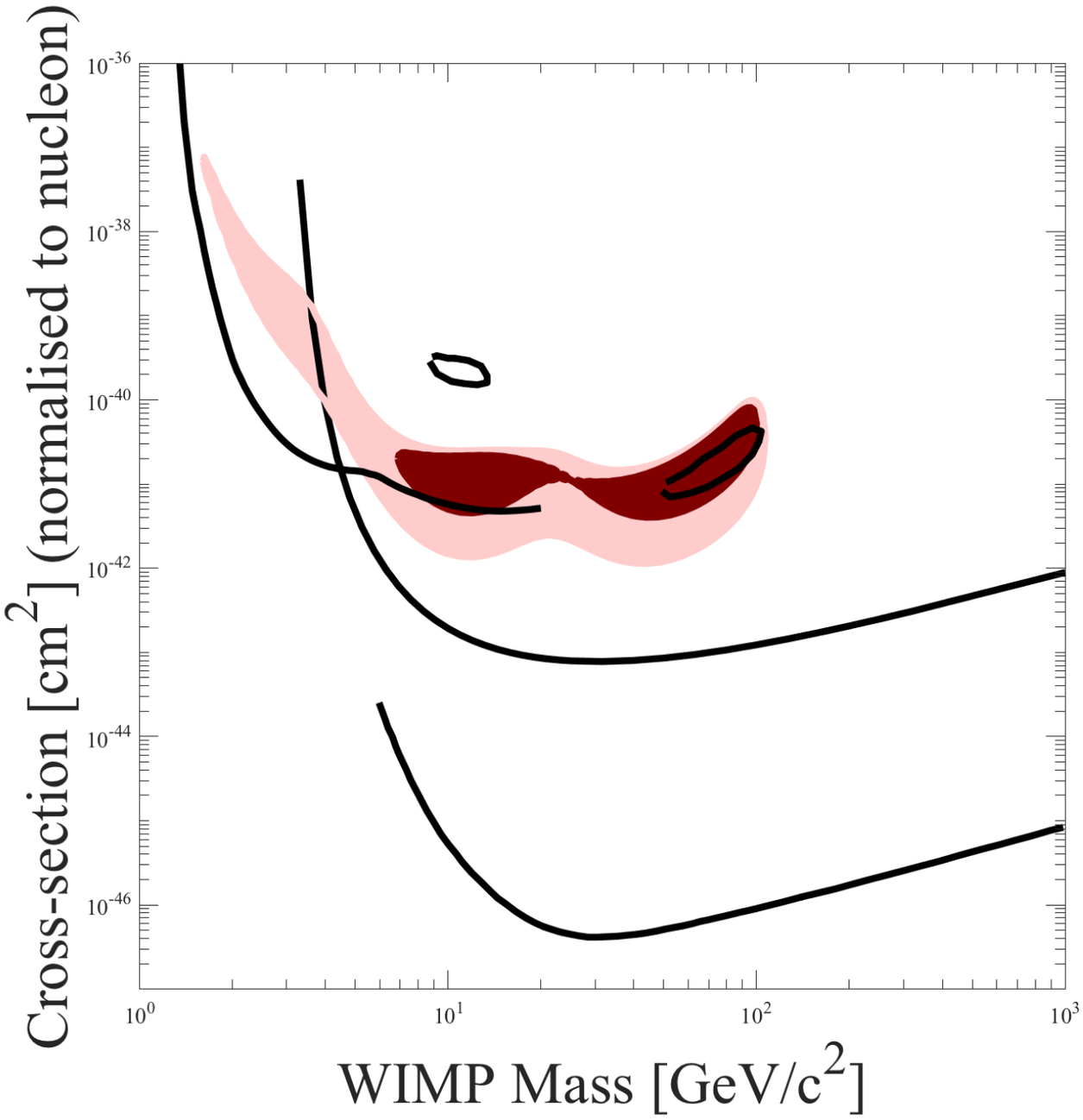

- DAMA and interpretations shown as probably contours

- PICO 60 SI limit, SuperCDMSlite and Xenon 1T shown for comparison

Cosine 100 Experiment

Cosine-100

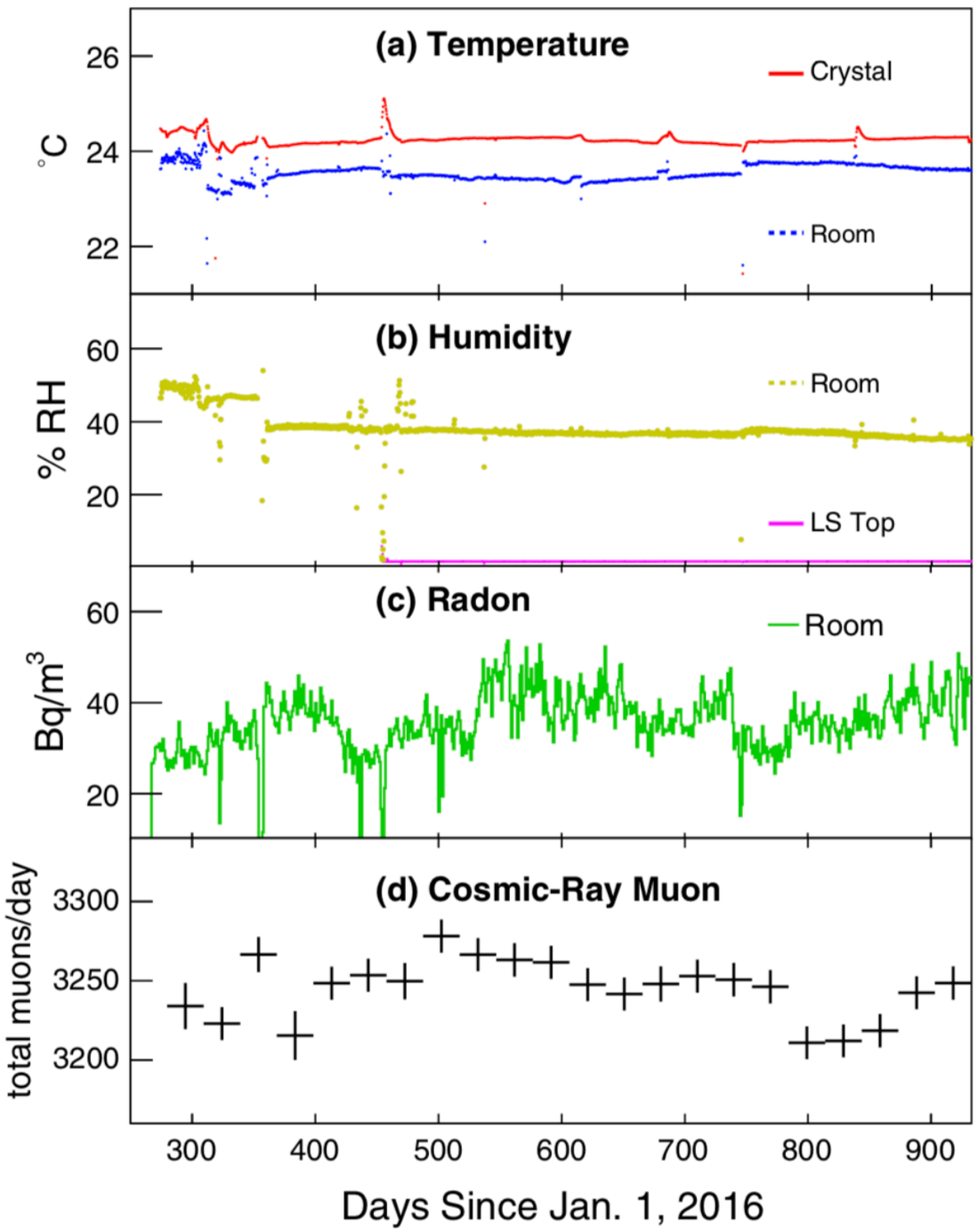

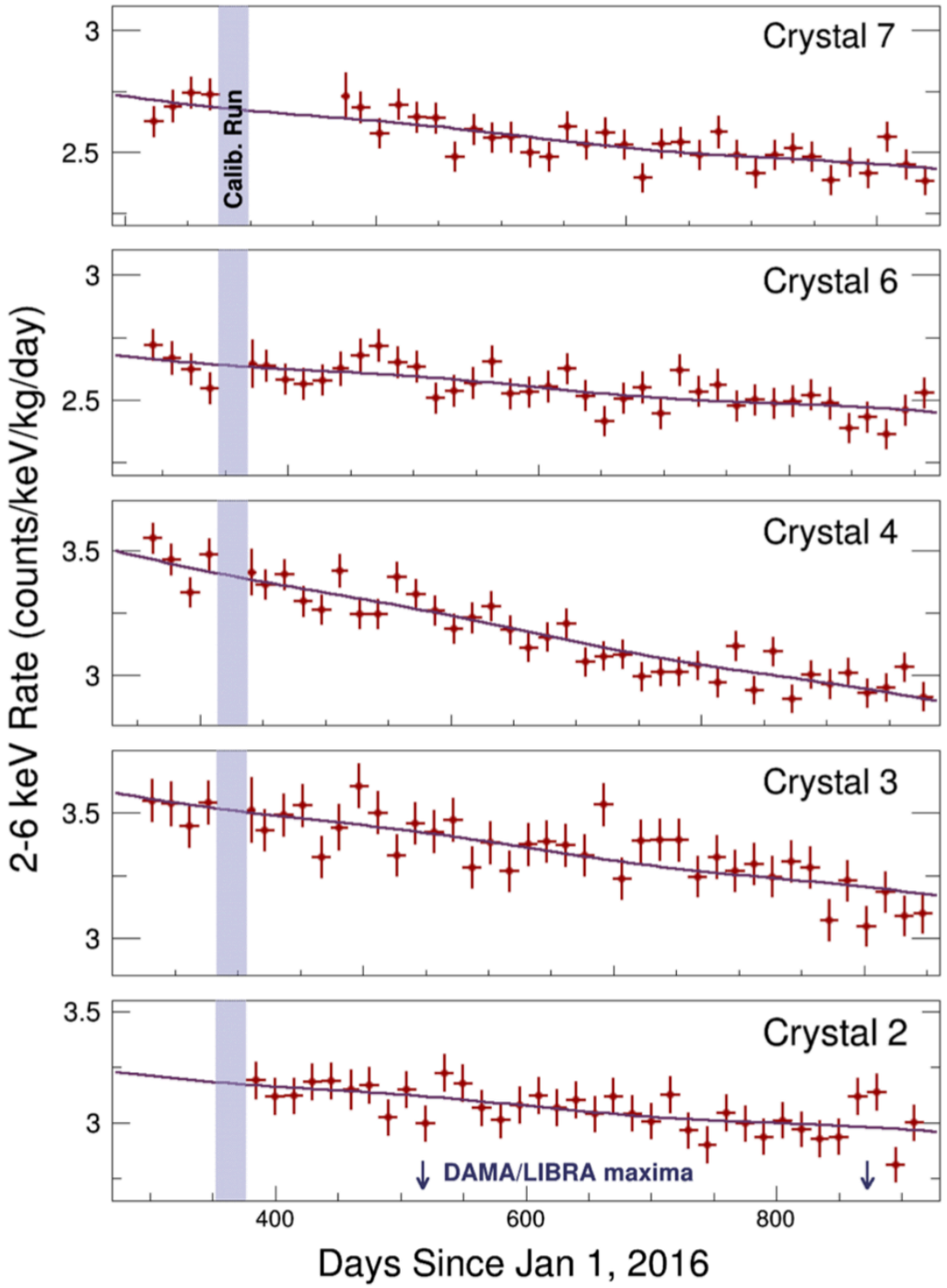

PHYSICAL REVIEW LETTERS 123, 031302 (2019)

Phase amplitude Diagram

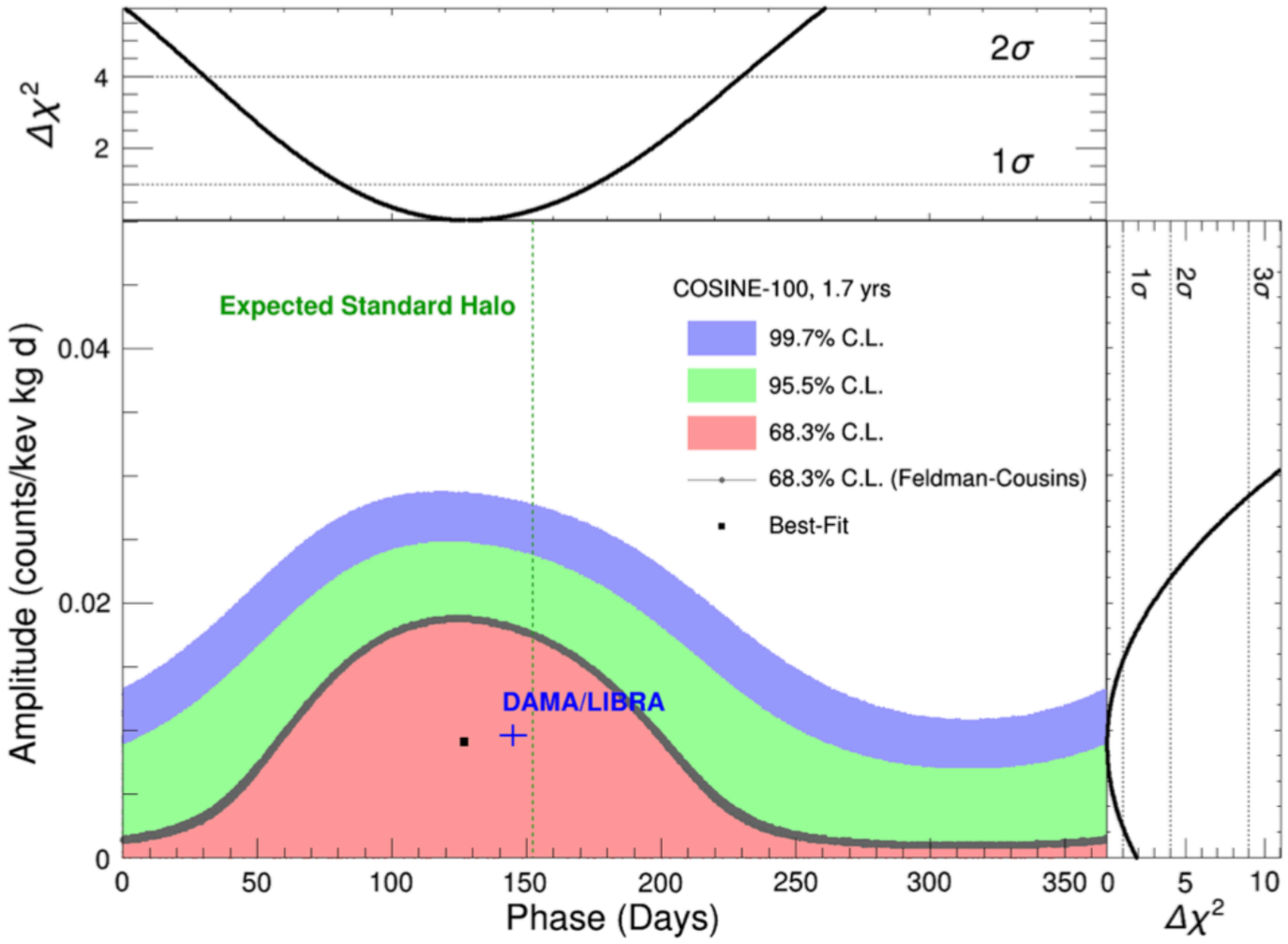

=> Need more data!

Summary

- Many exciting technologies have been developed to search for dark matter

- Experiments get larger and more expensive: in the US only ADMX, SuperCDMS and LZ are currently funded - there is a need for everyone to be clever and innovate to push the field with great ideas

- It's now harder to be as excited for dark matter searches as ~5-7 years ago - there is opposition in the theory community that question the viability of supersymmetry post LHC

- There is still no better testable theory. We have not tested the space accessibly to experiments yet!